

**FIELD EVALUATION AND ANALYSIS OF A
LIQUID DESICCANT AIR HANDLING SYSTEM**

by

BENJAMIN MARCUS JONES

A thesis submitted to the
Department of Mechanical and Materials Engineering
in conformity with the requirements for
the degree of Master of Science (Engineering)

Queen's University
Kingston, Ontario, Canada
Submitted September 2008

Copyright © Benjamin Marcus Jones, 2008

Abstract

A thermal liquid desiccant air handling machine was procured, installed, and field tested. The goal of the present investigation is to evaluate the field performance of the machine and characterize its operation for the temperature range of a solar thermal array. The system studied includes a natural gas boiler supplying the heat, and a cooling tower for heat rejection. System performance was evaluated for the 50 to 90°C temperature range, the operating range of solar thermal collectors. Cooling power varied between 4.3 kW and 22.8 kW for this range of temperature, with a latent heat ratio between 1.1 and 1.9, confirming that the unit is significantly dehumidifying the process air stream. Electrical COP varied between 0.58 and 4.48. Performance data indicates higher temperature solar collectors such as evacuated tube or double glazed flat plat collectors would be optimum in a solar cooling application with this system. Empirical correlations for the regenerator and conditioner components were obtained using a multivariate linear regression model. 5 empirical relations were derived and can be used to characterize the thermal dehumidification concept. These relations and methods will be used in future work to simulate and optimize a solar thermal driven dehumidification system for dedicated outdoor air systems.

Acknowledgments

First and foremost I would like to thank Professor S.J Harrison for inspiring my interest in solar energy and providing the resources, patience, and encouragement to expand my knowledge in this field. His tireless dedication and ambition seen in the many projects and communities both internal and external to the Queen's Solar Calorimetry Laboratory are responsible for much needed progress in understanding and bringing solar thermal technology to Canada.

I would like to thank the many individuals that make up the Queen's Solar Lab community my fellow students and friends. With the support and friendship of my fellow M.Sc. candidates, my time at the solar lab has been a defining and memorable experience.

I thank those who took a direct part in the ongoing Solar Cooling research at Queen's, the many summer students, graduate students, and technicians. Thanks go to Dr. Lucio Mesquita for the time taken in explaining the concept and his own research. The support of AIL Research is also appreciated, lending an expert voice to the analysis and installation required in this complex project.

This project has been supported by the Solar Calorimetry Laboratory of Queen's University and was made possible through support provided by Natural Resources Canada and the Solar Buildings Research Network.

Nomenclature

Symbols

A	Area	m^2
C _p	Specific heat	$kJ/kg \cdot K$
E	Energy	kJ
ϵ	Effectiveness	—
η	Efficiency	—
G	Incident solar radiation	W/m^2
h	Specific enthalpy	kJ/kg
\dot{m}	Mass flow rate	kg/s
p	Pressure	Pa
Q	Heat	kJ
\dot{q}	Heat flow rate	kW
T	Temperature	$^\circ C$
t	Time	s
VLI	Ventilation load index	$kWh/m^3 \cdot hr$
W	Humidity ratio	kg_v/kg_a

Subscripts

a	Air
d	Desiccant component of solution
c	Conditioner, also known as absorber
cw	Cooling water
fg	Heat of condensation or vaporization
hw	Heating water
HX	Heat exchanger
in	Inlet condition
OA	Outside air
out	Outlet condition
r	Regenerator, also known as desorber
set	Setpoint
sol	Liquid desiccant solution
T	Total
u	usable, in reference to solar thermal energy
v	Water vapor in air, or transported between solution and air
w	Water component of solution
x - y	Property transport from stream 'x' to 'y'

Acronyms

COP	Coefficient of performance
DOAS	Dedicated outdoor air system
IAQ	Indoor air quality
LHR	Latent heat ratio
SHR	Sensible heat ratio

Table of Contents

Abstract	i
Acknowledgments	ii
Nomenclature	iii
Table of Contents	vi
List of Tables	ix
List of Figures	x
Chapter 1:	
Introduction	1
1.1 Building Ventilation Air Requirements	1
1.2 Air Handling Systems	5
1.3 Solar Thermal Low Flow Liquid Desiccant Air Conditioning	11
1.4 Literature Review	13
1.5 Principle Advantages	16
1.6 Objectives and scope of study	17

Chapter 2:

Theory	20
2.1 Solar Thermal Collector Performance	20
2.2 Liquid Desiccants for Dehumidification	22
2.3 Liquid Desiccant Component Energy Analysis	27
2.4 System Performance Parameters	35

Chapter 3:

System Description	39
3.1 Component Overview	39
3.2 Air Handling System	40
3.3 Thermal Components	43
3.4 Data acquisition and control	45

Chapter 4:

Experiment and analysis methods	49
4.1 Experimental Procedure	49
4.2 Data analysis	51
4.3 Solar profile generation	53

Chapter 5:

Results and Analysis	56
5.1 Enthalpy balance	56
5.2 Daily performance data	60
5.3 Coefficients of performance	61
5.4 Sensitivity study	67

5.5 Regression analysis	68
5.6 Discussion	73
 Chapter 6:	
Conclusions and Recommendations	77
6.1 Conclusions	77
6.2 Recommendations & future work	79
 Bibliography	79
 Appendix A:	
Experimental results	83
A.1 Data set	83
A.2 Daily profiles	91
A.3 Regression correlations	91
 Appendix B:	
Data acquisition and control	102
 Appendix C:	
Matlab data processing	108
 Appendix D:	
Conditioner Assembly Drawings	116

List of Tables

3.1	Air handling system experimental values	45
3.2	CR10X analog input ranges	45
4.1	Data collection schedule for regenerator temperature	49
4.2	Solar profile temperatures - 30 minute resolution	55
5.1	Daily system operation summary	60
5.2	Regenerator performance parameters	68
5.3	Conditioner performance parameters	68
5.4	Regression fit summary	72
A.1	Daily performance table	88
A.2	Daily performance table continued	89
A.3	Daily performance table continued	90
B.1	Data acquisition specification and cross reference	105

List of Figures

1.1	Ventilation Load Index for Canadian Cities	4
1.2	Conventional HVAC Strategy	6
1.3	Ontario 2007 electricity demand and solar irradiation on horizontal for Toronto, Ontario	8
1.4	Dedicated Outdoor Air System HVAC configuration	9
1.5	Psychrometric chart showing three different ventilation air handling processes	10
1.6	Solar Cooling Overview	12
1.7	Research flow chart and scope	19
2.1	Concentration properties of $LiCl$	23
2.2	Vapor pressure p_{sol} , of aqueous $LiCl$	24
2.3	Relative vapor pressure variation of aqueous $LiCl$	25
2.4	Latent heats of absorption and desorption in $LiCl$	27
2.5	Process flow heat and mass transfer	28
2.6	Conceptual diagram of plate exchanger concept	30
2.7	Absorber mass and energy flows	31
2.8	Regenerator mass and energy flows	34
3.1	Overview of process flows	41

3.2	System layout	42
3.3	System layout	43
3.4	Model of air handling unit	44
3.5	Flate plate mass and heat exchangers	46
4.1	Solar thermal efficiency curves	53
4.2	Simulation schematic	54
5.1	Enthalpy flow in conditioner	57
5.2	Enthalpy flow in regenerator	58
5.3	Enthalpy balance in conditioner	59
5.4	Enthalpy balance in regenerator	59
5.5	Conditioner performance - July 25th	62
5.6	Heating temperature & performance figures - July 25th	63
5.7	Daily thermal coefficients of performance	65
5.8	Daily thermal coefficients of performance	66
5.9	Process air temperature change correlation for 2 variables	70
5.10	Process air temperature change correlation for 3 variables	71
A.1	Regenerator heating water temperature drop for various parameters .	84
A.2	Regenerator concentration change for various parameters	85
A.3	Conditioner water absorption rate for various parameters	86
A.4	Conditioner water absorption rate for various parameters	87
A.5	Conditioner performance - July 10th	92
A.6	Heating temperature & performance figures - July 10th	93
A.7	Conditioner performance - July 13th	94

A.8	Heating temperature & performance figures - July 13th	95
A.9	Conditioner performance - July 20th	96
A.10	Heating temperature & performance figures - July 20th	97
A.11	Water absorption correlation for 2 variables	98
A.12	Water absorption correlation for 3 variables	98
A.13	Cooling water temperature change correlation for 2 variables	99
A.14	Cooling water temperature change correlation for 3 variables	99
A.15	Heating temperature change correlation for 2 variables	100
A.16	Heating temperature change correlation for 3 variables	100
A.17	Heating temperature change correlation for 2 variables	101
A.18	Heating temperature change correlation for 3 variables	101
B.1	Data Acquisition System Wiring	103
B.2	Programmable Logic Controller Wiring	104
B.3	Programmable Logic Controller Initialization Stage	106
B.4	Programmable Logic Controller Control Stage	107
D.1	Conditioner assembly diagrams (U.S. patent 6745826)	117

Chapter 1

Introduction

In this chapter, the motivation for the project will be outlined. The method of meeting building ventilation air requirements and associated cooling loads will be discussed. The subject of this study, the solar thermal liquid desiccant dedicated outdoor air system, is introduced as an alternative to address the disadvantages associated with conventional ventilation air handling. The scope of the study is also presented.

1.1 Building Ventilation Air Requirements

1.1.1 Indoor Air Quality and Ventilation Air Requirements

Ventilation of buildings has a substantial influence on building energy consumption, the health of occupants, and the productivity and satisfaction of occupants. Ventilation of buildings is accomplished by circulating fresh outdoor air (OA) through the building and exhausting indoor air that has accumulated pollutants that negatively affect indoor air quality (IAQ). The minimum acceptable ventilation rate in Canada

follows the standards defined by the American Society of Heating, Refrigerating and Air-Conditioning Engineers (ASHRAE). Standard 62.1 gives the default minimum acceptable ventilation rate in units of $\frac{L/s}{person}$. This rate can vary from 17 $\frac{L/s}{person}$ for office spaces and classrooms to 26 $\frac{L/s}{person}$ for spaces such as health clubs and beauty salons [1]. There is also evidence that increasing the ventilation rate, and therefore the indoor air quality of the space, can have significant benefits in areas such as office productivity and student performance in the classroom [2].

1.1.2 Ventilation Air Cooling Loads

The cooling load of a building to be met by the air handling system can be divided into two types; the sensible cooling load, and the latent cooling load. The sensible cooling load, which is the requirement to reduce the dry bulb air temperature within the space, results from thermal sources such as;

- Incident sunlight through windows, skylights, or glass doors
- Exterior walls
- Air infiltration through cracks in the building, doors, and windows
- People in the building
- Equipment and appliances
- Lights
- Ventilation air

The latent cooling load, which is the requirement to reduce the humidity level of the space, results from;

- People
- Equipment and appliances
- Air infiltration through cracks in the building, doors, and windows
- Ventilation air

Typically, the largest sensible and latent cooling loads arise from the outdoor air requirement for the space. A building with a 20% outdoor air requirement must condition this outdoor air to meet the building comfort set point. As defined by ASHRAE, the comfort set-point is 24°C dry-bulb, and 50% relative humidity. This corresponds to a humidity ratio of 9.338 g_v/kg_a . The Ventilation Load Index (VLI) can be used to indicate the latent, sensible, and total ventilation cooling loads for a given location. The ventilation load index calculates the latent and sensible energy differences between the outdoor air and the comfort set-point of the room. Using the procedure of Harriman, Plager, and Kosar, a ventilation load index in SI units is defined using equations 1.1 and 1.2 below [3].

$$VLI_L = \int \frac{(W_{OA} - W_{set}) h_{fg}(T) \rho_a(T)}{W_{OA} + 1} dt \quad (1.1)$$

$$VLI_S = \int (T_{OA} - T_{set}) C p_a(T) \rho_a(T) dt \quad (1.2)$$

The latent ventilation cooling load, VLI_L , is proportional to the excess vapor in the air, $W_{OA} - W_{set}$, multiplied by the latent heat of condensation at that temperature, $h_{fg}(T)$. The sensible cooling requirement is equal to the dry-bulb temperature difference $T_{OA} - T_{set}$, multiplied by the specific heat capacity of the air, $C p_a(T)$.

These energy differences are multiplied by a unit flow rate and integrated over a year, with each hour of latent and sensible energy above the set point energy contributing to the total. This integral can be expressed in units of energy per unit flow rate of air; $\frac{kWh}{m^3/hr}$. The ventilation load index for several Canadian cities is presented in Fig. 1.1.

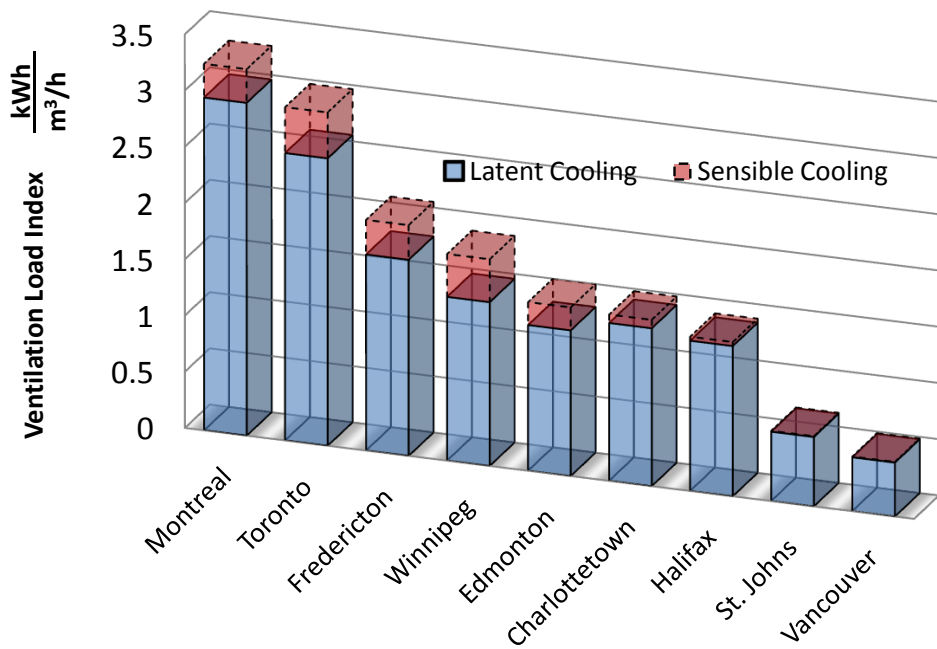


Figure 1.1: Ventilation Load Index for Canadian Cities

In the city of Toronto, 86% of the total ventilation load index is latent, while in Vancouver, humidity accounts for 99% of the cooling load. Improper handling of the building humidity load can lead to poor IAQ, occupant dissatisfaction, and microbial growth contamination.

1.2 Air Handling Systems

1.2.1 Conventional Air Handling Equipment

Conventional air conditioning equipment can lead to over-sizing of equipment and parasitic energy requirements. Many installed air handling systems simply fail to meet the latent cooling load of a building for humid days. Conventional AC equipment must cool the air passing the cooling coils below the dewpoint to remove moisture by condensation. Because the air dewpoint is below the comfort set-point, the air must then be reheated to comfort conditions. This is known as ‘parasitic heating’. Fig. 1.2 is representative of a conventional building HVAC strategy, with an electrically driven compressor and electrical reheat.

The effectiveness of AC equipment in dehumidifying the air is characterized by how closely the sensible heat ratio capacity of the air handling system matches the building SHR (Sensible Heat Ratio). The SHR is defined as the ratio of sensible cooling load to the total cooling load. A low SHR leads to a higher percentage of latent cooling for a building, requiring the AC equipment to provide more dehumidification relative to sensible cooling. Changing building standards have contributed to a decrease in the Sensible Heat Ratio over the past 30 years. The two standards governing building energy and ventilation in Canada and the U.S. are;

- ASHRAE Standard 90 - Energy standards for buildings [4]
- ASHRAE Standard 62 - Ventilation for Acceptable Indoor Air Quality [1]

These standards were created in the early 1970’s to govern ventilation and energy aspects of building design. Since 1970, they have undergone many revisions. With the

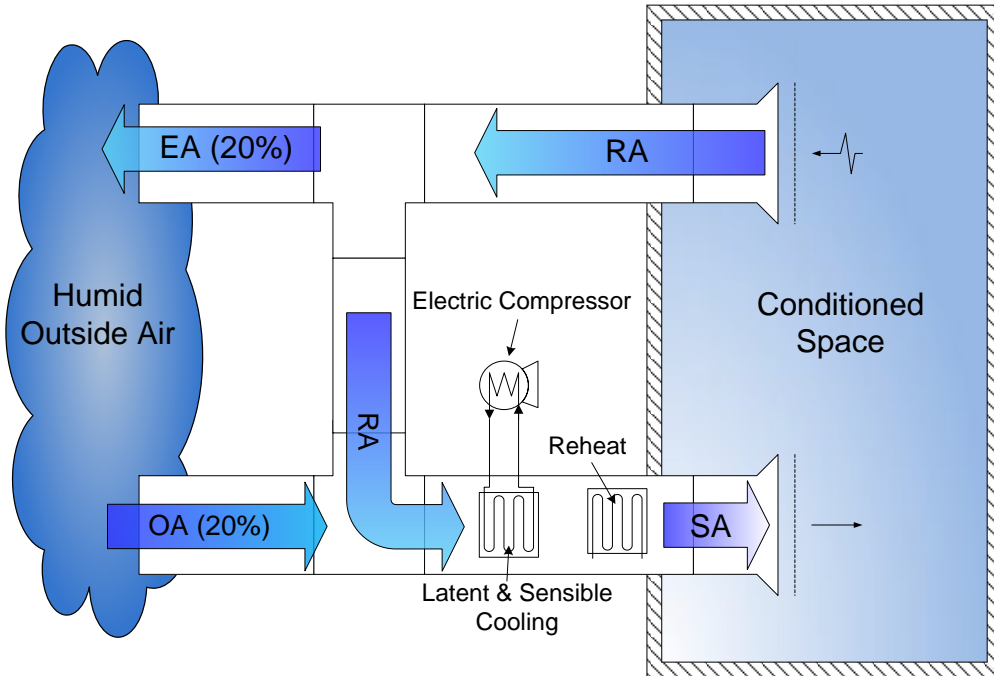


Figure 1.2: Conventional HVAC Strategy

advances in building insulation and increased focus on energy efficiency, ASHRAE Standard 90, governing the efficiency and usage of building energy systems, now demands R-values approximately 30% higher than in the 1970's. A tighter building envelope leads to a lower SHR for buildings. When the SHR of the AC system does not match the SHR of the building, the comfort set-point cannot be effectively achieved [5]. The HVAC industry is motivated to improve the latent cooling capacity of building energy systems to effectively and efficiently remove the humidity in ventilation air.

1.2.2 Energy Efficiency

Air conditioning, with its poor handling of humidity, places a strain on electricity generation capacity. Ontario has shifted from a winter to a summer peaking electricity load due to an increased demand for air conditioned residential and commercial space. Inefficient handling of ventilation air humidity contributes to this summer peaking demand. The Independent Electricity System Operator (IESO) is responsible for the day to day operation of Ontario's electric system. The president and CEO of the IESO remarked that for Ontario, peak summer hours "occurred during a hot summer day when air conditioning was no doubt running flat out" and that "[p]rice reflected the high demand on those days with the average price ... more than three times the annual average" [6]. Figure 1.3 is a plot of the 2007 electricity consumption in the province of Ontario showing the summer peak demand, as recorded by the IESO.

Electricity demand in Ontario was above 25,000 MWh on 6 days during the summer of 2007, with an average price for these days 30% higher than the annual average [7]. Average solar irradiation on the horizontal plane for the city of Toronto is plotted in Fig. 1.3 for reference. Summer peaking electricity, a consequence of air conditioning demand, is expensive and has increased environmental impacts when fossil fuel peak generators must be run to meet peak demand.

1.2.3 Dedicated Outdoor Air Systems

An effective approach to the problem of latent cooling demand is to decouple the latent and sensible cooling loads. This is accomplished by employing a dedicated outdoor air system (DOAS). A DOAS is designed to precondition the outside ventilation air required for the building by removing the moisture. The remaining sensible load is

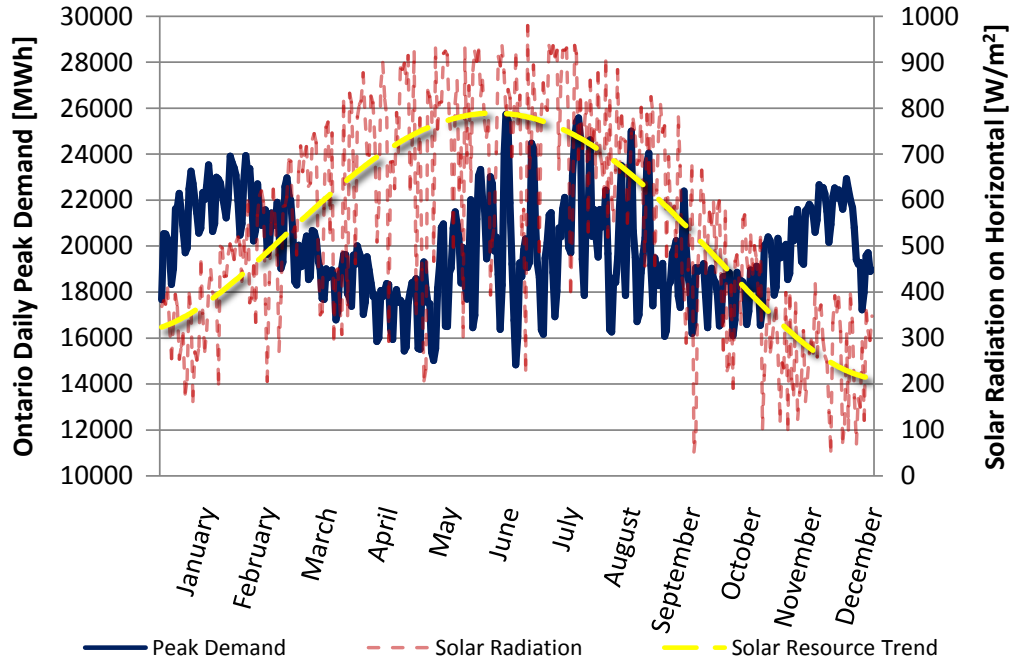


Figure 1.3: Ontario 2007 electricity demand and solar irradiation on horizontal for Toronto, Ontario

handled by a conventional AC system in the return air stream, avoiding overcooling and reheat. The conventional electric chiller is put in parallel with the dry outside air stream [8]. This decoupling allows each sub-system to be efficiently designed for the type of cooling load (latent or sensible). Not only does this improve energy efficiency of the overall system, but the system is now able to properly handle a wider range of cooling loads. Figure 1.4 shows a DOAS configuration, with RA, OA, EA, and SA referring respectively to the Return, Outside, Exhaust, and Supply Air streams.

Common dedicated outdoor air systems are based on various technologies such as electric chillers designed for dehumidification or enthalpy wheel recovery units. An enthalpy wheel is a rotary heat exchanger embedded with a solid desiccant material

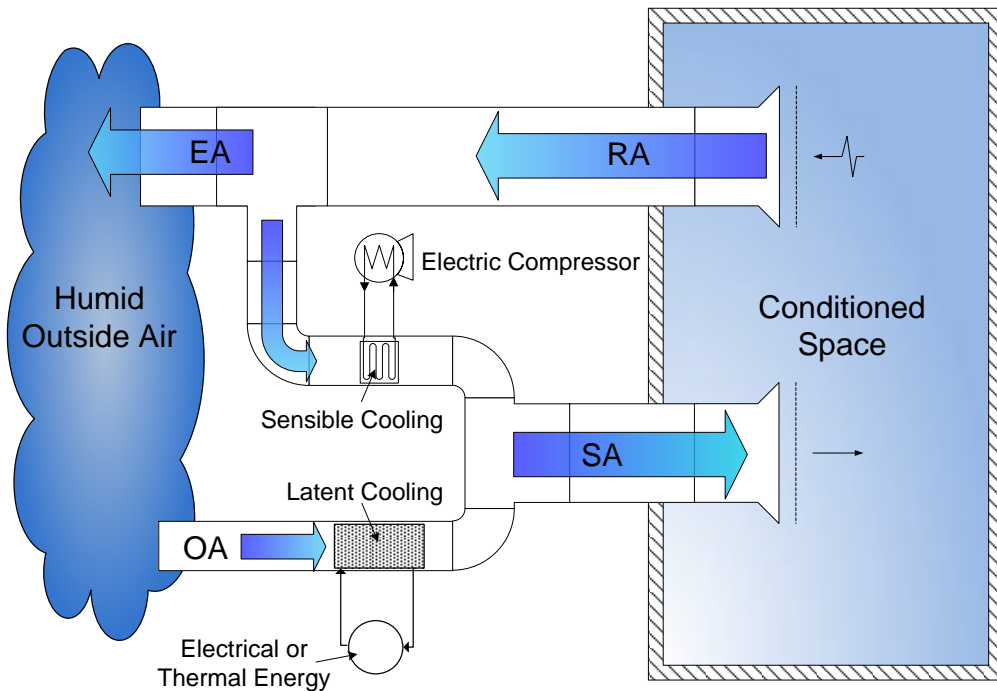


Figure 1.4: Dedicated Outdoor Air System HVAC configuration

which adsorbs moisture from the OA stream and is regenerated (dried) in the RA stream. One promising technology, the subject of this investigation, is based on liquid desiccant dehumidification systems.

Figure 1.5 Displays the process lines of three air handling systems. B-A-C-D represents a traditional vapor compression system. The air is sensibly cooled until the dewpoint, A, where further cooling results in water condensing on the coils. The air must then be reheated, from C to D. Process B-F-E-D represents a solid desiccant or liquid desiccant system with no internal cooling. As water vapor is adsorbed or absorbed by the desiccant, the latent heat is released, resulting in an increased dry bulb temperature. The dry air is then brought to the set-point through a combination

of sensible cooling and rehumidification. Process B-E-D represents an internally cooled desiccant system. Cooling water is used to absorb the latent heat of absorption or adsorption. This results in less sensible cooling required to reach the set-point, and can increase the dehumidification ability of the desiccant by cooling it as it becomes diluted and heated.

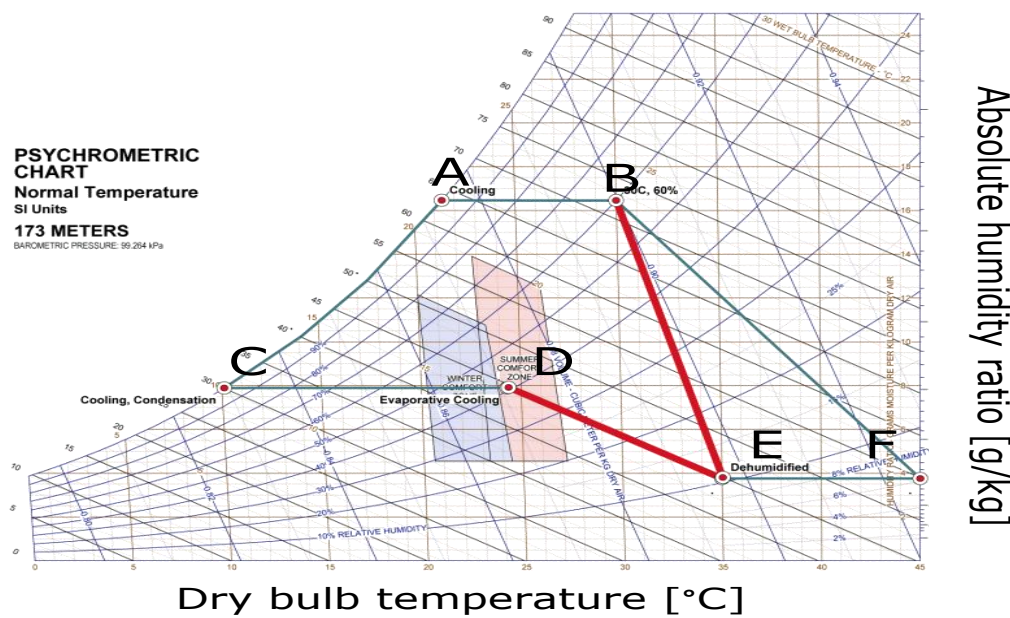


Figure 1.5: Psychrometric chart showing three different ventilation air handling processes

1.3 Solar Thermal Low Flow Liquid Desiccant Air Conditioning

1.3.1 Solar Cooling Technologies

Referring to Fig. 1.3, it can be seen that the peak summer electricity demand for Ontario is in phase with the solar energy resource. Thermal energy is suitable for air conditioning, attaining a higher exergetic efficiency when compared to electrically driven chillers [9]. Solar thermal energy conversion, the conversion of solar irradiance into fluid thermal energy, is efficient and inexpensive when compared to conversion of solar irradiance into electricity with photovoltaics. Solar water heating is achieved using technologies such as flat plate absorbers for low temperature, or concentrating and evacuated tube collectors for higher temperature operation. Solar thermal collectors are widely used for domestic hot water heating. Solar thermal air conditioning is a particularly attractive application as a method of utilizing the solar resource at its peak to offset peak electricity demands. The annual utilization of a solar thermal array is therefore increased, providing air or water heating in the winter, and air conditioning during the summer in what is known as a solar combi-system arrangement.

Solar driven air conditioning can be categorized according to Fig. 1.6 [10]. Liquid desiccant dehumidification, an open cycle system, has advantages over closed cycle absorption technology for solar applications. Open cycle systems require driving temperatures achievable by evacuated tube or flat plate absorbers. An absorption chiller requires temperatures in the 90°C to 220°C range. Liquid desiccant systems can be operated in the 50°C to 90°C temperature range. A closed cycle absorption chiller provides mainly sensible cooling, whereas an open cycle system is designed to

dehumidify the air stream.

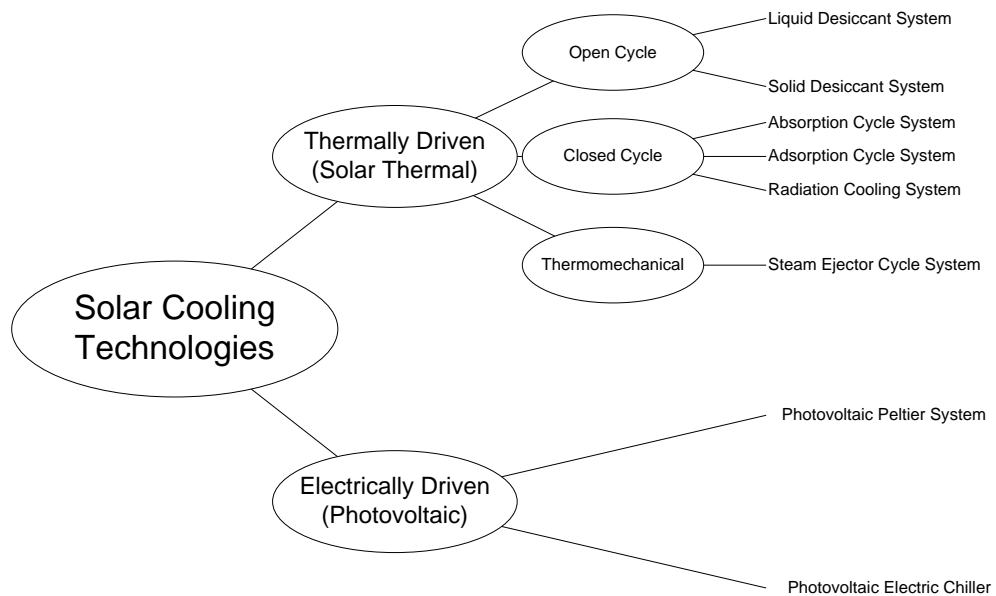


Figure 1.6: Solar Cooling Overview

1.3.2 Liquid Desiccant Systems

Liquid desiccant dehumidification can be further divided into packed tower spray systems and falling film systems. A packed tower arrangement sprays liquid desiccant into the process air stream in counterflow, through a random packing material. Drawbacks to the packed tower arrangement include higher system air pressure drop and desiccant carryover, which leads to corrosion of duct work. A falling film liquid desiccant dehumidification system is designed such that the liquid salt solution is brought into contact with the air stream in a flat plate arrangement. This arrangement

can be used to decrease the system pressure drop and decrease the flow rate of desiccant, eliminating desiccant carryover. A falling film can also be internally cooled or heated to offset the latent heat of condensation or evaporation of water.

1.4 Literature Review

The concept of desiccant air conditioning was initially explored relatively early by Löf in 1955 [11]. Interest was renewed during the early 1990's as energy prices increased along with increasing demand for air conditioning. The body of work in the field of solar driven liquid desiccant dehumidification continues to grow in the areas of solar integration and component optimization. Many different system configurations are possible, and many standards of efficiency and merit exist.

1.4.1 Review Papers

Öberg and Goswami [12] reviewed common system configurations in the field of desiccant dehumidification using calcium chloride, lithium chloride, lithium bromide, and triethylene glycol as solutes. A table of thermal coefficients of performance from research literature is given. It was concluded that COP and efficiency can be defined in a variety of ways, and that basing a comparison on a single figure of merit can lead to errors in evaluating different schemes of air conditioning. Daou, Wang, and Xia [13] reviewed the benefit of desiccant air conditioning for humid climates. It was concluded that energy savings, humidity control, and indoor air quality brought about by contaminant removal are all improved. Mei and Dai [14] discussed the importance of the regenerator required to concentrate the weakened desiccant in their review

paper. Different configurations of solar thermal regenerators are presented. Hwang, Radermacher, Al Alili, and Kubo [10] reviewed the general field of solar cooling, citing an average open cycle liquid desiccant thermal COP as 0.74, higher than that of 0.51 for solid desiccant open cycles. Single effect absorption chillers were quoted as having a COP of 0.50 to 0.73, with typical driving temperatures above 97°C. This is contrasted with a typical quoted liquid desiccant driving temperature of 67°C.

1.4.2 Liquid Desiccant Solutions

Al-Farayedhi, Gandhidasan, Antar, and Abdul Gaffar [15] listed several important considerations in choosing or designing the optimal liquid desiccant solution for a dehumidification application;

- High vapor pressure of water in solution
- Low vapor pressure of solute
- Performance of solution steady over large concentration range
- Non-corrosive and chemically stable
- Low viscosity
- High solubility
- Low regeneration temperature
- Non-toxic, harmless
- Low cost

Lithium chloride ($LiCl$), Calcium Chloride ($CaCl_2$), Lithium Bromide ($LiBr$), and tri-ethylene glycol (TEG) are common liquid desiccant materials meeting the above performance characteristics to varying degrees. $LiCl$ and $CaCl_2$ dominate the most recent research efforts into liquid desiccant dehumidification systems. Wimby and Berntsson [16] investigated aqueous solutions of various desiccants, including $LiCl$ and $CaCl_2$, producing experimental data of density as a function of temperature and mass fraction. This data is of critical importance when experimenting with liquid desiccant materials, providing concentration as a function of density, which is relatively easy to measure in the laboratory. A mixture of $LiCl$ and $CaCl_2$ was the subject of study by Ertas, Anderson, and Kiris [17]. $LiCl$ has excellent regeneration performance and stability but high cost, while $CaCl_2$ has lower performance but low cost. A mixture of the two at various ratios was analyzed to produce functions of vapor pressure for various temperatures. In an important study of aqueous $LiCl$ and $CaCl_2$, Conde [18] gathered data from 1850 and onwards and fit empirical curves to selected data. Functions of density, heat capacity, enthalpy of dilution, vapor pressure, solubility, and others, were presented. These correlations were used extensively in the present study. The concept of storage was explicitly investigated by Peng, Zhang, and Yin [19], with the conclusion that liquid desiccant regeneration equipment performance is improved with desiccant storage.

1.4.3 Low Flow Liquid Desiccant Systems

Falling film liquid desiccant dehumidification systems can be internally heated or cooled while conditioning the air or regenerating the desiccant. This has significant potential performance benefits. A 2-dimensional numerical analysis of an internally

cooled or heated flat plate liquid desiccant system was conducted by Mesquita and Harrison [20]. A further experimental analysis of a single channel low flow flat plate liquid desiccant system was conducted by Mesquita [21]. The system was operated under both isothermal and non-isothermal conditions. It was concluded that water temperature and mass flow rate of desiccant have a strong effect on the performance of the flat plate dehumidifier and regenerator. A pre-commercial prototype low flow liquid desiccant system was built and tested by Lowenstein, Slayzak, and Kozubal [22]. The benefit of zero desiccant process air carryover was emphasized, and a solar thermal driving source was investigated. An important benefit of a liquid desiccant system coupled to a solar thermal array, the lossless chemical storage of liquid desiccant, was investigated by Miller and Lowenstein [23]. A preliminary cost benefit analysis of a 6000 CFM unit charged with $CaCl_2$ was conducted, showing a simple payback of 10 years with a 30% investment tax credit. The system described by Lowenstein, Slayzak, and Kozubal [22] is the subject of the current investigation.

1.5 Principle Advantages

With increasing importance placed on climate change, energy conservation, energy security, and air quality, the low flow liquid desiccant dedicated outdoor air system driven by solar thermal energy is an attractive technology. It has significant potential advantages over many alternative building energy schemes. The important advantages of the solar thermal low flow liquid desiccant concept are summarized;

- Sustainable clean solar thermal energy source

- Solar combi-system arrangements possible, increasing solar thermal array usability
- No global warming potential associated with common refrigerants
- Low system pressure drop
- Zero carryover of corrosive desiccant material
- Air cleaning and filtering
- Lossless storage of solar cooling power in liquid salt solution

The performance of the solar driven liquid desiccant dehumidification concept will be investigated in the present study. Low temperature regeneration associated with solar thermal collectors will be experimentally verified. Low temperature performance data will be used to validate simulation of a complete solar thermal air conditioning system in future work.

1.6 Objectives and scope of study

The main objective of this study is to characterize the performance of a liquid desiccant air handling system for the solar thermal temperature range of 50 to 90°C. The scope of the study is presented in Fig. 1.7. Outcomes of this study will support further investigation of the solar cooling concept and include;

- Installed and commissioned liquid desiccant system including boiler and cooling tower
- Data acquisition system and software

- Control system and software
- Performance data for the temperature range of 50 to 90°C
- Performance data for machine driven by a simulated solar thermal heat profile
- Preliminary mathematical modeling of performance data to support future simulation of solar thermal system
- Procedures for data collection and analysis
- Recommendations for further research and system optimization

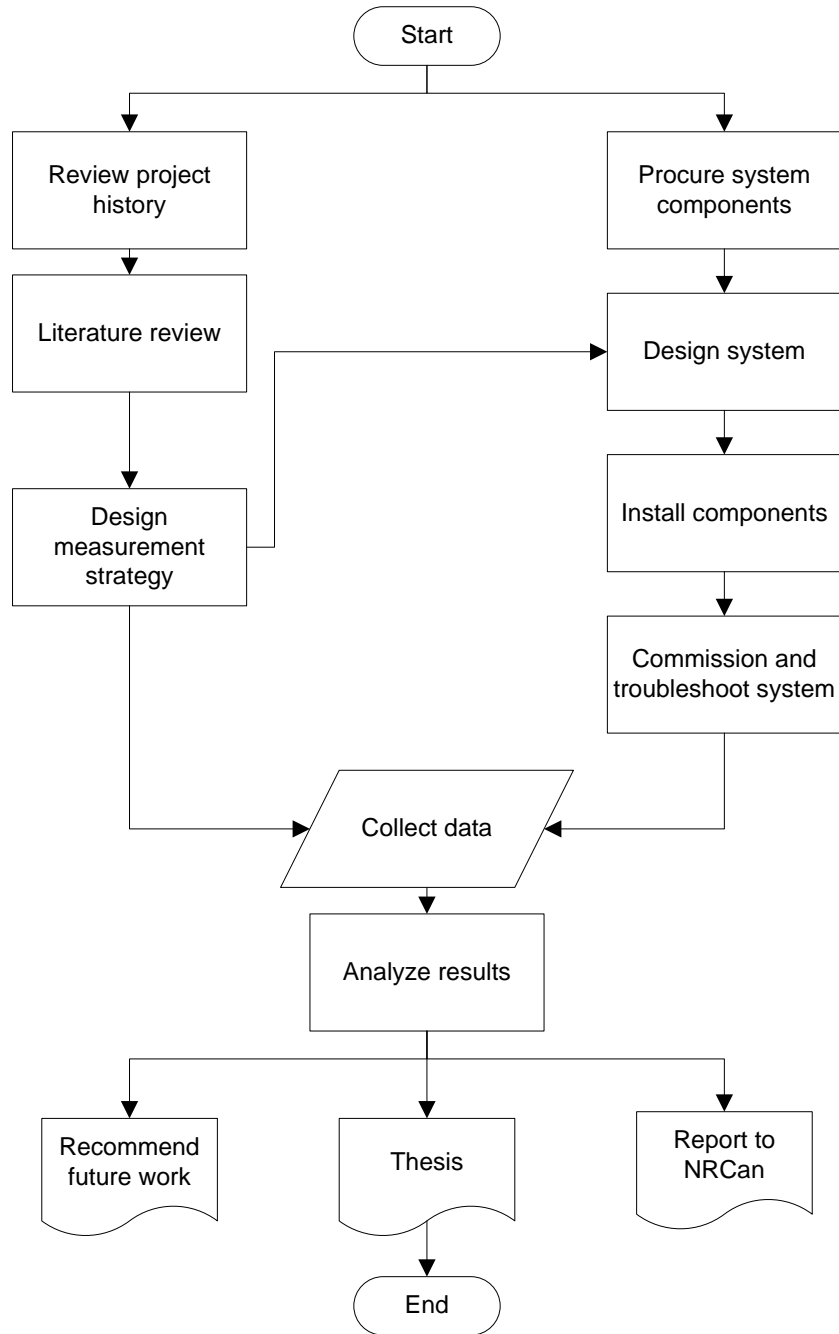


Figure 1.7: Research flow chart and scope

Chapter 2

Theory

In this chapter, the definition of efficiency for a solar thermal collector will be developed. The fundamental theory of liquid desiccant dehumidification will then be presented with the thermodynamic properties of a lithium chloride desiccant solution. The first law of thermodynamics will be applied to the conditioner and regenerator components. Various system performance figures of the air handling system under investigation will be presented.

2.1 Solar Thermal Collector Performance

As defined in the procedure of Duffie and Beckman [24], the efficiency of a solar thermal collector is the ratio of useable solar thermal energy per unit area, Q_u , to the total incident radiant energy on the collector, G_T , shown in equation 2.1.

$$\eta_{\text{collector}} = \frac{Q_u}{A_c G_T} \quad (2.1)$$

The usable solar thermal energy is given by equation 2.2.

$$Q_u = A_c F_R [S - U_L (T_i - T_a)] \quad (2.2)$$

U_L is the total heat loss coefficient of the collector. F_R is the heat removal factor, equivalent to the effectiveness of a conventional heat exchanger, and is given by equation 2.3.

$$F_R = \frac{\dot{m} C_p (T_{fo} - T_{fi})}{A_c [S - U_L (T_{fi} - T_a)]} \quad (2.3)$$

S is the total absorbed radiation, equation 2.4.

$$\begin{aligned} S &= Beam + Diffuse + Ground\ Reflected\ Radiation \\ &= I_b R_b K_{\tau\alpha,b} (\tau\alpha)_b + I_d K_{\tau\alpha,d} (\tau\alpha)_d \left(\frac{1 + \cos\beta}{2} \right) \\ &\quad + I \rho_g K_{\tau\alpha,g} (\tau\alpha)_n \left(\frac{1 + \cos\beta}{2} \right) \end{aligned} \quad (2.4)$$

with I the incident direct, diffuse, or ground reflected radiation, K the incident angle modifier, and $(\tau\alpha)$ the absorption-transmission product of the collector. The incident angle modifier accounts for the variation in absorbed radiation with angle of incidence of solar radiation. These equations and properties are developed and explained fully in Duffie and Beckman [24].

The Solar Rating and Certification Corporation (SRCC) provides standardized testing of solar thermal collectors. Efficiency curves based on gross collector area are presented in the form of equation 2.5.

$$\eta_{collector} = a_1 + a_2 \frac{(T_i - T_a)}{G_T} + a_3 \frac{(T_i - T_a)^2}{G_T} \quad (2.5)$$

with the coefficients a_i provided. The incident angle modifier is also given as a second order empirical curve fit, equation 2.6.

$$K_{\alpha\tau} = 1 + a_1 \left(\frac{1}{\cos \theta} - 1 \right) + a_2 \left(\frac{1}{\cos \theta} - 1 \right)^2 \quad (2.6)$$

This equation is suitable for flat plate absorbers, while vacuum tube collectors require a biaxial incident angle modifier for a complete analysis. The standardized curves of 2.5 and 2.6 can be used in simulating the performance of a rated solar thermal collector in varying ambient conditions.

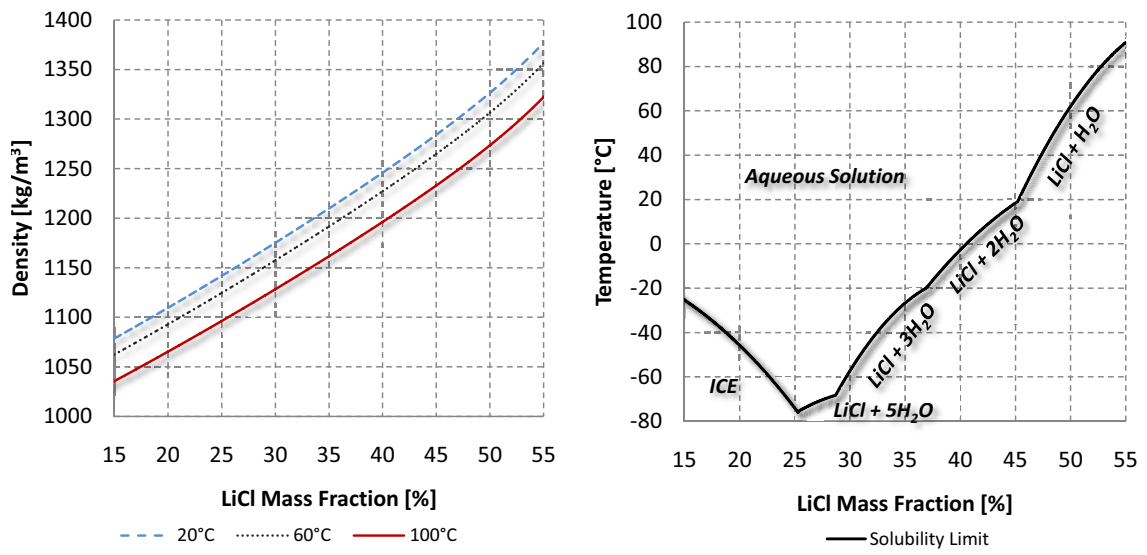
2.2 Liquid Desiccants for Dehumidification

Many types of liquid desiccants suitable for process air dehumidification exist. In this study, only $LiCl$ will be investigated. $CaCl_2$, either pure or mixed with $LiCl$, could also be suitable for solar thermal applications, having a lower unit cost but decreased dehumidification performance. A cost benefit analysis between these two common desiccants is suggested as future work for the solar thermal liquid desiccant dehumidification concept.

2.2.1 Desiccant Concentration and Solubility

An aqueous solution of $LiCl$ consists of disassociated salt ions (the solute) in water (the solvent). To determine the concentration of a sample of $LiCl$, an empirical correlation between density and concentration is used. This correlation is slightly affected by temperature, as shown in Fig. 2.1a. The solubility limit of the salt is another important parameter in liquid desiccant dehumidification systems. Solid desiccant

build-up can constrict and block flow through pipes, causing serious maintenance problems in a standalone air handling system. The solubility limit for $LiCl$ is presented in Fig. 2.1b. Solubility is a function of both temperature and concentration. At the solubility boundary, $LiCl$ forms water ice and various solid hydrates. A practical upper concentration limit for avoiding problems using $LiCl$ in liquid desiccant dehumidification is 43%.



(a) Density and concentration correlation for $LiCl$ (b) Solubility limits of $LiCl$ ice and hydrates at various temperatures

Figure 2.1: Concentration properties of $LiCl$

2.2.2 Vapor pressure

Vapor pressure is the pressure of a vapor in equilibrium with its non-vapor phase. Liquids have a tendency to evaporate to a gaseous form, and gases have a tendency to condense back into a liquid. Depending on temperature, this process will reach a dynamic equilibrium. A sealed quantity of fluid with its gaseous phase will exert a

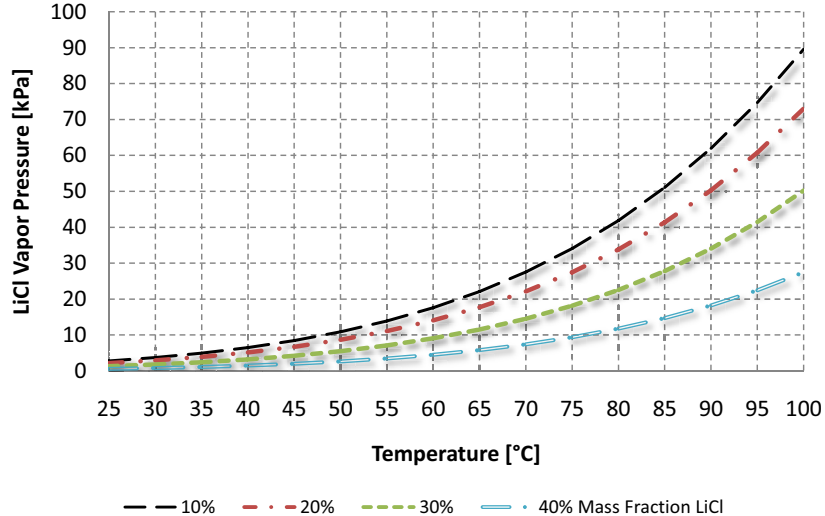


Figure 2.2: Vapor pressure p_{sol} , of aqueous $LiCl$

pressure on the surrounding container. For a desiccant solution, this pressure will vary with concentration as well as temperature. The absolute vapor pressures of water for four concentrations of $LiCl$ solution are plotted as a function of temperature using the empirical relation found in Conde [18]. The absolute vapor pressure of $LiCl$ increases rapidly with temperature and decreases with concentration. A higher solution vapor pressure will increase the tendency for water to be desorbed from the solution. This property is used in the regenerator, where the low concentration desiccant solution is heated and re-concentrated. In the conditioner, concentrated desiccant solution is cooled, absorbing water vapor from the air stream. The absorption rate is a function of the equilibrium vapor pressure between the solution and the vapor pressure of the moisture in the air stream. The variation in equilibrium vapor pressure with temperature is the driving principle in a low flow liquid desiccant dehumidification

cycle.

The relative vapor pressure of $LiCl$ solution is shown in Fig. 2.3 for the same 4 solution concentrations. The relative vapor pressure is defined as the ratio of the vapor pressure of the solution to the vapor pressure of pure water. This figure further illustrates that as the concentration of the desiccant in solution increases, the ability of the solution to absorb water vapor increases. To benefit from this effect, desiccant solution should be concentrated for the conditioner, and desiccant solution of lowest concentration should be supplied to the regenerator. An important consideration for the regenerator is the crystallization limit of the solution. Crystallization can lead to solid build up in piping, pumps, and plates, requiring time consuming maintenance. Careful control of solution temperature and concentration is required to avoid the crystallization line seen in Fig. 2.1b. An example of plate operation near this crystallization limit is also shown in Fig. 3.5b, section 3.2

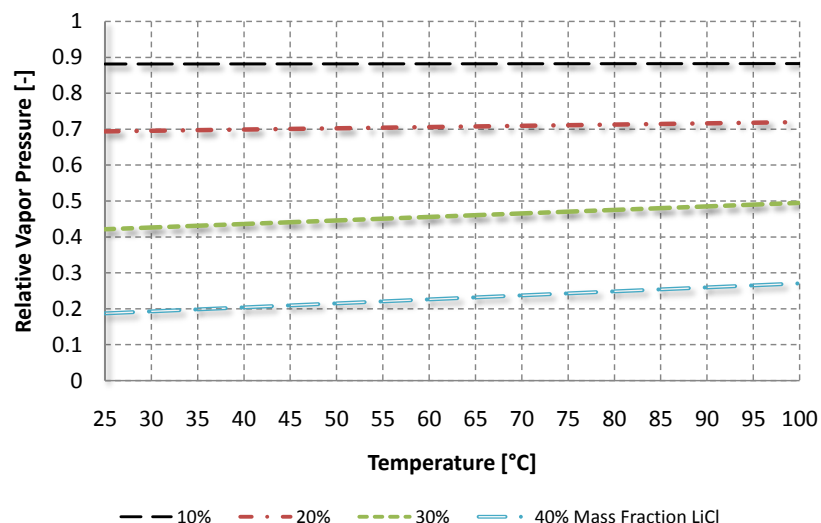
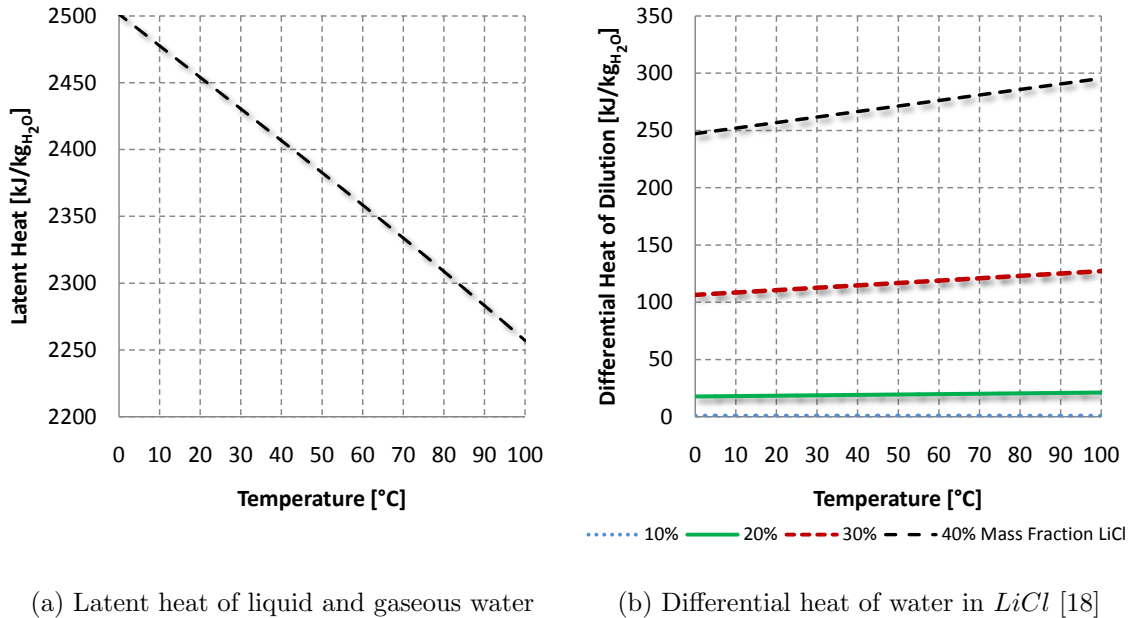


Figure 2.3: Relative vapor pressure variation of aqueous $LiCl$

2.2.3 Latent Enthalpy and Enthalpy of Solution

The latent enthalpy of condensation and vaporization of water is another important property when considering moisture transport between the solution and air streams. When gaseous water is absorbed into solution in the conditioner or desorbed from solution in the regenerator the latent enthalpy of water is released from or absorbed by the desiccant solution. The latent enthalpy of water, h_{fg} , is a function of temperature, plotted in Fig. 2.4a using data from a standard thermodynamics text [25]. However, the thermal energy required or liberated during absorption or desorption in a salt solution is greater than the latent heat of water alone. This difference constitutes the differential enthalpy of solution, plotted in Fig. 2.4b. The differential enthalpy of solution decreases as the mass fraction of $LiCl$ decreases, or as the solution approaches pure water.

In addition to providing cooling to the conditioner to lower the temperature of the desiccant and thereby decrease its vapor pressure according to Fig. 2.2, the cooling water also absorbs the latent enthalpy of condensation and enthalpy of solution. If the cooling water is not sufficiently cold, the enthalpy of the absorbed water will be converted to sensible heat in the desiccant stream, which consequently will increase the temperature of the air stream. This represents the conversion from latent heat into sensible heat. Similarly, the heating water in the regenerator supplies the latent enthalpy of vaporization and enthalpy of solution in order to maintain the high desiccant temperature required for effective desorption of water.

Figure 2.4: Latent heats of absorption and desorption in *LiCl*

2.3 Liquid Desiccant Component Energy Analysis

The conditioner and regenerator are similar in operation and design. Both are designed as heat and mass exchangers operating with three working fluids. The three working fluids are moist air, desiccant solution, and water. The operation of the absorber and regenerator are complimentary, and when working in conjunction, the two components complete a thermodynamic cycle for open cycle dehumidification by chemical absorption. The cycle is driven by the dilution and regeneration of a liquid desiccant solution. The desorption and absorption of water is controlled by varying the equilibrium vapor pressure of the desiccant solution with the air, according to Fig. 2.2. The two controlled desiccant properties are temperature and concentration. A detailed mass and energy balance on the absorber and regenerator components is required in understanding and evaluating the performance of the system.

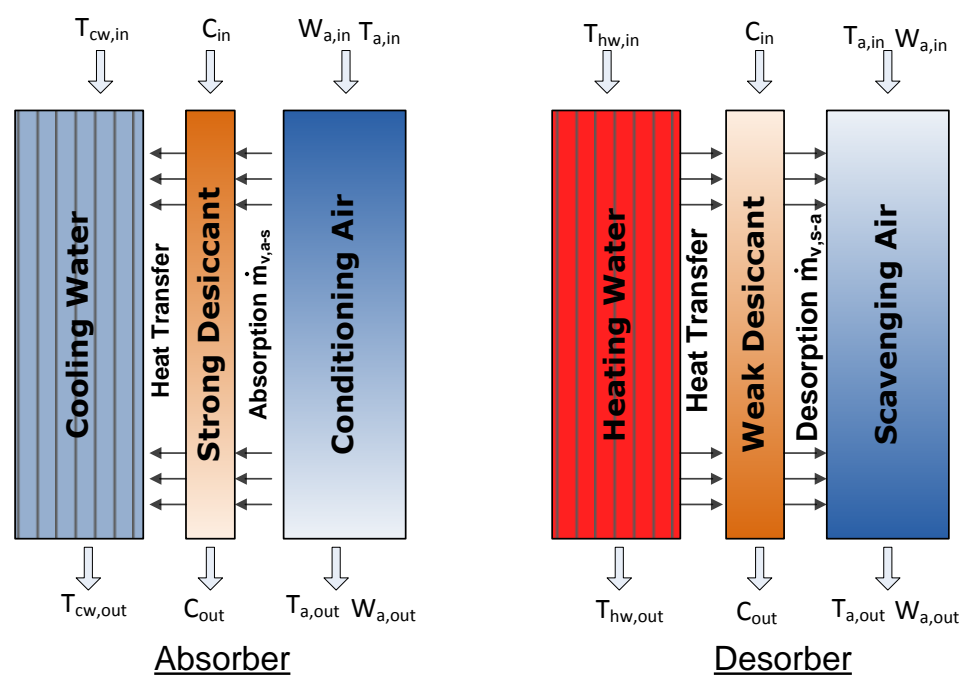


Figure 2.5: Process flow heat and mass transfer

Figure 2.5 compares the absorber and desorber operation, with the temperature of the internal water flow affecting the vapor pressure of the water in solution. A simplified diagram of the plate exchanger flow geometry is shown in Fig. 2.6. The cooling or heating water flows inside each plate, with the desiccant falling down the plates in a thin film. Air is blown across the desiccant flow between the plates. Plate geometry is repeated with a 2.5 mm air gap between plates. The cross section of each conditioner plate is 2.5 mm thick by 305 mm wide. Assembly drawings of the conditioner are shown in appendix D (U.S. patent 6,745,826) [26]. The conditioner plates are curved to add to the structural support of the assembly. The design for the regenerator is similar, consisting of a series of plates with the heating water inlet and outlet located at the same ends of the plates, allowing the plates to hang. This allows for unconstrained thermal expansion. The regenerator plates are 3 mm thick and 114 mm wide. Both the conditioner and regenerator plates have a thin (approximately 0.5 mm) wick covering their surfaces to ensure even wetting. These figures are used to derive the first law enthalpy balance for the conditioner/absorber and regenerator/desorber plate heat and mass exchangers.

2.3.1 Absorber

As shown in Fig. 2.7, the absorber, or conditioner, is operated such that water vapor from the process air stream is absorbed by the desiccant solution. The moist air stream can be divided into dry air and moisture components. The desiccant solution can also be divided into the solute and solvent. Cooling water is supplied to lower the equilibrium vapor pressure of the desiccant. The absorbed moisture releases the heat of condensation and dilution into the desiccant stream. This is the conversion of

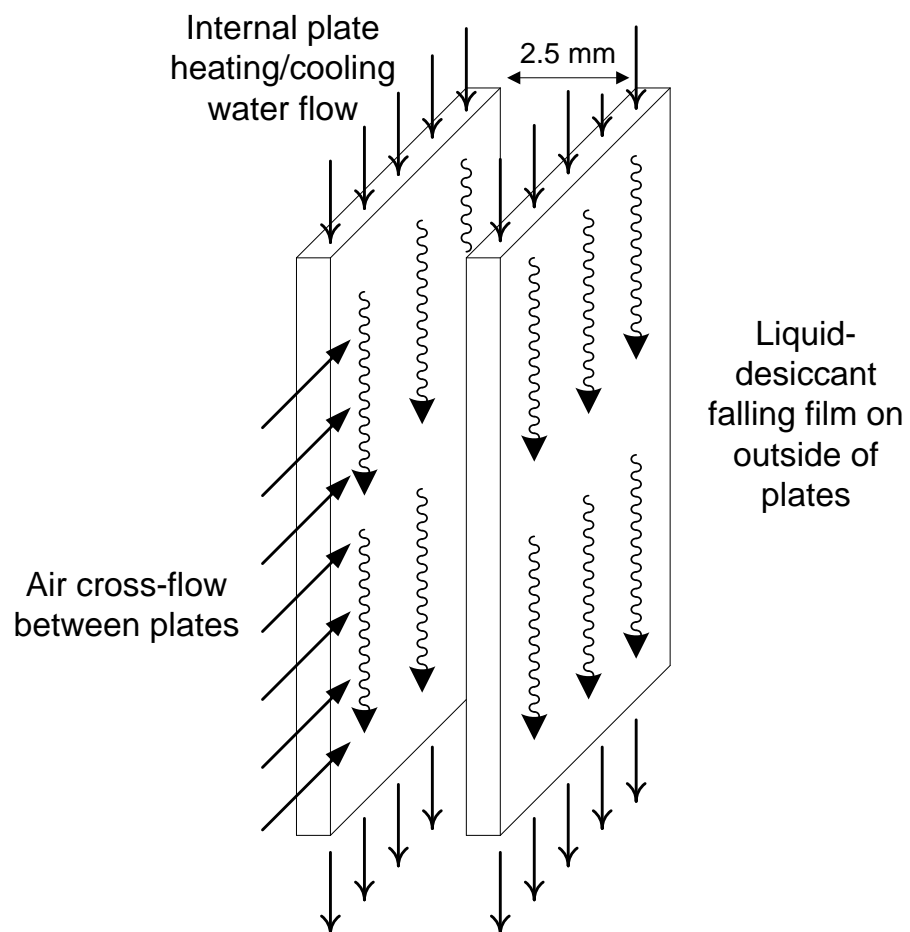


Figure 2.6: Conceptual diagram of plate exchanger concept

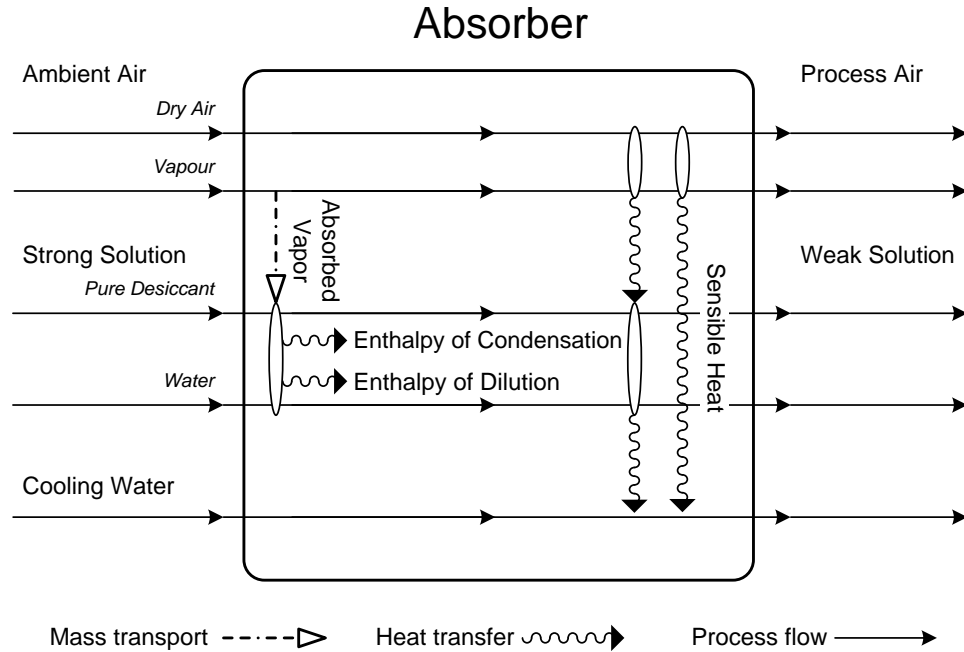


Figure 2.7: Absorber mass and energy flows

latent heat into sensible.

A mass and energy balance is defined for each process stream in the conditioner.

The conditioner is assumed adiabatic.

Process air stream

The mass flow rate of the dry air component, equation 2.7, is unaffected in the process.

$$\dot{m}_{a,in,c} = \dot{m}_{a,out,c} = \dot{m}_{a,c} \quad (2.7)$$

The air is dehumidified in the process air stream, with $\dot{m}_{v,a-s,c}$ being absorbed by the desiccant, resulting in a lower humidity ratio $W_{out,c}$, calculated using equation 2.8.

$$\dot{m}_{a,c}W_{in,c} = \dot{m}_{v,a-s,c} + \dot{m}_{a,c}W_{out,c} \quad (2.8)$$

The conditioner is operated such that the process air stream enthalpy is decreased. This enthalpy change is equal to the sum of the enthalpy absorbed by the desiccant solution from the absorption of water and the heat transferred between the air and desiccant, $\dot{q}_{a-s,c}$, and the air and cooling water streams, $\dot{q}_{a-cw,c}$. The enthalpy released into the desiccant stream is equal to the sum of the enthalpy of condensation and the enthalpy of dilution. The total enthalpy transfer due to the absorption of water is therefore given by $\dot{m}_{v,a-s,c} (h_{fg} + h_{dil})$. The enthalpies of condensation and dilution are both functions of temperature. The total energy balance on the process air stream is given by equation 2.9.

$$\dot{m}_{a,c}h_{a,in,c} = \dot{q}_{a-s,c} + \dot{q}_{a-cw,c} + \dot{m}_{v,a-s,c} (h_{fg} + h_{dil}) + \dot{m}_{a,c}h_{a,out,c} \quad (2.9)$$

The enthalpy change of the process air is due primarily to the amount of water absorbed. The dry bulb temperature of the air stream can be lower or higher than ambient, dependant on the temperatures of the air stream, the desiccant solution, and the cooling water.

Desiccant Solution

The solution concentrations at the inlet and outlet of conditioner are given by equations 2.10 and 2.11.

$$C_{in,c} = \frac{\dot{m}_{d,c}}{\dot{m}_{d,c} + \dot{m}_{w,in,c}} \quad (2.10)$$

$$C_{out,c} = \frac{\dot{m}_{d,c}}{\dot{m}_{d,c} + \dot{m}_{w,in,c} + \dot{m}_{v,a-s,c}} \quad (2.11)$$

The mass of the desiccant component of the solution is unchanged in the conditioner, equation 2.12.

$$\dot{m}_{d,in,c} = \dot{m}_{d,out,c} = \dot{m}_{d,c} \quad (2.12)$$

The solution will absorb $\dot{m}_{v,a-s,c}$ from the air stream, lowering the concentration of the solution. This mass flow rate change is represented by equation 2.13.

$$\dot{m}_{s,out,c} = \dot{m}_{d,c} + \dot{m}_{w,in,c} + \dot{m}_{v,a-s,c} \quad (2.13)$$

The energy balance of the desiccant solution is due to the thermal contact with the process air and cooling water, and the heat of condensation and dilution of the absorbed water vapor. The overall desiccant energy balance is given by equation 2.14.

$$h_{s,in,c}\dot{m}_{s,in,c} + \dot{q}_{a-s,c} + (h_{fg} + h_{dil})\dot{m}_{v,a-s,c} = h_{s,out,c}\dot{m}_{s,out,c} + \dot{q}_{s-cw,c} \quad (2.14)$$

Cooling water

The mass flow of cooling water is unchanged. The cooling water will absorb heat from the air stream and the solution stream (equation 2.15). This energy balance is given by equation 2.15.

$$h_{cw,in,c}\dot{m}_{cw,c} + \dot{q}_{s-cw,c} + \dot{q}_{a-cw,c} = h_{cw,out,c}\dot{m}_{cw,c} \quad (2.15)$$

2.3.2 Regenerator

The regenerator is similar to the absorber in operation, and is analyzed with a corresponding set of equations. The regenerator component, seen in Fig. 2.8, operates with heating water such that the temperature of the desiccant stream is elevated. This heated desiccant is brought into contact with an air stream. This air stream, called the scavenging air stream, carries away the desorbed water and is rejected back into the atmosphere.

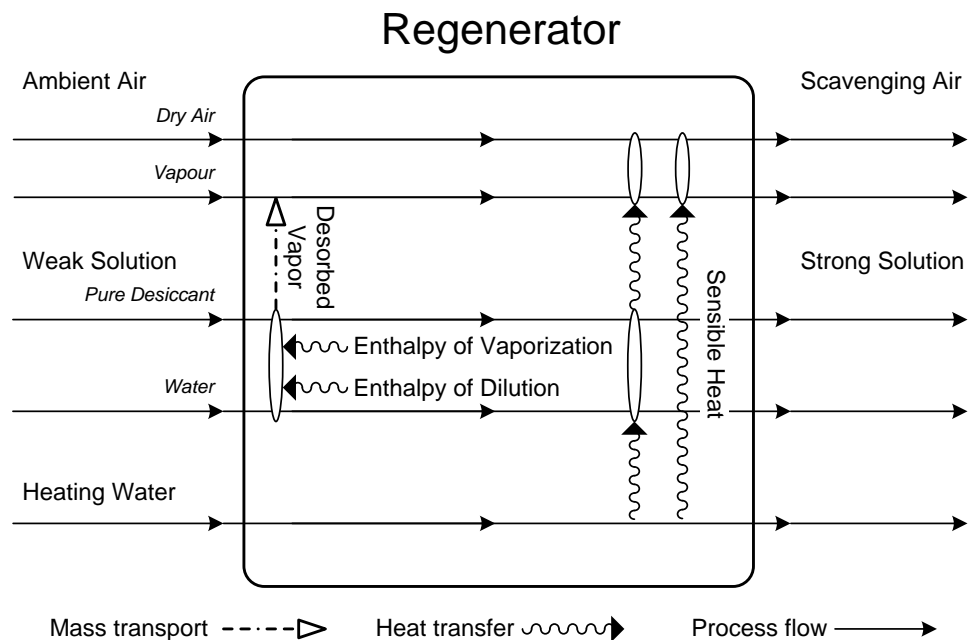


Figure 2.8: Regenerator mass and energy flows

Scavenging Air Stream

The enthalpy of the waste air stream, $\dot{m}_{a,r}h_{a,r}$, is increased according to equation 2.16.

$$\dot{m}_{a,r}h_{a,in,r} + \dot{q}_{s-a,r} + \dot{q}_{hw-a,r} + \dot{m}_{v,s-a,r}(h_{fg} + h_{dil}) = \dot{m}_{a,r}h_{a,out,r} \quad (2.16)$$

Desiccant Solution

The desiccant solution is in thermal contact with the air and heating water. The heating water supplies thermal energy, $\dot{q}_{hw-s,r}$, to the desiccant to offset that lost by the desorption of water, $\dot{m}_{v,s-a,r}(h_{fg} + h_{dil})$. The complete energy balance on the solution stream is presented in equation 2.17.

$$h_{s,in,r}\dot{m}_{s,in,r} + \dot{q}_{hw-s,r} = q_{s-a,r} + \dot{m}_{v,s-a,r}(h_{fg} + h_{dil}) + h_{s,out,r}\dot{m}_{s,out,r} \quad (2.17)$$

Heating Water

The energy balance on the heating water in the regenerator is given by equation 2.18 and accounts for the heat transfer between the heating water and the air and desiccant streams.

$$h_{hw,in,r}\dot{m}_{hw,r} = q_{hw-s,r} + q_{hw-a,r} + h_{hw,out,r}\dot{m}_{hw,r} \quad (2.18)$$

2.4 System Performance Parameters

The cooling power of the dehumidifier is used to size the unit to a specific application. The cooling power of the conditioner can be described by the the dry bulb temperature change of the air stream (sensible cooling) and the humidity change of the air stream

(latent cooling).

$$\dot{Q}_{latent} = \dot{m}_{v,a-s,c} h_{v,fg,c} \quad (2.19)$$

$$\dot{Q}_{sensible} = \dot{m}_{a,c} C p_{a,c} (T_{a,out,c} - T_{a,in,c}) \quad (2.20)$$

The amount of energy removed from the air stream by the conditioner, the total cooling, is the enthalpy change of the air stream, or the sum of the latent and sensible cooling.

$$\dot{Q}_{cooling} = \dot{m}_{a,c} (h_{in,c} - h_{out,c}) \quad (2.21)$$

$$= \dot{Q}_{latent} + \dot{Q}_{sensible} \quad (2.22)$$

The ratio of sensible to total cooling is called the sensible heat ratio with SHR = $\dot{Q}_{sensible}/\dot{Q}_{total}$. The amount of water absorbed or desorbed from a desiccant stream in contact with an air stream can be evaluated from the change in humidity ratio of the air stream (equation 2.23), or the change in concentration of the desiccant stream. Equation 2.24 shows these two methods, where C is the mass fraction of *LiCl* in solution.

$$\dot{m}_{v,a-s} = \dot{m}_a (W_{in} - W_{out}) \quad (2.23)$$

$$\dot{m}_{v,a-s} = \dot{m}_{sol} \left(\frac{C_{in}}{C_{out}} - 1 \right) \quad (2.24)$$

A heat exchanger is used to transfer heat from the desiccant stream leaving the regenerator to the stream entering. This also decreases the sensible heat load in the conditioner. The effectiveness of the heat exchanger is defined in equation 2.25. The mass flow rates are equal, and the specific heat of the desiccant solution on each side of the exchanger are assumed constant over this temperature range, giving equation 2.26.

$$\epsilon_{HX} = \frac{\dot{m}_{sol,in,r} C_{p,sol,in} (T_{sol,out,r} - T_{sol,out,HX})}{\dot{m}_{sol,out,r} C_{p,sol,out} (T_{sol,out,r} - T_{sol,in,HX})} \quad (2.25)$$

$$= \frac{T_{sol,out,r} - T_{sol,out,HX}}{T_{sol,out,r} - T_{sol,in,HX}} \quad (2.26)$$

The thermal coefficient of performance of the regenerator is defined as the ratio of the amount of water desorbed from the solution expressed in terms of enthalpy to the amount of heat absorbed in the regenerator. The enthalpy of the water desorbed is the theoretical minimum amount of energy required, and is equal to the sum of the enthalpy of vaporization and dilution at the solution temperature. Similarly, the cooling COP is the amount of cooling divided by the amount of heat required.

$$COP_{th,r} = \frac{\dot{m}_{v,s-a,r} h_{v,fg,r}}{\dot{m}_{hw,r} C_{p,hw} (T_{hw,in,r} - T_{hw,out,r})} \quad (2.27)$$

$$COP_{th,c} = \frac{\dot{Q}_{cooling}}{\dot{m}_{hw,r} C_{p,r} (T_{hw,in,r} - T_{hw,out,r})} \quad (2.28)$$

The electrical COP is simply defined as the amount of cooling produced per unit of electricity consumed.

$$COP_{elec,c} = \frac{\dot{Q}_{cooling}}{\dot{E}_{electricity}} \quad (2.29)$$

The above performance parameters represent instantaneous values. These equations can easily be integrated to yield average or total values for a specified time period.

Chapter 3

System Description

In this chapter, the apparatus is presented. Various system diagrams and pictures are provided to explain the installation of the dehumidifier and its support components. The control and data acquisition system is outlined.

3.1 Component Overview

The primary components of the dehumidification system under investigation include the heat rejection system, the air handling system, and the thermal source system. The process flows for these systems are presented in Fig. 3.1. The air handling system is a self contained pre-commercial prototype, and includes blowers, pumps, and data acquisition and control equipment. The air handling system is contained in the rounded box of Fig. 3.1. The main process loops, and their components are listed;

- Cooling water heat rejection loop [cooling tower, absorber]
- Solar thermal heat source loop [solar thermal array, desorber]

- Auxilliary heat loop [boiler, desorber]
- Process air loop [ambient, absorber]
- Scavenging air loop [ambient, desorber]
- Strong desiccant loop [sump, absorber]
- Weak desiccant loop [sump, heat exchanger, desorber]

Figure 3.1 indicates the positions of sensors within the overall apparatus. Sensors are placed such that an energy balance on the sub components can be performed, and to evaluate the performance of the system. An energy balance is calculated for the system components according to equations 2.7 to 2.18, using flow meters and inlet/outlet temperature probes.

Figure 3.2 is a photograph of the air handling apparatus and the cooling tower. Prominent features of the system are labelled.

Figure 3.3 is a schematic of the complete installed apparatus. All dimensions are in meters. The solar thermal array is not installed as part of this investigation. The apparatus is installed on the north west side of a university research building in Kingston, Ontario. Components were sited and oriented such that thermal interference between exhaust and inlet air streams would be minimized. Heating and cooling piping was $1\frac{1}{2}$ inch copper and PVC, respectively.

3.2 Air Handling System

A beta-prototype liquid desiccant dedicated outdoor air system was procured from a manufacturer. Figure 3.4 is a simplified graphic of the internal components of this

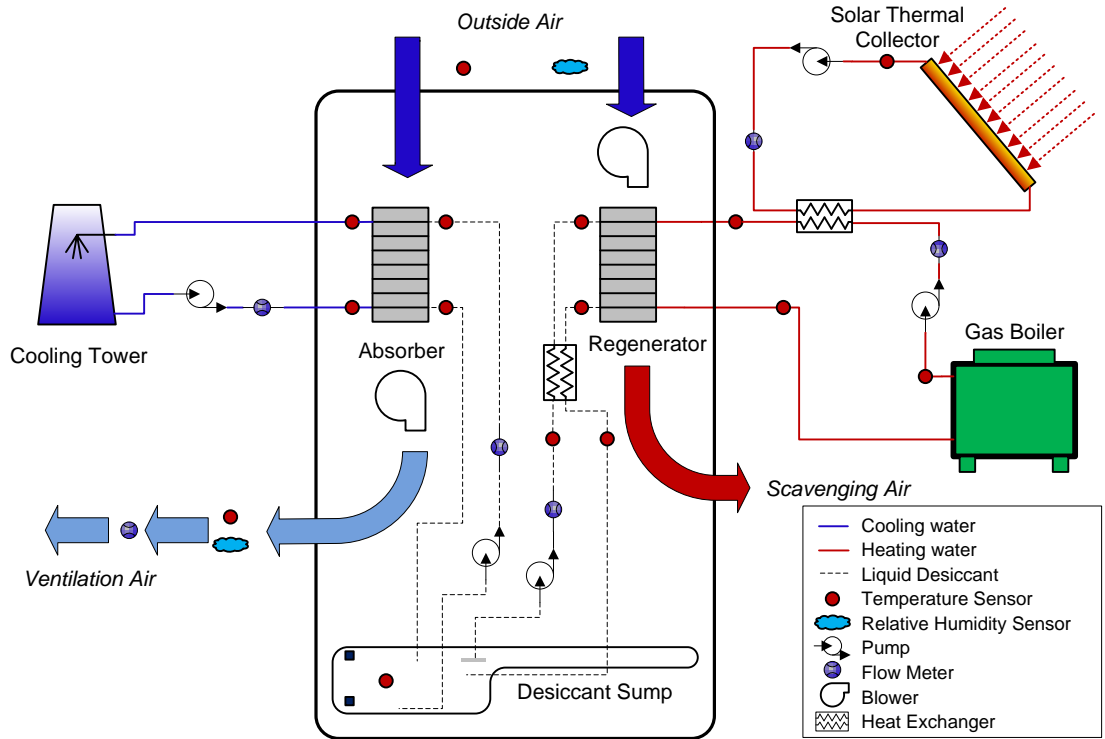


Figure 3.1: Overview of process flows

machine [22]. The conditioner is on the left side of Fig. 3.4, with strong desiccant from the sump being pumped to the top of the plate array. Cooling water is pumped through a loop internal to each plate. Process air is blown in a cross flow arrangement, and brought into contact with the strong desiccant. Weakened desiccant is pumped through the heat exchanger to be preheated, and flows down the regenerator plates. Heating water is pumped through the plates, and scavenging air is brought into contact with the weak desiccant, carrying away water vapor. The performance values for this machine used in experiment are presented in table 3.1.

Temperature was the primary variable under investigation in this experiment.

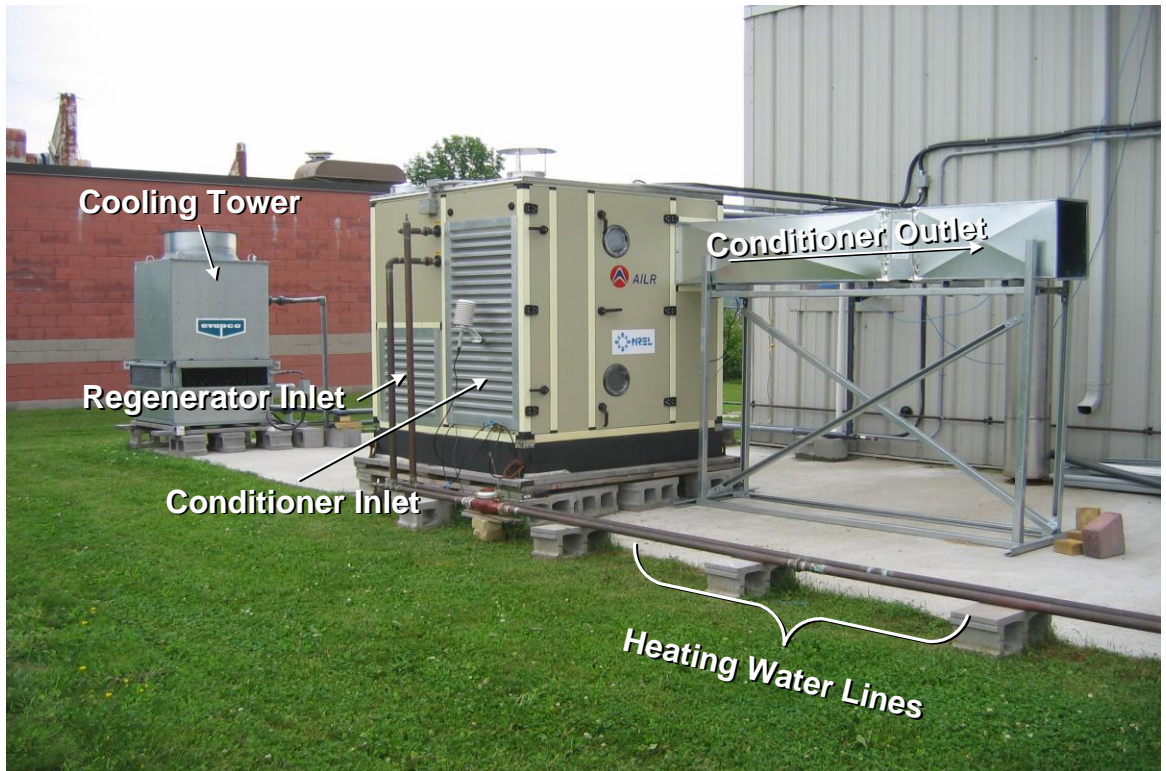


Figure 3.2: System layout

Variation and optimization of fluid flow rates and desiccant material is recommended in future work.

Figure 3.5 shows the flat plate mass and heat exchanger found in the conditioner and regenerator. These components are similar in operation and designed for different temperature ranges. The conditioner consists of a series of standing plates. Conditioner plate depth is 305 mm, and each plate is 2.5 mm wide. Cooling water is internally circulated through the flat plate array. The plate surfaces are coated with a thin wick material to improve the wetting and distribution of liquid desiccant. The regenerator consists of a series of parallel plates, each 114 mm by 3 mm. Figure 3.5b displays

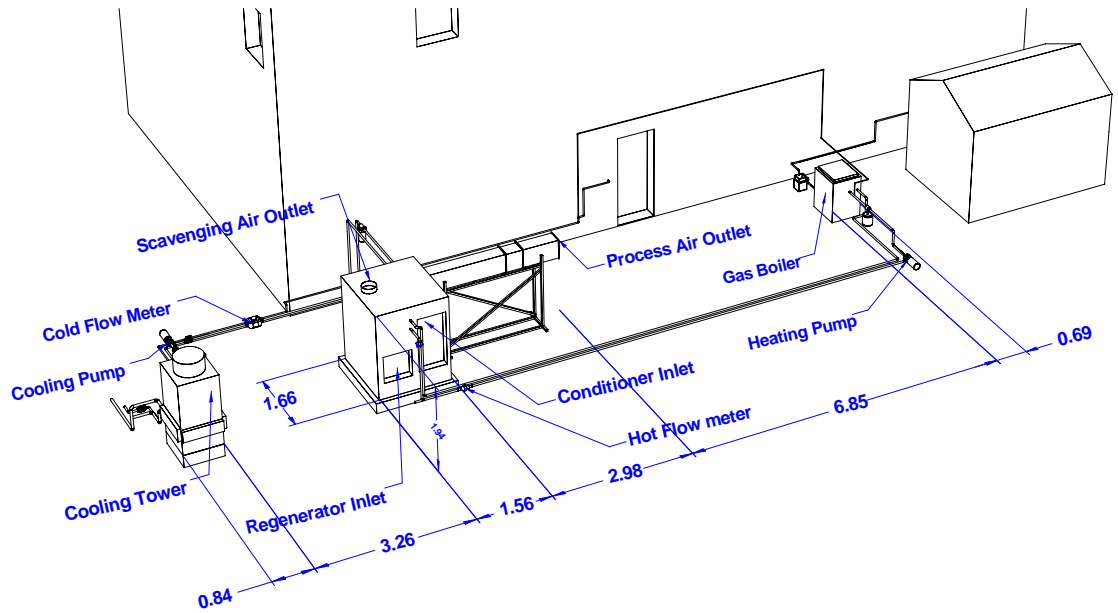


Figure 3.3: System layout

operation at close to the desiccant solution solubility limit, with one plate beginning to generate solid desiccant.

3.3 Thermal Components

3.3.1 Auxiliary heat and heat rejection

The auxiliary heating system is a 90 kW natural gas boiler with a 2 stage valve. The control system attempts to achieve a set-point boiler outlet temperature by alternating between boiler Off/Low/High firing. This control strategy causes the temperature

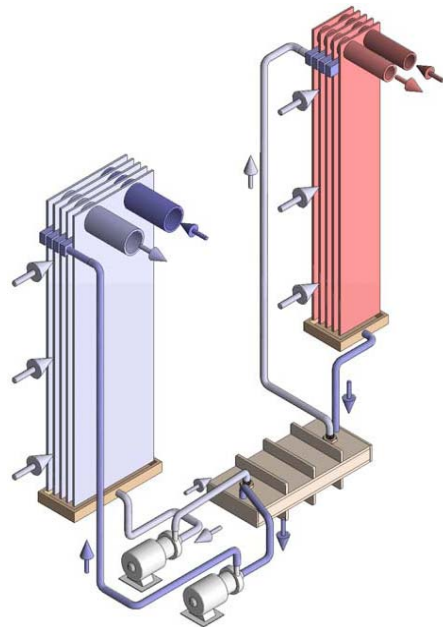


Figure 3.4: Model of air handling unit

to fluctuate within the heating loop. The heat rejection system consists of a 65kW cooling tower. The cooling tower fan is driven by a 0.8kW electric motor. Heating and cooling water are circulated using 2kW electric pumps. Balancing valves are placed after the pumps to control the flow rate through the lines.

Table 3.1: Air handling system experimental values

	Experiment
Air Flow	1700 L/s
Hot water flow	110 L/min
Cold water flow	85 L/min
Desiccant charge	43% LiCl
Desiccant flow	0.126 L/s
Regeneration thermal COP	0.70 - 1.00
Hot water temperature	50 - 90 C
Total Cooling	4.2 - 22.8 kW
Latent Cooling Ratio	1.0 - 1.9

3.4 Data acquisition and control

3.4.1 Data acquisition system

A CR10X Campbell Scientific datalogger was used to collect sensor data. The datalogger capability was expanded with a Campbell Scientific SDM-SW8A pulse count module and a Campbell Scientific AM16/32A relay multiplexer. A wiring diagram of the data logger can be found in Fig. B.1, Appendix B. This data acquisition system has a capacity of 40 single ended (20 differential) voltage channels and 10 pulse counter channels. Various single channel input ranges are selectable, and are listed in table 3.2.

Table 3.2: CR10X analog input ranges

Full Scale Range [mV]	Accuracy [mV]
2500	2.5
250	0.25
25	0.025
2.5	0.0025

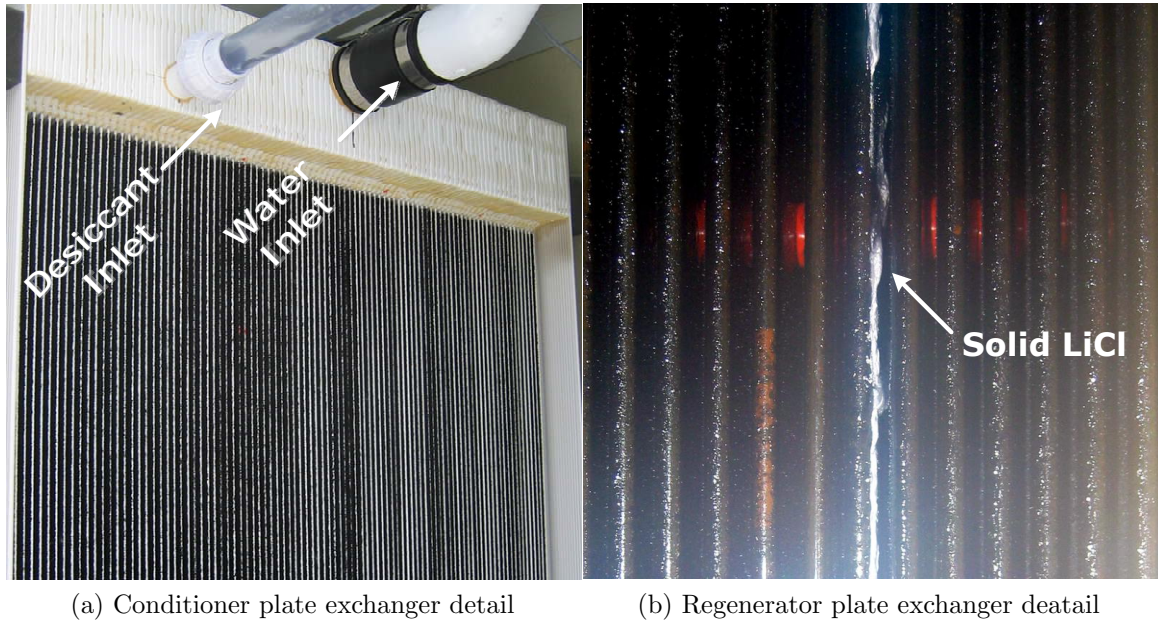


Figure 3.5: Flate plate mass and heat exchangers

3.4.2 Automatic control system

Control of the system was achieved using a programmable logic controller (PLC). A Direct Logic 06 PLC was used with two expansion modules; a 4 channel RTD input module and a digital/analog expansion module. A wiring diagram of the PLC, Fig. B.2, is located in Appendix B. The system control parameters are listed below.

- Input signals
 - Various system faults
 - Desiccant sump minimum/maximum level
 - Process air stream pressure
 - Regenerator desiccant concentration (currently disabled)
 - Regenerator inlet temperature

- Desiccant sump temperature
- Output signals
 - Cooling tower supply valve
 - Cooling tower drain valve
 - Boiler off/low/high fire
 - Cooling tower fan
 - Regenerator heating water pump
 - Absorber cooling water pump
 - Regenerator desiccant pump
 - Absorber desiccant pump
 - Process air blower
 - Scavenging air blower
 - Process air fan speed

The PLC is programmed using staged relay ladder logic. The stages are listed in Figs. B.3 and B.4 in appendix B [27]. A summary of the control scheme used in this experiment is listed below. The system was run with a constant temperature profile from 9 am to 5 pm each day, or with a varying temperature profile over the same period.

- AUTO mode
 - Initialize PLC (9am)

- Initialize PLC memory
- Load control set points
- Monitor AUTO/OFF mode switch (loop)
- Run desiccant pumps to fully wet flat plate exchangers (5 minutes)
- Power up motors (staged)
- Update temperature profile according to time (loop)
- Monitor faults (loop)
- Shut down system (5pm)

Chapter 4

Experiment and analysis methods

The method of data acquisition is explained in this chapter. A schedule of operation is presented, and the generation of the data set used in this investigation is outlined. The computer simulation incorporating the data set is introduced.

4.1 Experimental Procedure

The system was operated starting on July 9th 2008. For this investigation, performance data was collected over varying regeneration temperatures, the most important parameter when considering a solar thermal driven system. The data collection schedule is summarized in Table 4.1.

Table 4.1: Data collection schedule for regenerator temperature

Day	1	2	3	4	5	6	7	8
Temperature	50	50	70	70	70	70	70	90
Day	9	10	11	12	13	14	15	16
Temperature	80	80	60	90	90	**	**	Off
Day	17	18	19	20	21	22		
Temperature	**	Off	Off	50	70	90		

** - solar heat profile, see Fig. 5.6

The temperature set point indicates the control signal sent to the two stage modulating boiler. This temperature was maintained during each day from 9am to 5pm. Average regenerator inlet temperature was within 1 degree of the set point temperature for all days. This comprises the complete data set used for subsequent analysis. A varying solar heat profile was used for three days in this period to validate operation over daily varying temperatures. Data was stored from all sensors according to table B.1 and downloaded from the datalogger to a PC. This data is internally averaged over a one minute period.

4.1.1 Desiccant measurement

To determine the concentration of desiccant, samples were taken and analyzed using a DMA 4000 Anton Paar density meter with a rated repeatability of $5 \times 10^{-5} \text{ g/cm}^3$.

1. 6 mL of desiccant was taken using a syringe from the following locations
 - Conditioner inlet port (flushed before sampling)
 - Conditioner outlet tray
 - Regenerator inlet port (flushed before sampling)
 - Regenerator outlet tray
2. 3 mL of desiccant solution was injected into the DMA 4000
3. The sample was automatically cooled to 20° and the density was recorded
4. 6 mL of distilled water was used to flush the DMA 4000

5. The distilled water was pumped clear of the DMA 4000
6. The above procedure was repeated for the remaining three samples
7. The density of distilled water (0.9982 kg/L) was measured every four sample runs to confirm the accuracy and cleanliness of DMA 4000
8. At the end of the day, the waste desiccant and distilled water were returned to the air handling machine desiccant sump

The density determined from these measurements was converted to a solution concentration using the correlation presented in Fig. 2.1a. Manual density measurements were taken every 30 minutes. The concentration was linearly interpolated between measurements on a 1 minute interval.

4.2 Data analysis

All data was collected and analysed using Matlab using the following procedure;

1. Datalogger data was loaded from comma separated value file representing each minute
2. Thermodynamic properties of water and air were loaded for interpolation
3. Manual desiccant concentration data was loaded and expanded over one minute interval
4. Air state properties were calculated using ASHRAE correlations for temperature, T and relative humidity, ϕ

- Absolute humidity ratio $W = f(T, p, \phi)$ in units of [g/kg] [28]
 - Air enthalpy $h = f(T, W)$ in units of [kj/kg] [28]
5. Water enthalpy states were interpolated using thermodynamic relations [25]
 6. Desiccant enthalpy and enthalpy of dilution was calculated using relations [18]
 7. All flow rates were converted from volumetric to mass rates in units of [kg/hr] using average of inlet/outlet temperatures and density data from thermodynamic property tables
 8. Enthalpy states were multiplied by mass flow rates to obtain enthalpy flow rates in units of [kJ/hr] for each inlet and outlet point
 9. Water absorbed by desiccant from process air stream was calculated using two methods
 - Change in absolute humidity ratio in process air stream
 - Change in desiccant concentration
 10. Water desorbed from desiccant into scavenging air stream was calculated using the same two methods, with the outlet humidity ratio calculated using an enthalpy balance on the regenerator
 11. Performance parameters were calculated using average, instantaneous, or total values of enthalpies, water flow rates, and energy rates described in section 2.4

4.3 Solar profile generation

Figure 4.1 shows efficiency curves for two solar thermal collectors, generated using equation 2.5 and standardized performance test data. The flat plate collector is a single glazed collector while the evacuated tube collector is arranged in headers of 20 individual tubes. The efficiencies below are based on gross collector area.

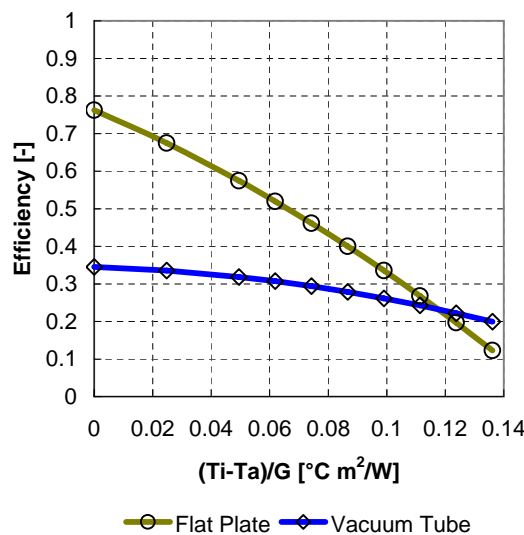


Figure 4.1: Solar thermal efficiency curves

Figure 4.2 is an overview of a simulation developed to generate a heating profile for a solar thermal collector. Details of the simulation can be found in a previous study done by Jones and Harrison [29]. This basic simulation was implemented using the software package TRNSYS, a transient simulation program used primarily for analyzing solar energy systems [30]. This simulation program uses a constant 5 degree temperature decrease from the outlet to inlet of the collector to simulate a regeneration load. There are many options when coupling the thermal source to the regenerator.

Some interesting options include eliminating the auxiliary heat source, replacing the water storage tank with a mixing valve, and various temperature control strategies described in section 6.2. A detailed investigation into these different options is beyond the scope of the present work.

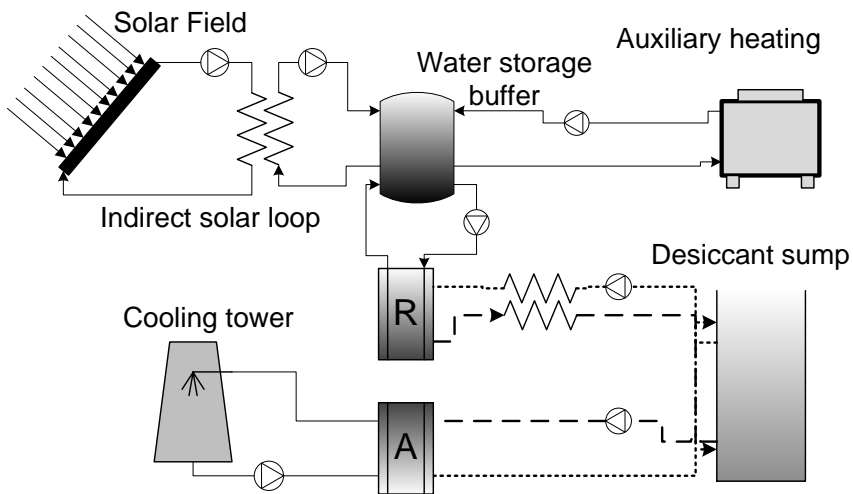


Figure 4.2: Simulation schematic

A typical meteorological year weather file is loaded for Toronto, the closest available city in the weather file database. The simulation is arranged such that the area of flat plate or vacuum tube collectors can be varied. For the solar profile used in the experimental study, the solar thermal array consisted of 70 square meters of vacuum tube collectors. The water buffer storage is set at 400 L. The cooling tower and boiler performance parameters are set to the manufacturers values for the installed components. The result of this simulation was the hot water setpoint temperature. This setpoint temperature was updated by the PLC every 30 minutes while above

50°C. Operation between 9 am and 5 pm is presented in table 4.2.

Time	$T_{hw, set}$ [°C]
9:30	51.1
10:00	62.3
10:30	62.4
11:00	64.9
11:30	66.1
12:00	70.1
12:30	73.7
13:00	76.3
13:30	77.2
14:00	78.2
14:30	77.2
15:00	77.0
15:30	76.9
16:00	73.9
16:30	68.1

Table 4.2: Solar profile temperatures - 30 minute resolution

Chapter 5

Results and Analysis

In this chapter, observations relevant to the characterization of the system for solar thermal applications are presented. Enthalpy flows for the regenerator and conditioner are plotted, and coefficients of performance are given for the data set. A sensitivity analysis is used to identify important independent variables upon which a regression analysis is performed to yield an empirical model of the system performance.

5.1 Enthalpy balance

Figures 5.1 to 5.4 summarize the enthalpy flow rates through the conditioner and regenerator for a day of operation, the 15th of July. These results are typical for all days with constant heating water temperature, and provide an example of operation. These figures are derived from the equations in section 2.2.3. The enthalpy flows are calculated from temperature, concentration, humidity and flow rate data using Matlab. Selected Matlab scripts used for analysis are in appendix section C.

Figure 5.1 shows the enthalpy flow rates over a constant 50°C regenerator setpoint.

It can be seen that the cooling water gains enthalpy from the air and desiccant streams. This enthalpy is rejected by the cooling tower, and is primarily the latent heat of absorption of the water vapor. The sharp spikes in the air flow enthalpy occur during the opening of the conditioner door to take the manual desiccant concentration sample. When the door is opened, a safety interlock opens the circuit to the process air blower, which could otherwise represent a safety hazard with the door open.

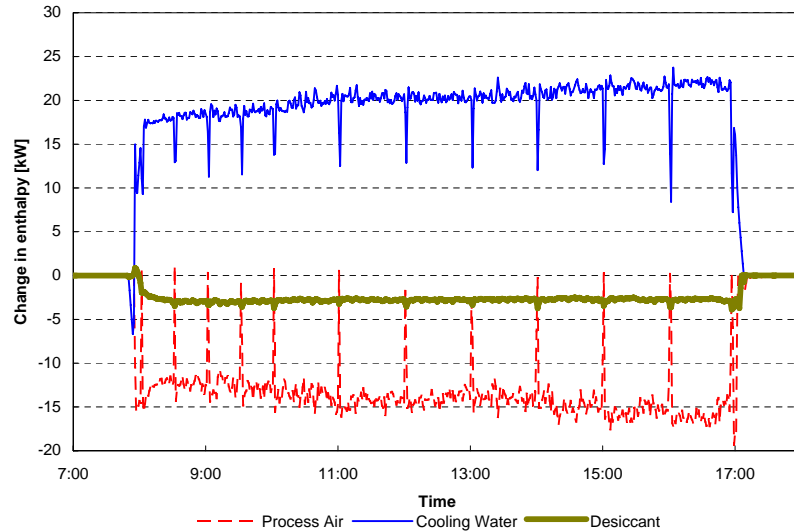


Figure 5.1: Enthalpy flow in conditioner

In the regenerator, Fig. 5.2, the heating water is the dominating enthalpy flow, with a flow rate of 80 [L/min] and a temperature range of 50 to 90°C. The air flows at a lower rate compared to the conditioner, at 250 [L/s]. The weak desiccant flows at 7.5 [L/min], similar to the conditioner. Compared to the heating water, these two flows are at a lower temperature. The heating water flow is an important optimization parameter in the design of a complete system due to this large enthalpy flow. The

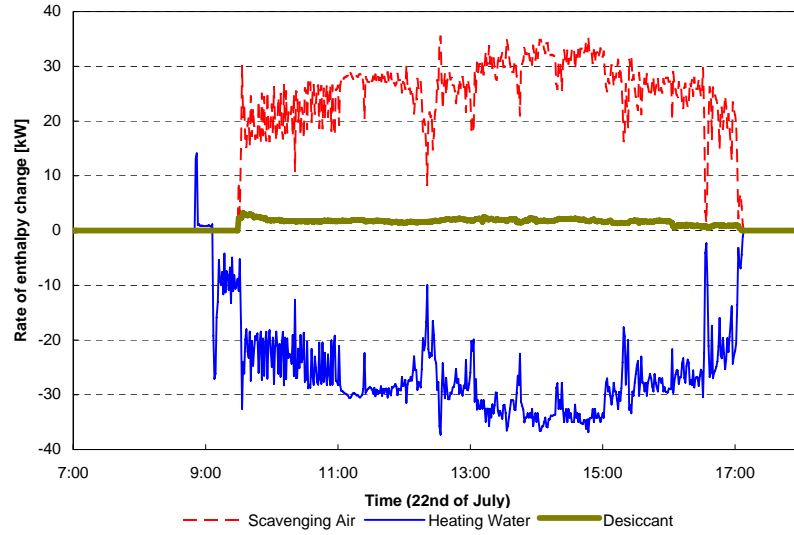


Figure 5.2: Enthalpy flow in regenerator

enthalpy change of the heating water through the regenerator represents the latent heat of desorption of water from the desiccant to the scavenging air stream.

Figures 5.3 and 5.4 show the sum of all enthalpy flows into the conditioner and regenerator along with the sum of the flows leaving, this is a complete enthalpy balance of the control volume defined by Figs. 2.7 and 2.8. These two figures show close agreement obtained in the enthalpy balance and show that there are no major errors in the data acquisition system. The conditioner deviation, averaging an increase of 0.77 kW, is less than 3% of the total cooling rate. The regenerator deviation is less than 1% of the heating water enthalpy change. Because of this agreement, the assumption that the regenerator and conditioner are adiabatic is also valid for these control volumes.

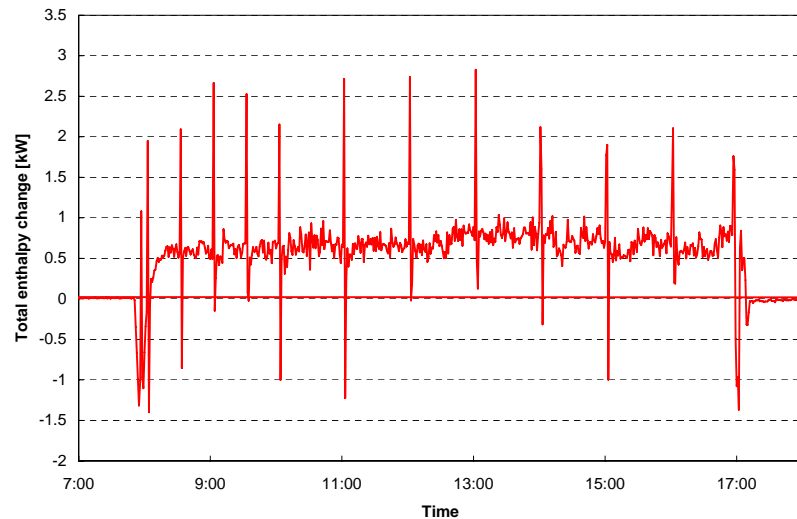


Figure 5.3: Enthalpy balance in conditioner

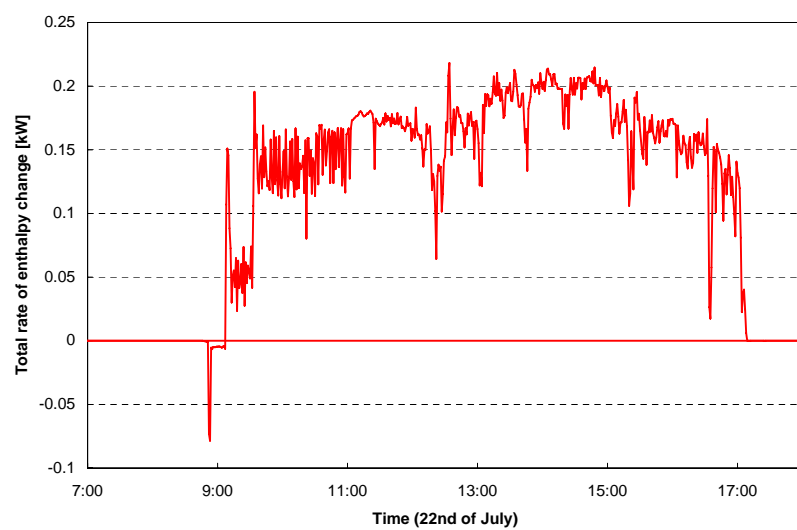


Figure 5.4: Enthalpy balance in regenerator

Quantity	Symbol	Note	Unit	Day (July 2008)			
				10	13	20	25
Start time	t_{start}	Time	hr	9.0	9.0	11.0	9.0
Time Period	Δt	Time	hr	7.0	6.0	5.0	7.0
Hot water inlet	$T_{hw,in}$	Avg.	°C	50.5	68.7	86.6	Solar
Hot water change	$\Delta T_{hw,in}$	Avg.	°C	-1.7	-3.4	-5.0	-3.5
Hot water flow	\dot{m}_{hw}	Avg.	kg/hr	6295.9	6250.2	6793.5	6779.2
Cold water in	$T_{cw,in}$	Avg.	°C	18.7	22.3	24.4	23.1
Cold water change	ΔT_{cw}	Avg.	°C	1.8	3.1	4.4	3.2
Cold water flow	$\dot{m}_{cw,c}$	Avg.	kg/hr	5148.5	5188.6	5210.2	5004.2
Ambient temperature	$T_{air,in}$	Avg.	°C	21.0	21.2	22.9	23.8
Ambient change	ΔT_{air}	Avg.	°C	0.1	3.7	5.2	2.4
Ambient humidity	W_{amb}	Avg.	g/kg	8.7	12.4	14.3	11.9
Ambient humidity change	ΔW	Avg.	g/kg	-1.0	-4.0	-6.5	-3.6
Air flow rate	\dot{m}_{air}	Avg.	kg/hr	7417.9	7511.5	7365.2	7415.3
Total cooling rate	\dot{Q}_{total}	Avg.	kW	4.9	13.4	20.0	13.5
Latent cooling rate	\dot{Q}_{latent}	Avg.	kW	5.1	21.5	30.4	18.4
Latent heat ratio	LHR	Avg.	-	1.0	1.6	1.5	1.4
Heating rate	\dot{Q}_{regen}	Avg.	kW	12.9	24.8	40.3	28.0
Water desorbed	$\dot{m}_{v,s-a,r}$	Tot.	kg	91.3	214.5	214.1	190.2
Desorption rate	$\dot{Q}_{v,s-a,r}$	Avg.	kW	8.9	25.0	30.4	19.1
Water absorbed	$\dot{m}_{v,a-s,c}$	Tot.	kg	50.8	181.4	208.9	0.0
Absorption rate	$\dot{Q}_{v,a-s,c}$	Avg.	kW	5.1	21.5	30.4	18.4
Thermal COP	$COP_{thermal}$	Avg.	-	0.70	1.01	0.75	0.68
Cooling COP	$COP_{cooling}$	Avg.	-	0.38	0.54	0.50	0.48
f COP	COP_{elec}	Avg.	-	0.96	2.60	3.86	2.68
Regen. conc. in	$C_{in,c}$	Avg.	Wt. %	26.88	32.18	37.30	32.78
Regen. conc. change	ΔC_c	Avg.	Wt. %	-1.00	-1.85	-2.97	-2.21
Cond. conc. In	$C_{in,r}$	Avg.	Wt. %	26.57	31.16	35.20	31.80
Cond. conc. change	ΔC_r	Avg.	Wt. %	0.72	2.36	3.22	1.88

Table 5.1: Daily system operation summary

5.2 Daily performance data

Table 5.1 is a summary listing of the daily operation of the air handling system under 4 types of regenerator heating profile. The 10th, 13th, and 20th correspond to the 50, 70, and 90°C heating setpoint. The 25th was operated on the time varying solar heating profile discussed in 4.3. The remaining daily operation data is found in table A.1, appendix A.

System operation plots for the 25th of July are presented in Figs. 5.5 and 5.6. The

data for the remaining three constant temperature days are plotted in Figs. A.5 to A.10 in appendix section . Figure 5.5 is a plot of the conditioner performance. The system begins operation when the temperature of the solat thermal array reaches 50°C, at 9:30 in the morning. The temperature profile can be seen in the top section of Fig. 5.6. The temperature profile approaches 80° as the day progresses and the incident radiation on the simulated vacuum tube collector increases. The temperature profile is adjusted by the programmable logic controller every 30 minutes. From table 5.1, we see that the average cooling rate is 13.5 kW with a latent heat ratio of 1.4. From the middle section of Fig. 5.5, one can observe the temperature at the process air inlet and outlet. The temperature rises an average of 2.4°C for this day. The bottom section of Fig. 5.5 shows a significant dehumidification effect, a change in absolute humidity averaging 3.6 g/kg. This amounts to a total absorption of 208.9 kg of water for this day. From the middle section of Fig. 5.6, is is observed that the absorption and desorption rates are similar. This indicates that the unit is approaching steady state operation even over a varying temperature profile The total amount of water desorbed for this day is 214.1 kg. The bottom section plots the coefficients of performance for this day. The average thermal COP for the 25th is 0.68, the average cooling COP is 0.48, and the average electrical COP is 2.68 for this solar temperature profile.

5.3 Coefficients of performance

Figures 5.7 and 5.8 display the average daily coefficients of performance for the data set. The thermal and electrical COP's are defined in equations 2.27 to 2.29. Overall, the regenerator COP averaged 0.81 for the days of constant heating temperature operation, while the cooling COP is an average of 0.53. The cooling COP is lower

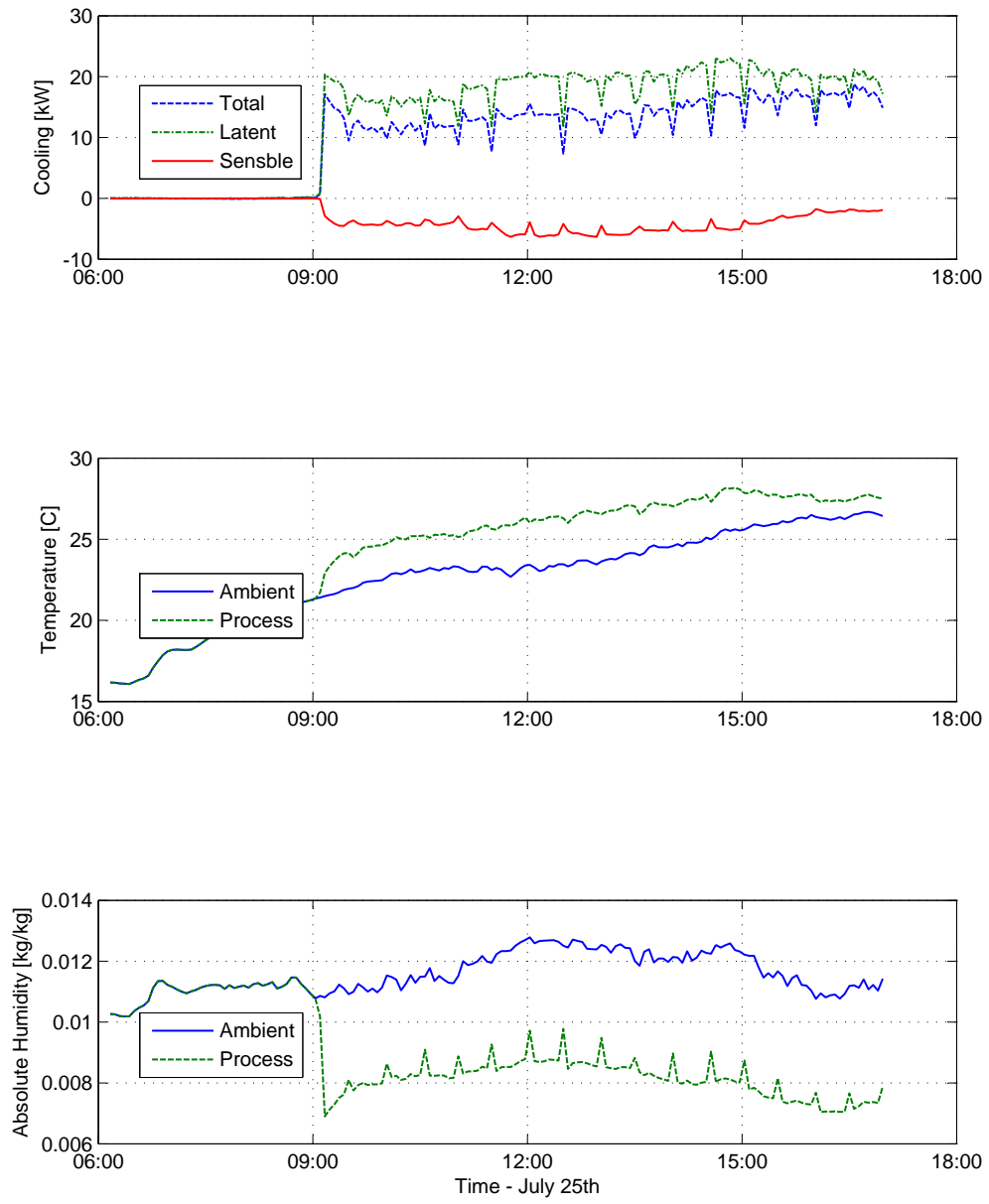


Figure 5.5: Conditioner performance - July 25th

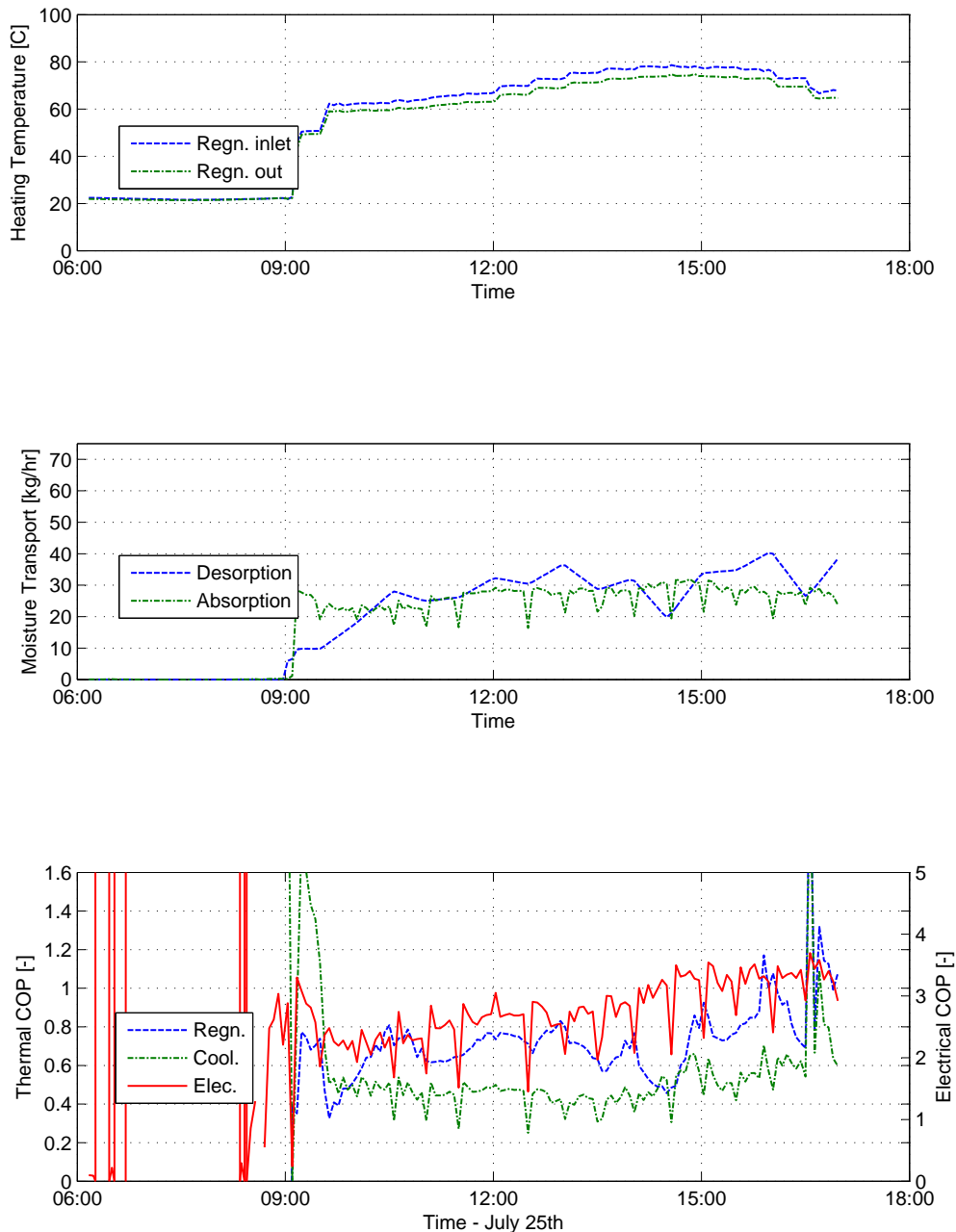


Figure 5.6: Heating temperature & performance figures - July 25th

due to the enthalpy gained by the desiccant as it condenses and absorbs water vapor from the process air. The cooling COP can be improved with a higher capacity heat rejection system. Figure 5.8 summarizes the electrical COP values derived for all days of operation. The electrical consumption of the system was normally 5.5 kW. The majority of this power goes to pumps and blowers.

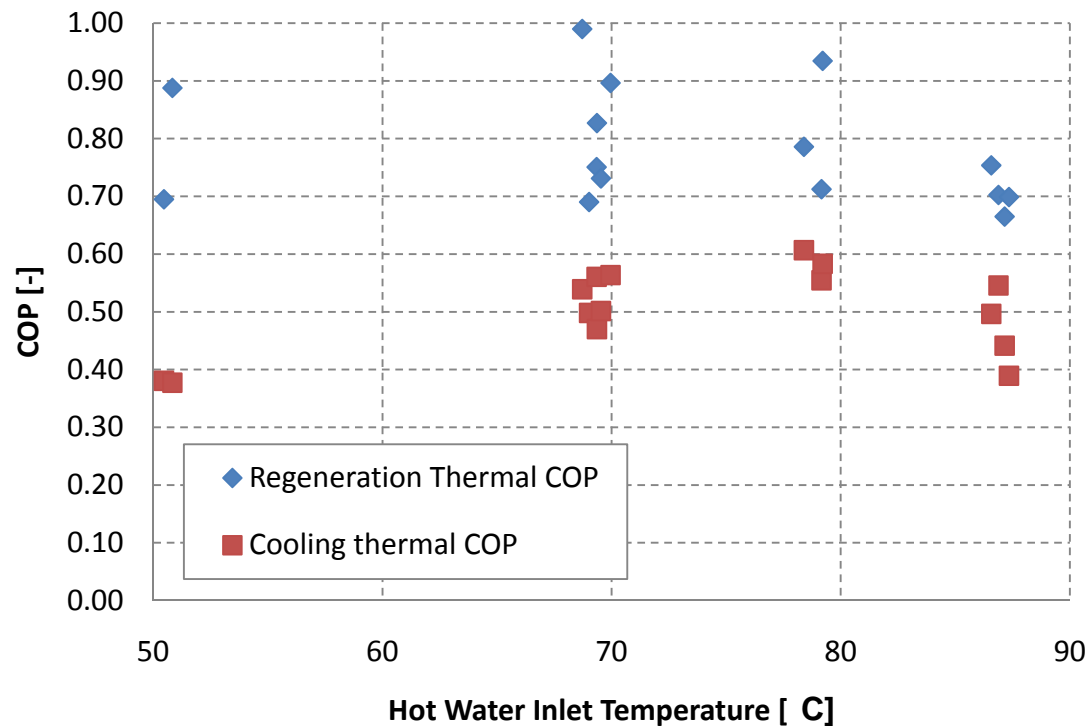


Figure 5.7: Daily thermal coefficients of performance

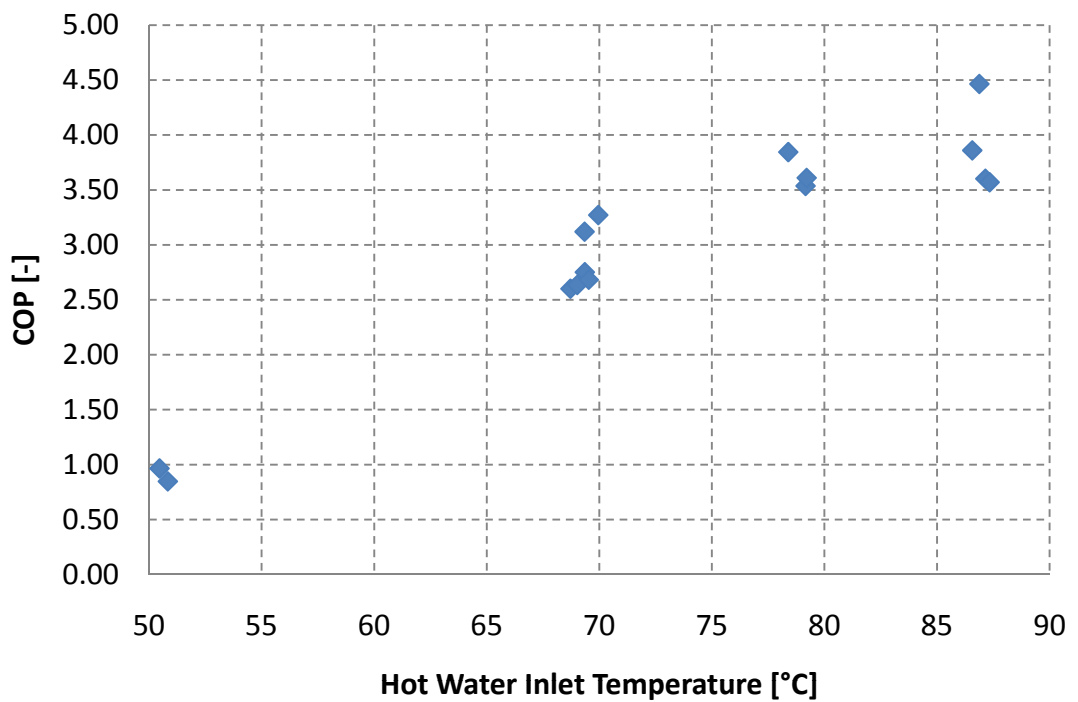


Figure 5.8: Daily thermal coefficients of performance

5.4 Sensitivity study

From Figs. 2.7 and 2.8 and equations (2.7) to (2.18), 13 input variables for the combined conditioner and regenerator unit can be listed. The ambient air requires two psychrometric properties to define the state, the desiccant solution likewise requires two state variables, and the water streams require one. There are additionally the flow rates for each stream. In this field test, the flow rates were held constant. The outside environment during July and August specified the inlet to both the process and scavenging air streams, as well as indirectly specifying the cooling tower water temperature. The heating water was the primary independent variable varied in this investigation, used to characterize the system operating at temperatures common to solar thermal collectors. The temperature was varied according to table 4.1.

The data obtained and processed from the is given in appendix A, Figs. A.1 to A.4. These figures show all data for constant temperature days according to table 4.1. The data is grouped according to the regenerator hot water inlet set point temperature for that day. Upon visual inspection of these graphs, it is clear that the data set is scattered according to varying ambient conditions. Observed outlet conditions are not simple functions of one inlet condition and require non-linear multivariate regression to be fully defined. For example, the concentration change of desiccant through the regenerator is primarily a function of the hot water temperature, but also depends on the ambient air humidity. During these experiments, the regenerator and conditioner were run simultaneously. Tables 5.2 and 5.3 list the independent variables and two dependant variables for the conditioner and regenerator. The trend of each independent variable on the dependent variable is summarized in these tables, based on visual inspection and regression analysis of Figs. A.1 to A.4. Selected dependent

output variables are used to predict the overall performance of the conditioner and regenerator.

Table 5.2: Regenerator performance parameters

Parameter	Heating Water Temperature Change ΔT	Regenerator Concentration Change ΔC
$T_{hw,in}$	Positive correlation	Positive correlation
\dot{m}_{hw}	Constant	Constant
$T_{air,in}$	Negative correlation	Positive correlation
$W_{air,in}$	Positive correlation	Negative correlation
\dot{m}_{air}	Constant	Constant
C_{in}	Negative correlation	Negative correlation
$T_{sol,in}$	Positive correlation	Positive correlation
\dot{m}_{sol}	Constant	Constant

Table 5.3: Conditioner performance parameters

Parameter	Water Absorption $\dot{m}_{v,a-s,c}$	Cooling Water Temperature ΔT
$T_{cw,in}$	Positive correlation	Positive correlation
\dot{m}_{cw}	Constant	Constant
$T_{air,in}$	Negative correlation	Negative correlation
$W_{air,in}$	Negative correlation	Negative correlation
\dot{m}_{air}	Constant	Constant
C_{in}	Positive correlation	Positive correlation
$T_{sol,in}$	Negative correlation	Negative correlation
\dot{m}_{sol}	Constant	Constant

5.5 Regression analysis

The dependent variables of interest are functions of more than one independent variable. As an approximation, the independent variables with strongest influence on the dependent variable are first chosen as the predictors, with the response given by

the dependent variables. The regression coefficients are computed for a linear model with an interaction term in the form $y = a + x_1b + x_2c + x_1x_2d$ for 2 independent variables, or $y = a + x_1b + x_2c + x_3d + x_1x_2x_3e$ for 3. Matlab was used to generate fit coefficients and regression statistics. The script can be found in appendix C.

Independent variables with a strong correlation on the dependent variable were chosen for the fit. To characterize the conditioner, three dependent output variables were chosen; $\dot{m}_{v,a-s,c}$, the water absorption rate from the air stream into the desiccant, ΔT_{cw} , the change in temperature of the cooling water, and ΔT_{air} , the change in temperature of the process air. With these three variables, a simulation could be run to predict total and latent cooling, and cooling tower performance. For the regenerator, the water desorption rate, $\dot{m}_{v,s-a,r}$, and the heating water temperature change, $\Delta T_{hw,in}$, are chosen as the primary dependent variables. It was found that $T_{hw,in}$, $C_{in,r}$, and W_{in} were strong predictors of the regenerator performance. With $\dot{m}_{v,s-a,r}$ and $\Delta T_{hw,in}$ known, the thermal COP of the regenerator as well as the inlet temperature to the solar array can be determined.

Figures 5.9 and 5.10 display the result of the regression analysis performed on ΔT_{air} , the change in air temperature for the process air stream through the conditioner. In the left hand plot of 5.9, the correlation between the model and data are displayed. A perfect correlation between the two would lie on the line. The residuals of the fit are plotted beside the correlation. Figure 5.9 shows a large residual compared to the original data. The standard deviation of the residual (r-SD), is 1.117. Additionally, the residual displays an increasing trend. In this case, a new model is fit for the three independent variables $C_{in,c}$ and $T_{air,in}$. The correlation of this 3 term regression is presented in Fig. 5.10. The new model has a standard deviation of

0.189, and the residuals are more evenly distributed about the mean. This process could be continued to explore higher order mathematical models, or incorporate more independent variables. As an approximation, this study will limit the regression to a three term linear model with interaction. Table 5.4 summarizes this modeling effort. The remaining correlation plots are found in Figs. A.11 to A.18, appendix A.

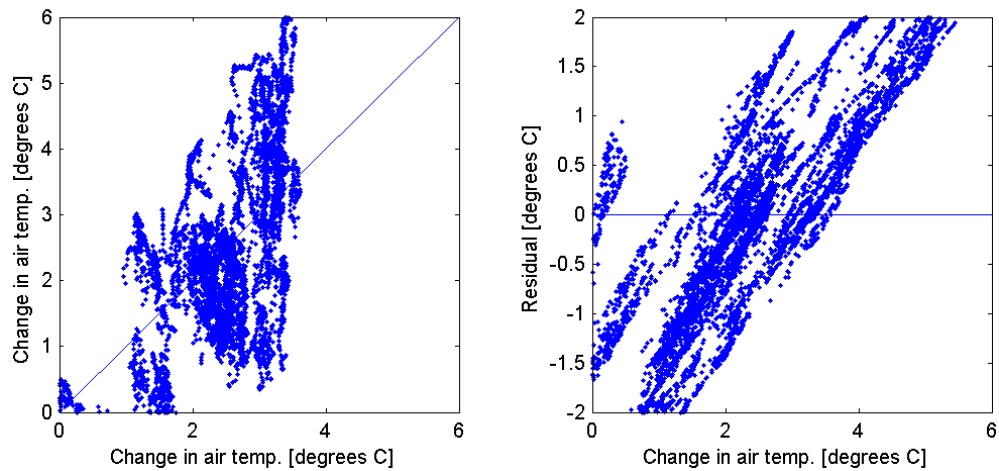


Figure 5.9: Process air temperature change correlation for 2 variables

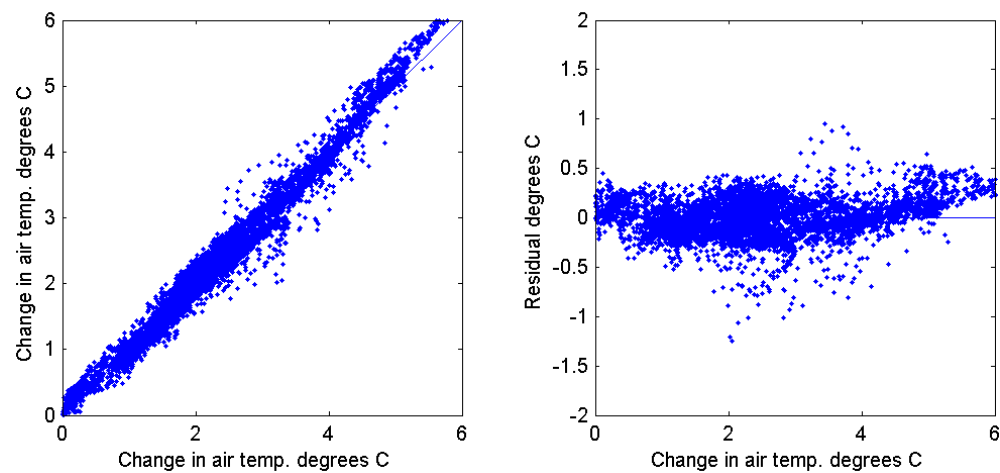


Figure 5.10: Process air temperature change correlation for 3 variables

Table 5.4: Regression fit summary

Figure	Parameters				Coefficients					Residual r-SD
	y	x1	x2	x3	a	b	c	d	e	
A.11	$\dot{m}_{v,a-s,c}$	W_{amb}	$C_{in,c}$		-1.900	-4275.400	-0.200	224.900		4.970
A.12	ΔT_{cw}	W_{amb}	$C_{in,c}$		-1.326	-176.962	0.073	11.527		0.415
A.13	ΔT_{air}	W_{amb}	$C_{in,c}$		-11.209	0.385	0.268	-0.005		1.117
A.14	$\dot{m}_{v,a-s,c}$	W_{amb}	$C_{in,c}$	$T_{air,in}$	22.139	-963.690	1.028	-2.938	5.756	4.841
5.9	ΔT_{cw}	W_{amb}	$C_{in,c}$	$T_{air,in}$	-0.755	-54.846	0.126	-0.092	0.313	0.415
5.10	ΔT_{air}	W_{amb}	$C_{in,c}$	$T_{air,in}$	0.178	0.849	0.073	-0.912	0.00012	0.189
A.15	ΔT_{hw}	$T_{hw,in}$	$C_{in,r}$		-7.295	0.184	0.100	-0.002		0.545
A.16	$\dot{m}_{v,s-a,r}$	$T_{hw,in}$	$C_{in,r}$		-104.223	2.342	2.186	-0.043		5.753
A.17	ΔT_{hw}	$T_{hw,in}$	$C_{in,r}$	W_{amb}	-3.233	0.179	-0.113	-18.029	-0.068	0.256
A.18	$\dot{m}_{v,s-a,r}$	$T_{hw,in}$	$C_{in,r}$	W_{amb}	-0.370	0.010	-0.001	7.447	-0.004	3.001

5.6 Discussion

5.6.1 High temperature operation

Figure 5.7 indicates that the thermal COP of the regenerator decreases slightly at only the highest temperature. The thermal regeneration COP is defined as the amount of energy liberated from the desiccant by desorbed water divided by the amount of energy lost by the heating water through the plate exchanger. As recorded in table 5.1, the cooling power of the system increases from roughly 4 to 20 kW over the range of 50 to 90°C. This increase corresponds directly to the electrical system efficiency, which is the cooling power divided by the electrical power consumed.

This suggests that a solar thermal array can be operated at high temperature to achieve a favorable electrical COP. Evacuated tube collectors or double glazed flat plate collectors are designed to sustain these higher temperatures, whereas an unglazed or single glazed collector would have difficulty since the collector heat losses are higher for these types. Furthermore, higher temperatures are required to maintain a higher cooling power. It was shown that a $70\ m^2$ evacuated tube collector, reaching a peak temperature of 78.6° can provide an average of 13.5 kW of cooling.

5.6.2 System components

From figure 5.8 it can be seen that the system operates with an electrical COP similar to an electrically driven chiller. For example, a 50kW electrically driven dedicated outdoor air unit has a COP of approximately 4, while the system under study only approached a COP of 4 for high temperature operation. The high power consumption found in this experiment should therefore be investigated. Electrical consumption can

be reduced using variable speed drives for the two water pump motors and cooling tower fan motor. Flow rates could be further optimized in a more detailed TRNSYS simulation.

Further investigation should be done on the coupling of the thermal heat source to the regenerator. Figure 4.2 is only one possible arrangement incorporating the solar thermal array and auxiliary heat source. Many more combinations are possible. For example, the water storage system could be replaced with a mixing valve (another parallel heat source arrangement), or the heating loop could flow through both the solar thermal array and the auxiliary heat source (a series arrangement). The heat rejection component could also be investigated as a component to replace. Cooling towers often require frequent maintenance as well as consume electricity and water.

5.6.3 Experimental apparatus

Several possible improvements to the data acquisition system were noted during summer operation.

For a more complete enthalpy balance on the regenerator, a temperature and humidity (T/RH) sensor should be installed on the scavenging air outlet. A T/RH sensor on the scavenging air stream will need to withstand high temperature and humidity conditions.

Tables 5.2 and 5.3 list the thermodynamic variables of interest. A more accurate model of the regenerator and conditioner can be obtained by varying these parameters in a more controlled setting. Ideally, only one parameter should be varied and the system should be allowed to achieve steady state. Such an investigation would involve moving the machine indoors and installing an air handling system capable of generating

a wide range of ambient humidity and temperature conditions for the process air flow. A full system simulation with the aim of optimization would vary all independent variables including flow rates.

The manual desiccant density measuring process described 4.1.1 was time consuming. Control of desiccant concentration is an important issue in liquid desiccant systems. Solid desiccant can damage a standalone air handling system. If a continuous desiccant concentration measurement was taken, system control and measurement would be significantly improved. The manufacturer attempted to incorporate such an automated measuring system based on the varying index of refraction of desiccant with concentration. This sensor was placed at the regenerator outlet. This sensor was unable to provide an adequate data resolution and was prone to error due to the high temperatures and variable flow found in the regenerator outlet.

The two flow rates that deviated from the manufacturers' specification in section 3.2 should be adjusted to their rated values. The process air stream was supplied at a rate higher than specified by the manufacturer, and the cooling water pump was under sized for the application, supplying approximately 80% of the specified flow. These two parameters will have an influence on the total cooling capacity of the machine.

5.6.4 Desiccant storage

In order to properly develop a model of the conditioner and regenerator for a solar thermal application, the concept of desiccant storage should be investigated. Storage of cooling energy in the form of a lossless chemical potential is a key advantage for a solar driven system. Storage will smooth out the available unpredictable solar resource and may allow for a higher solar fraction and a smaller solar thermal array.

Storage allows for humid but cloudy days and takes advantage of extra thermal regeneration during dry and sunny days. Previous work indicates that a 90% solar fraction system meeting the cooling load can be reduced from $140m^2$ to $100m^2$ of evacuated tube thermal collectors using 3000L of liquid desiccant storage [29]. Several recommendations for further study follow from this concept. Firstly, if a simulation is to be performed investigating the concept of storage, performance data on the regenerator and conditioner needs to be collected with the machines running decoupled. This would remove the influence of the desiccant being heated by the regenerator and immediately entering the conditioner, which lowers its cooling potential. Storage would likely incorporate the salt $CaCl_2$, in either a $CaCl_2/LiCl$ mixture, or pure $CaCl_2$ solution. $CaCl_2$ cannot cool the desiccant as effectively, but is significantly less expensive [23]. A preliminary study done by Miller and Lowenstein [23] using a double capacity air handling system (supplying 3000 L/s process air), suggests 12100L of storage of $CaCl_2$ solution to meet 12 hours of demand. In order to properly simulate the storage performance of the installed system under investigation, performance data for decoupled operation of the regenerator and conditioner should be obtained. This removes extra heat load on the conditioner from the warm desiccant leaving the regenerator. A solution storage system should be optimized to cool during the night, increasing the dehumidification potential of the liquid desiccant. In addition to heat rejection by a solution storage system, the tank should be designed such that the solution remains stratified, with strong, heavier desiccant being drawn from the bottom of the tank. Stratification will increase the exergy storage in the tank.

Chapter 6

Conclusions and Recommendations

The experiment and the important results are summarized in this final chapter. Future work for the project is discussed.

6.1 Conclusions

A liquid desiccant air handling system driven by thermal energy was procured. Piping, valves, motors, and thermal sub-components were purchased and connected. Transducers included flow meters, thermistors, and relative humidity sensors. Desiccant solution concentration was monitored using a batch process density meter and a density-concentration correlation. A data acquisition system was designed and installed. The system is controlled using a programmable logic controller using relay ladder logic controlling the drive units for pumps and fans, and monitoring system faults. The system commissioning included troubleshooting and government safety inspections.

The system was tested in a field environment. Operating specifications varied from

the manufacturer, with the air flow rate 13% higher, and cooling water flow rate 23% lower. This has the effect of increasing the latent heat ratio, since less sensible cooling is provided by the cooling tower. The regenerator was driven by hot water supplied by a natural gas boiler. Hot water temperature was varied over 50, 70, and 90°C, as well as varied over a typical solar thermal array hot water supply temperature. The system was operated to dehumidify ambient air over 19 days in July. Data was collected by 26 sensors giving thermodynamic state variables of the process flows. The process flows for the system are heating and cooling water loops, supply and scavenging air streams, and the liquid desiccant loop. Data was averaged and collected every minute.

The data set was processed giving enthalpy flows and performance figures for daily operation of the machine. An enthalpy balance on the system was used to check sensors and assumption of adiabatic operation. The assumption of an adiabatic control volume around the conditioner and regenerator was found to be valid. Regenerator thermal COP was calculated to be 0.76 to 0.99, and conditioner thermal COP was in the range of 0.38 to 0.61 for the entire data set over 50°C to 90°C. Electrical COP increased from 0.58 at 50°C to 4.48 at 90°C. The average latent heat ratio was 1.1, 1.3, and 1.5 respectively for the three temperatures evaluated, showing that the heat load on the conditioner increases as the desiccant is heated in the regenerator. The average cooling power was 4.3, 14.1, and 21.3 kW for the temperature range. Data indicates that high temperature solar thermal collectors would achieve better performance based on their ability to maintain a desired cooling power and their increased electrical COP. Performance data was used to derive multivariate empirical models of the regenerator and conditioner. These models, equations, and the methods to obtain them are to provide a basis for future work in characterizing and optimizing

the solar cooling concept.

6.2 Recommendations & future work

Several recommendations for future investigation can be made, some of which have been discussed in section 5.6.

- Improve electrical COP by upgrading drive units to variable speed drives
- Vary remaining independent variables (primarily flow rates) to investigate effect on system performance
- Refine data collection procedure by controlling all independent variables except one
- Investigate higher order curve fitting to data
- Utilize mathematical model to simulate system connected to solar thermal array
- Investigate alternative liquid desiccant solutions
- Investigate methods and control schemes for installing auxilliary heating system combined with solar heating system
- Design liquid desiccant storage system for solar thermal heating

References

- [1] ASHRAE. *Ventilation for acceptable indoor air quality*. ASHRAE, 1791 Tullie Circle NE, Atlanta, GA, 62.1 edition, 2007.
- [2] P. Wargocki and R. Djukanovic. Simulations of the potential revenue from investment in improved indoor air quality in an office building. *ASHRAE Transactions*, 111:699 – 711, 2005.
- [3] Lewis G. III Harriman, Dean Plager, and Douglas Kosar. Dehumidification and cooling loads from ventilation air. *Energy Engineering: Journal of the Association of Energy Engineering*, 96(6):31 – 45, 1999.
- [4] ASHRAE. *Energy standard for buildings except low-rise residential buildings*. 1791 Tullie Circle NE, Atlanta, GA, 90.1 edition, 2007.
- [5] TIAX LLC. Matching the sensible heat ratio of air conditioning equipment with the building load shr. Technical report, TIAX LLC, 2003.
- [6] Paul Murphy. Focus on the future - the electricity challenge in Ontario - an electricity system perspective. Presentation to Toronto Board of Trade, June 2007.
- [7] IESO Historical Data. Ontario demand and market prices. Technical report, (IESO), 2007.
- [8] Stanley A. Mumma. Doas and desiccants. *Engineered Systems*, 24(8):37 – 49, 2007.
- [9] Luigi. Marletta. Exergy analysis of solar cooling. Technical report, Solar Heating & Cooling Programme - Task 38, January 2008.
- [10] Yunho Hwang, Reinhard Radermacher, Ali Al Alili, and Isoroku Kubo. Review of solar cooling technologies. *HVAC and R Research*, 14(3):507 – 528, 2008.
- [11] Löf. House heating and cooling with solar energy. *Solar Energy Research*, pages 33–46, 1955.

- [12] V. Öberg and D.Y. Goswami. *Advances in Solar Energy*. American Solar Energy Society, 1998.
- [13] K. Daou, R.Z. Wang, and Z.Z. Xia. Desiccant cooling air conditioning: A review. *Renewable and Sustainable Energy Reviews*, 10(2):55 – 77, 2006.
- [14] L. Mei and Y.J. Dai. A technical review on use of liquid-desiccant dehumidification for air-conditioning application. *Renewable and Sustainable Energy Reviews*, 12 (3):662 – 89, 2008.
- [15] A.A. Al-Farayedhi, P. Gandhidasan, M.A. Antar, and M.S. Abdul Gaffar. Experimental study of an aqueous desiccant mixture system: air dehumidification and desiccant regeneration. *Proceedings of the Institution of Mechanical Engineers, Part A (Journal of Power and Energy)*, 219(A8):669 – 80, 2005.
- [16] J. Martin Wimby and Thore S. Berntsson. Viscosity and density of aqueous solutions of LiBr, LiCl, ZnBr₂, CaCl₂, and LiNO₃. 1. single-salt solutions. *Journal of Chemical and Engineering Data*, 39:68 – 72, 1994.
- [17] A. Ertas, E.E. Anderson, and I. Kiris. Properties of a new liquid desiccant solution-lithium chloride and calcium chloride mixture. *Solar Energy*, 49(3):205 – 12, 1992.
- [18] Manuel R. Conde. Properties of aqueous solutions of lithium and calcium chlorides: Formulations for use in air conditioning equipment design. *International Journal of Thermal Sciences*, 43(4):367 – 382, 2004.
- [19] Donggen Peng, Xiaosong Zhang, and Yonggao Yin. Theoretical storage capacity for solar air pretreatment liquid collector/regenerator. *Applied Thermal Engineering*, 28(11-12):1259 – 66, 2008.
- [20] L.C.S. Mesquita and S.J. Harrison. Non-isothermal, flat-plate liquid-desiccant regenerators: A numerical study. *International Solar Energy Conference*, pages 325 – 331, 2005.
- [21] Lucio Cesar De Souza Mesquita. *Analysis of a Flat-Plate, Liquid-Desiccant, Dehumidifier and Regenerator*. PhD thesis, Queen's University, 2007.
- [22] Andrew Lowenstein, Steven Slayzak, and Eric Kozubal. A zero carryover liquid-desiccant air conditioner for solar applications. *Proceedings of International Solar Energy Conference*, pages 397 – 407, 2007.
- [23] Jeffrey Miller and Andrew Lowenstein. The field operation of a thermally driven liquid-desiccant air conditioner. *International Solar Energy Conference*, 2008.

- [24] John A. Duffie and William A. Beckman. *Solar Engineering of Thermal Processes*. John Wiley & Sons, Inc, 3rd edition, 2006.
- [25] Michael J. Moran and Howard N. Shapiro. *Fundamentals of Engineering Thermodynamics*. John Wiley & Sons, 2008.
- [26] Andrew Lowenstein, Marc Sibilia, Jeffrey Miller, and Thomas S. Tonon. U.S. Patent 6,745,826. Heat Exchange Assembly, 2004.
- [27] Jeffrey Miller. *OA3000 RLLplus stage overview*. AIL Research, draft edition, 2008.
- [28] ASHRAE. *1997 ASHRAE Handbook - Fundamentals*. American Society of Heating, Refrigerating, and Air-Conditioning Engineers, SI edition edition, 1997.
- [29] B.M. Jones and S.J. Harrison. First results of a solar thermal liquid-desiccant air conditioning concept. *Proceedings of 33rd Solar Energy Society of Canada Inc. conference*, 2008.
- [30] TRNSYS. *TRNSYS: A Transient Simulation Program, Ver. 16*. Solar Energy Laboratory, 2006.

Appendix A

Experimental results

A.1 Data set

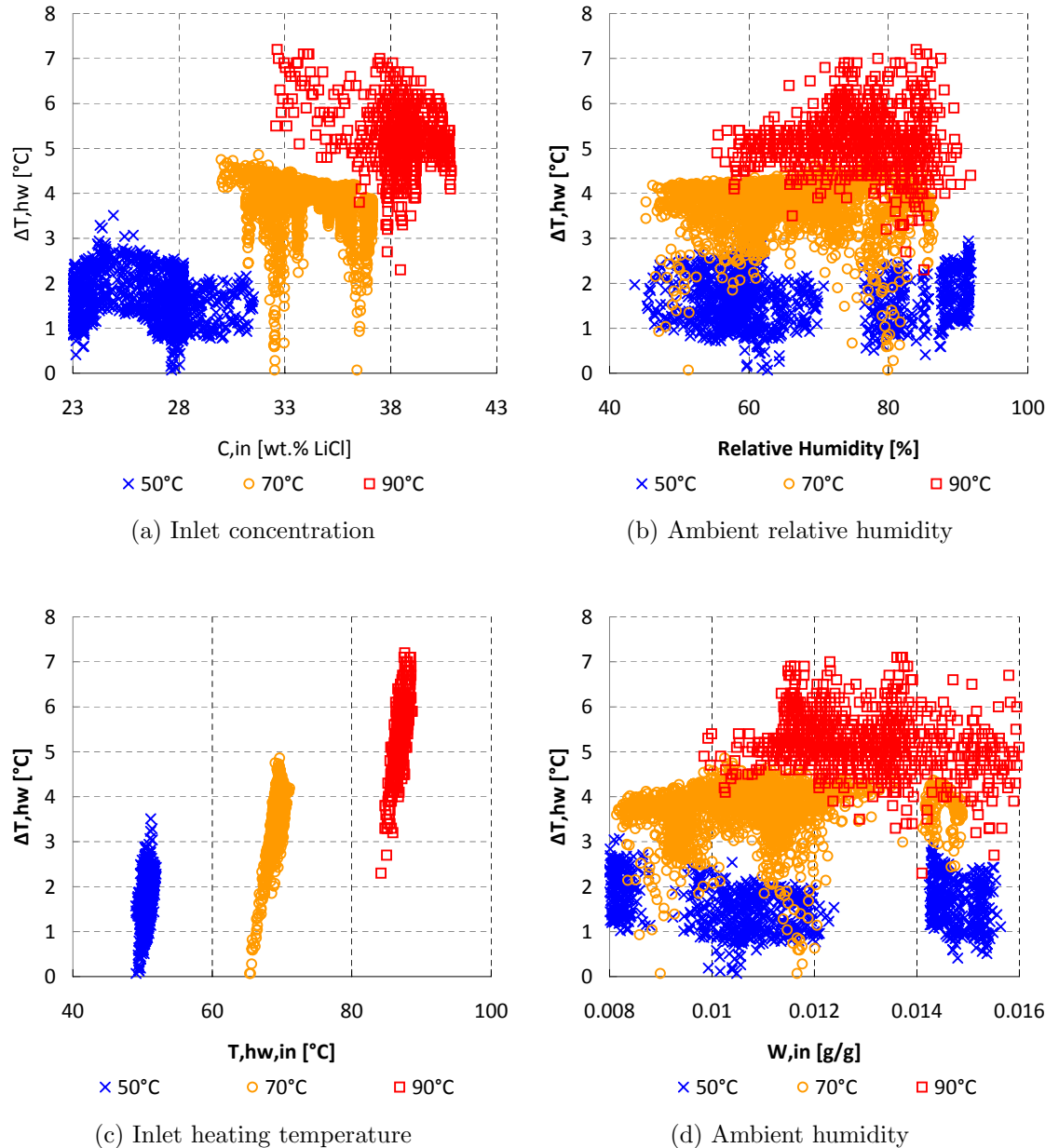


Figure A.1: Regenerator heating water temperature drop for various parameters

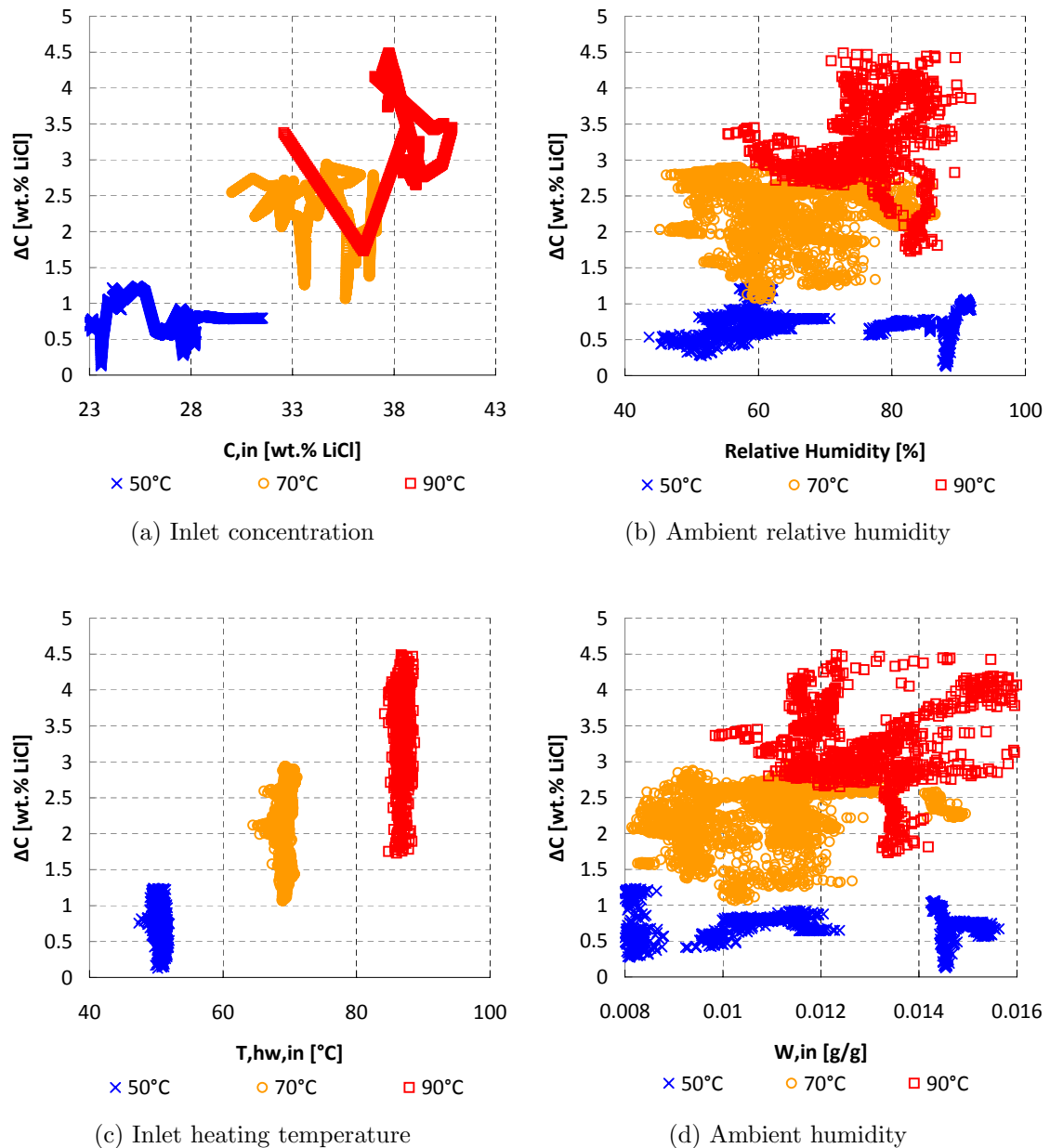


Figure A.2: Regenerator concentration change for various parameters

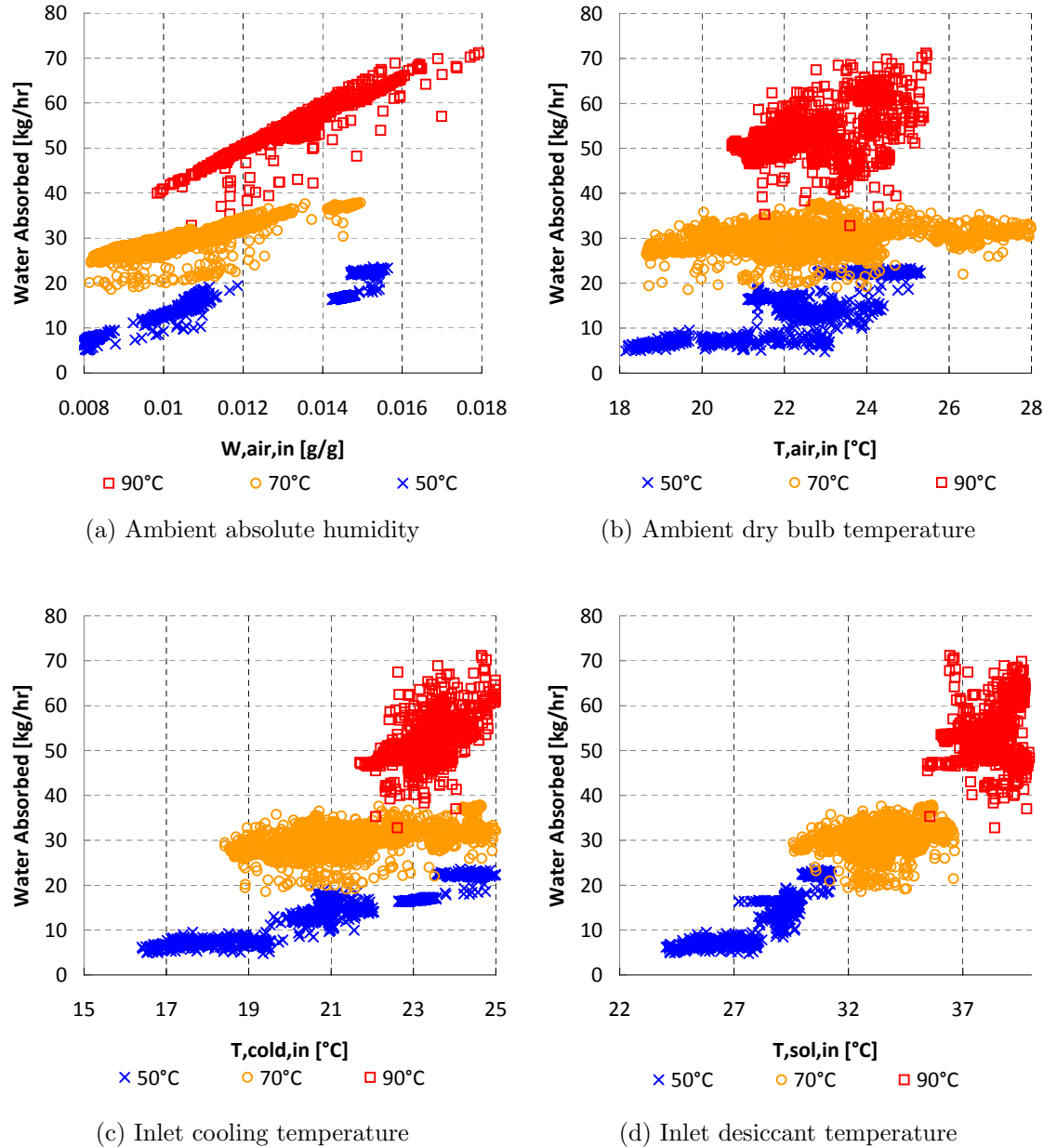


Figure A.3: Conditioner water absorption rate for various parameters

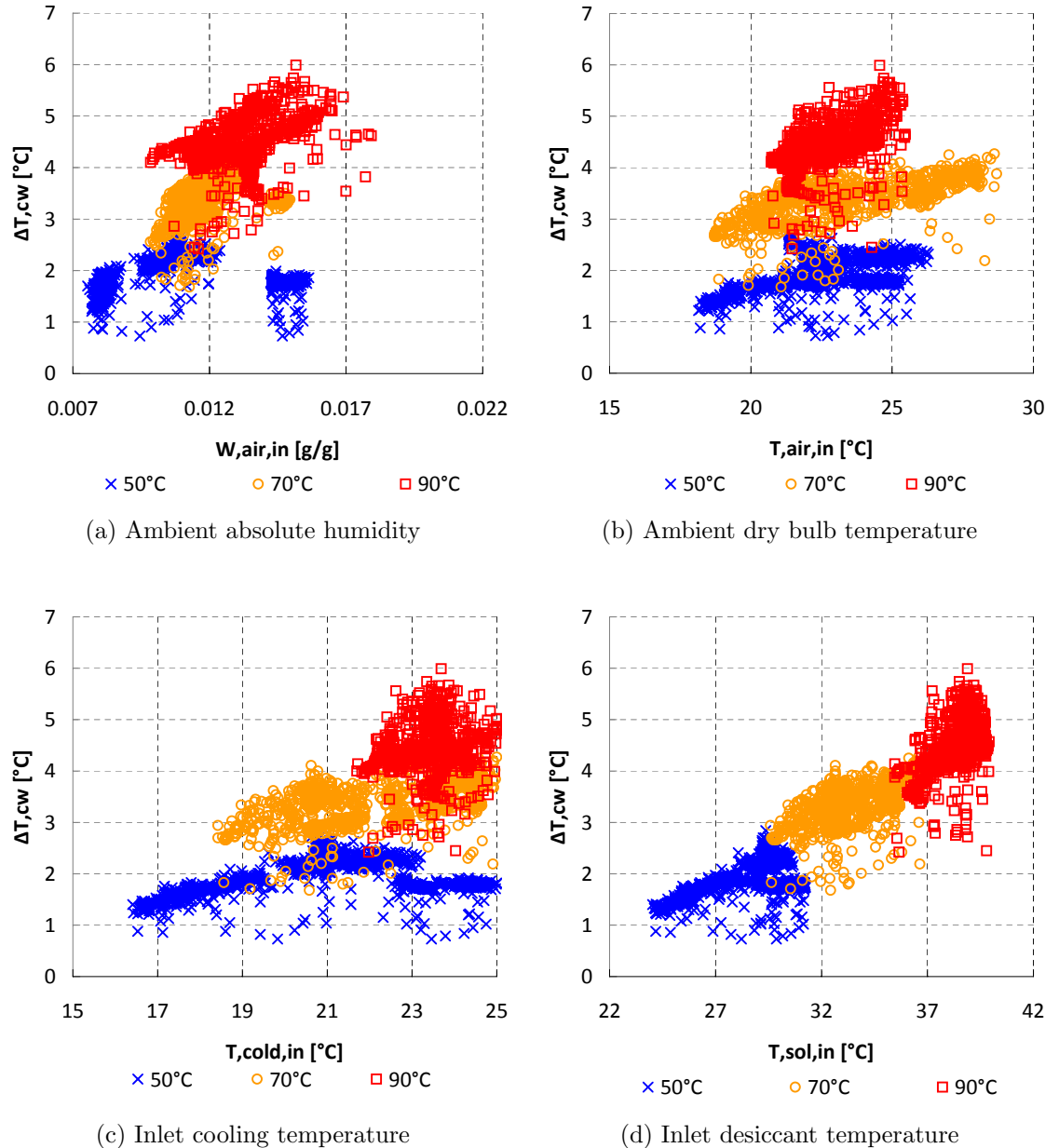


Figure A.4: Conditioner water absorption rate for various parameters

Quantity	Symbol	Note	Unit	Day (July 2008)					
				9-1	9-2	10	11	12	13
Start time	t_{start}	Time	hr	8.3	11.7	9.0	9.0	9.0	9.0
Time Period	Δt	Time	hr	2.9	2.9	7.0	7.0	7.0	6.0
Hot water inlet	$T_{hw,in}$	Avg.	°C	50.6	50.8	50.5	69.3	70.0	68.7
Hot water change	$\Delta T_{hw,in}$	Avg.	°C	-1.8	-1.5	-1.7	-3.9	-4.1	-3.4
Hot water flow	\dot{m}_{hw}	Avg.	kg/hr	6324.2	6274.3	6295.9	6225.8	6237.0	6250.2
Cold water in	$T_{cw,in}$	Avg.	°C	23.1	24.3	18.7	20.5	23.7	22.3
Cold water change	ΔT_{cw}	Avg.	°C	1.7	1.7	1.8	3.3	3.6	3.1
Cold water flow	$\dot{m}_{cw,c}$	Avg.	kg/hr	5188.9	5209.9	5148.5	5155.5	5197.5	5188.6
Ambient temperature	$T_{air,in}$	Avg.	°C	21.7	24.0	21.0	21.4	25.6	21.2
Ambient change	ΔT_{air}	Avg.	°C	2.7	2.2	0.1	2.2	1.5	3.7
Ambient humidity	W_{amb}	Avg.	g/kg	14.5	15.1	8.7	11.2	11.8	12.4
Ambient humidity change	ΔW	Avg.	g/kg	-2.6	-1.8	-1.0	-3.9	-3.8	-4.0
Air flow rate	\dot{m}_{air}	Avg.	kg/hr	7429.5	7241.1	7417.9	7354.2	7414.1	7511.5
Total cooling rate	\dot{Q}_{total}	Avg.	kW	4.4	4.2	4.9	15.9	16.9	13.4
Latent cooling rate	\dot{Q}_{latent}	Avg.	kW	7.9	8.1	5.1	20.9	20.4	21.5
Latent heat ratio	LHR	Avg.	-	1.8	1.9	1.0	1.3	1.2	1.6
Heating rate	\dot{Q}_{regen}	Avg.	kW	13.6	11.3	12.9	28.4	30.0	24.8
Water desorbed	$\dot{m}_{v,s-a,r}$	Tot.	kg	42.6	42.7	91.3	212.8	265.7	214.5
Desorption rate	$\dot{Q}_{v,s-a,r}$	Avg.	kW	10.0	10.0	8.9	21.3	26.9	25.0
Water absorbed	$\dot{m}_{v,a-s,c}$	Tot.	kg	39.5	34.0	50.8	204.5	198.4	181.4
Absorption rate	$\dot{Q}_{v,a-s,c}$	Avg.	kW	8.2	8.1	5.1	20.9	20.4	21.5
Thermal COP	$COP_{thermal}$	Avg.	-	0.74	0.89	0.70	0.75	0.90	1.01
Cooling COP	$COP_{cooling}$	Avg.	-	0.38	0.38	0.38	0.56	0.56	0.54
Electrical COP	COP_{elec}	Avg.	-	0.93	0.85	0.96	3.12	3.27	2.60
Regenerator concentration inlet	$C_{in,c}$	Avg.	Wt. %	23.85	23.04	26.88	33.00	34.32	32.18
Regenerator concentration change	ΔC_c	Avg.	Wt. %	-1.37	-1.20	-1.00	-2.18	-2.68	-1.85
Conditioner concentration inlet	$C_{in,r}$	Avg.	Wt. %	23.51	22.70	26.57	32.01	32.86	31.16
Conditioner concentration change	ΔC_r	Avg.	Wt. %	0.73	0.70	0.72	2.06	2.66	2.36

Table A.1: Daily performance table

Symbol	Note	Unit	Day (July 2008)							
			14	15	16-1	16-2	17	18	19	20
t_{start}	Time	hr	9.0	9.0	9.0	14.0	9.0	10.0	9.0	11.0
Δt	Time	hr	7.0	7.0	3.0	3.0	6.0	6.0	7.0	5.0
$T_{hw,in}$	Avg.	°C	69.0	69.5	87.1	79.2	79.2	78.4	60.8	86.6
$\Delta T_{hw,in}$	Avg.	°C	-3.6	-3.4	-5.2	-3.9	-4.1	-4.0	-2.5	-5.0
\dot{m}_{hw}	Avg.	kg/hr	6350.5	6863.3	6786.0	6776.1	6787.6	6785.2	6846.4	6793.5
$T_{cw,in}$	Avg.	°C	20.7	20.5	23.1	24.7	23.5	25.9	25.0	24.4
ΔT_{cw}	Avg.	°C	3.2	3.3	4.3	4.0	4.0	4.0	2.8	4.4
$\dot{m}_{cw,c}$	Avg.	kg/hr	5165.3	5145.7	5190.2	5173.9	5167.3	5190.6	5208.7	5210.2
$T_{air,in}$	Avg.	°C	21.9	21.3	22.7	26.7	25.3	25.8	26.4	22.9
ΔT_{air}	Avg.	°C	2.0	2.4	4.0	2.0	2.0	3.6	1.6	5.2
W_{amb}	Avg.	g/kg	9.5	9.2	11.5	12.0	11.5	14.8	13.8	14.3
ΔW	Avg.	g/kg	-3.3	-3.5	-5.1	-4.3	-4.3	-5.2	-2.9	-6.5
\dot{m}_{air}	Avg.	kg/hr	7332.3	7459.0	7361.4	7258.4	7295.2	7168.2	7335.2	7365.2
\dot{Q}_{total}	Avg.	kW	13.5	13.8	18.5	18.3	18.0	19.5	11.9	20.0
\dot{Q}_{latent}	Avg.	kW	18.2	19.6	28.0	23.1	22.7	27.0	15.0	30.4
LHR	Avg.	-	1.3	1.4	1.5	1.3	1.3	1.4	1.3	1.5
\dot{Q}_{regen}	Avg.	kW	27.1	27.6	41.8	31.4	32.4	32.1	20.0	40.3
$\dot{m}_{v,s-a,r}$	Tot.	kg	183.3	196.7	115.5	123.2	194.1	215.6	161.6	214.1
$\dot{Q}_{v,s-a,r}$	Avg.	kW	18.7	20.2	27.8	29.4	23.1	25.2	15.9	30.4
$\dot{m}_{v,a-s,c}$	Tot.	kg	175.0	187.1	114.0	95.5	187.5	227.2	149.9	208.9
$\dot{Q}_{v,a-s,c}$	Avg.	kW	18.2	19.6	28.0	23.1	22.7	27.0	15.0	30.4
$COP_{thermal}$	Avg.	-	0.69	0.73	0.67	0.93	0.71	0.79	0.80	0.75
$COP_{cooling}$	Avg.	-	0.50	0.50	0.44	0.58	0.55	0.61	0.59	0.50
COP_{elec}	Avg.	-	2.64	2.68	3.60	3.61	3.54	3.84	2.31	3.86
$C_{in,c}$	Avg.	Wt. %	35.67	36.94	39.73	36.95	36.76	34.23	29.24	37.30
ΔC_c	Avg.	Wt. %	-2.00	-2.33	-3.53	-3.03	-2.82	-3.26	-2.05	-2.97
$C_{in,r}$	Avg.	Wt. %	34.44	35.46	37.69	35.30	35.09	32.88	28.59	35.20
ΔC_r	Avg.	Wt. %	1.94	2.12	3.14	3.13	2.46	2.51	1.39	3.22

Table A.2: Daily performance table continued

Symbol	Note	Unit	Day (July 2008)						
			21	23	25	28	29	30 - 1	30 - 2
t_{start}	Time	hr	9.0	10.0	9.0	10.5	10.0	9.5	12.0
Δt	Time	hr	5.5	6.0	7.0	5.5	6.0	1.5	3.4
$T_{hw,in}$	Avg.	°C	86.9	Solar	Solar	50.7	69.4	87.3	77.7
$\Delta T_{hw,in}$	Avg.	°C	-5.2	-3.8	-3.5	-1.4	-3.8	-5.9	-3.8
\dot{m}_{hw}	Avg.	kg/hr	6765.8	6813.8	6779.2	6851.3	6826.9	6782.7	6788.5
$T_{cw,in}$	Avg.	°C	23.3	22.5	23.1	21.8	22.2	22.3	22.8
ΔT_{cw}	Avg.	°C	4.7	3.6	3.2	2.3	3.4	4.3	4.5
$\dot{m}_{cw,c}$	Avg.	kg/hr	5179.9	5128.0	5004.2	5094.4	5026.4	5026.4	4995.8
$T_{air,in}$	Avg.	°C	23.0	23.0	23.8	24.0	23.5	21.4	23.4
ΔT_{air}	Avg.	°C	4.1	2.7	2.4	0.7	2.2	4.3	3.3
W_{amb}	Avg.	g/kg	13.0	12.6	11.9	11.0	10.9	11.7	11.8
ΔW	Avg.	g/kg	-6.0	-4.5	-3.6	-1.9	-3.7	-5.4	-5.3
\dot{m}_{air}	Avg.	kg/hr	7285.7	7354.3	7415.3	7398.5	7416.2	7385.6	7417.9
\dot{Q}_{total}	Avg.	kW	22.8	17.1	13.5	8.3	14.2	18.5	20.1
\dot{Q}_{latent}	Avg.	kW	32.5	22.8	18.4	9.5	18.8	28.3	27.7
LHR	Avg.	-	1.4	1.3	1.4	1.1	1.3	1.5	1.4
\dot{Q}_{regen}	Avg.	kW	41.8	30.4	28.0	11.3	30.1	47.5	30.6
$\dot{m}_{v,s-a,r}$	Tot.	kg	224.9	202.6	190.2	72.7	210.1	68.9	132.0
$\dot{Q}_{v,s-a,r}$	Avg.	kW	29.4	23.7	19.1	9.1	24.9	33.2	28.4
$\dot{m}_{v,a-s,c}$	Tot.	kg	243.9	191.1	0.0	180.2	0.0	0.0	74.7
$\dot{Q}_{v,a-s,c}$	Avg.	kW	32.5	22.8	18.4	9.5	18.8	28.3	27.7
$COP_{thermal}$	Avg.	-	0.70	0.78	0.68	0.81	0.83	0.70	0.93
$COP_{cooling}$	Avg.	-	0.55	0.56	0.48	0.73	0.47	0.39	0.66
COP_{elec}	Avg.	-	4.47	3.37	2.68	1.63	2.75	3.57	3.89
$C_{in,c}$	Avg.	Wt. %	38.77	33.33	32.78	28.42	34.79	39.05	38.53
ΔC_c	Avg.	Wt. %	-3.76	-2.42	-2.21	-1.34	-2.37	-3.16	-3.54
$C_{in,r}$	Avg.	Wt. %	36.63	32.27	31.80	28.06	33.69	37.06	36.62
ΔC_r	Avg.	Wt. %	3.15	2.34	1.88	0.79	2.56	3.69	3.14

Table A.3: Daily performance table continued

A.2 Daily profiles

A.3 Regression correlations

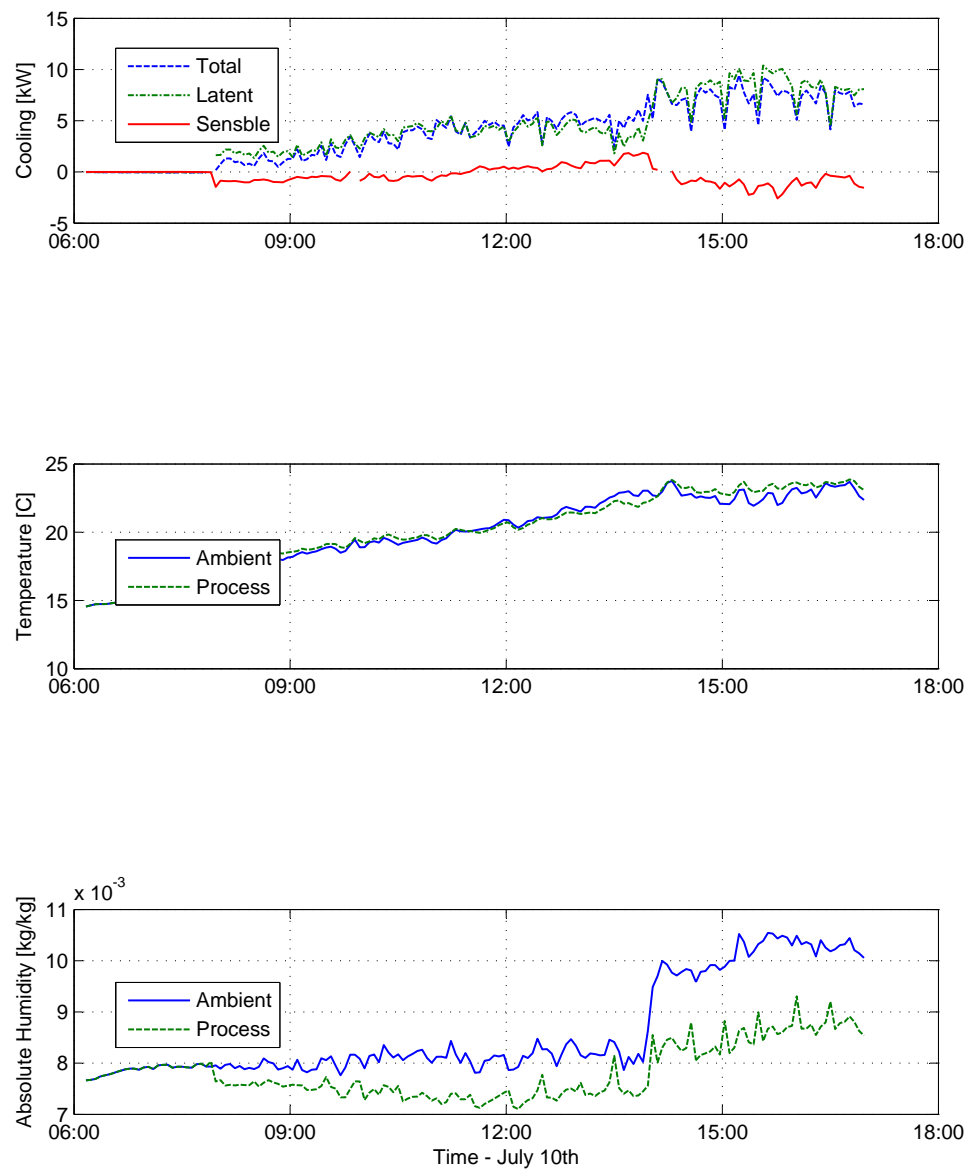


Figure A.5: Conditioner performance - July 10th

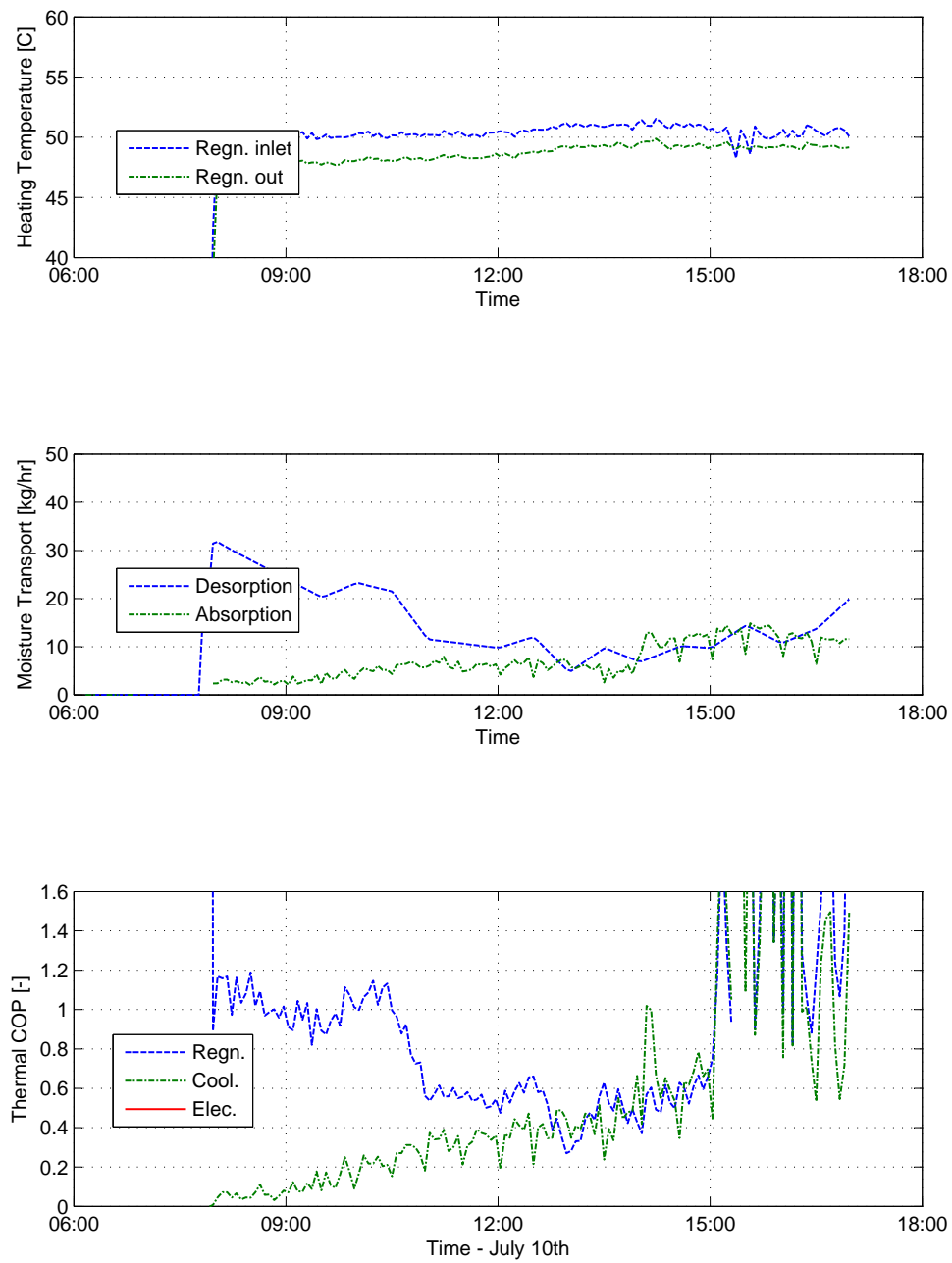


Figure A.6: Heating temperature & performance figures - July 10th

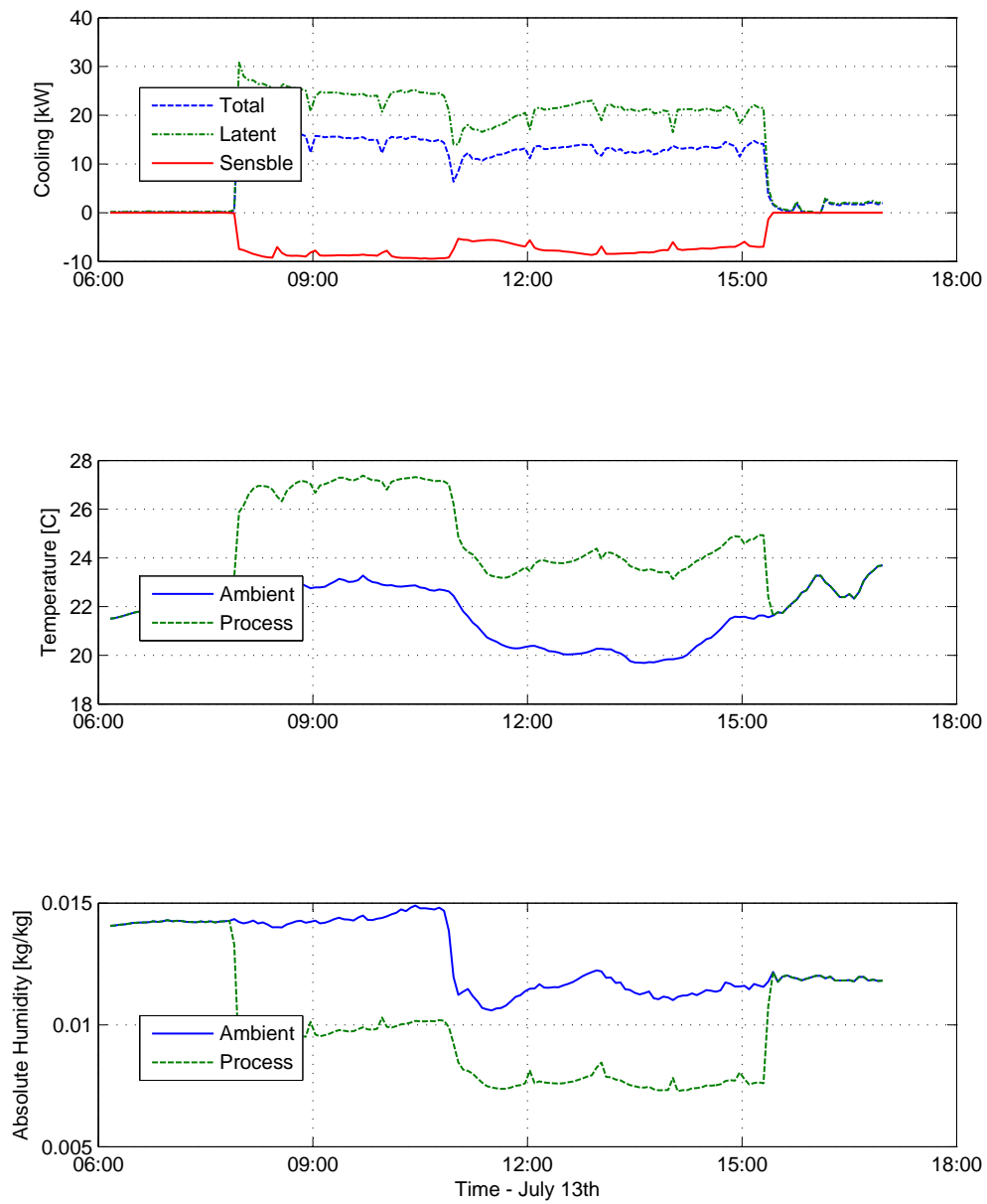


Figure A.7: Conditioner performance - July 13th

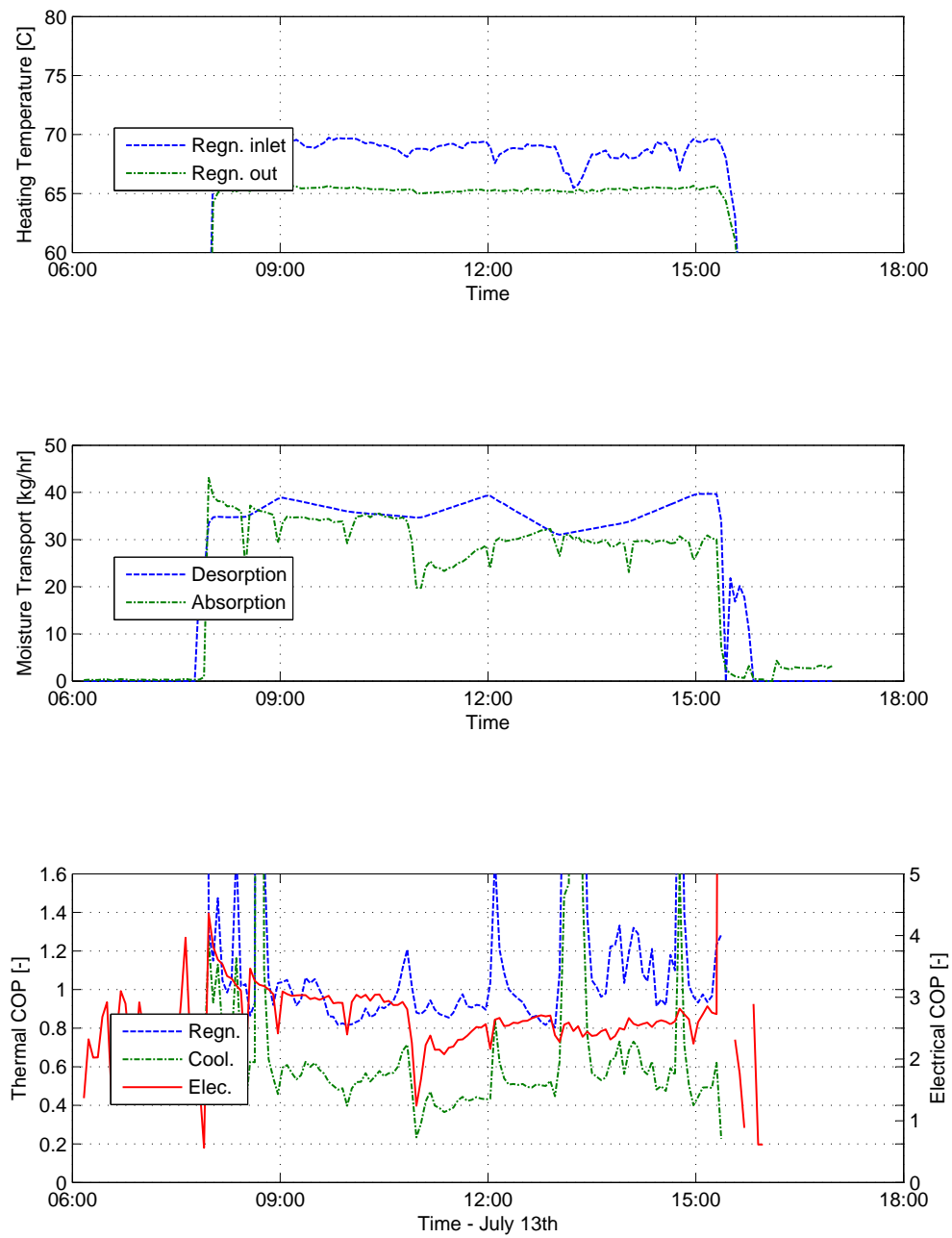


Figure A.8: Heating temperature & performance figures - July 13th

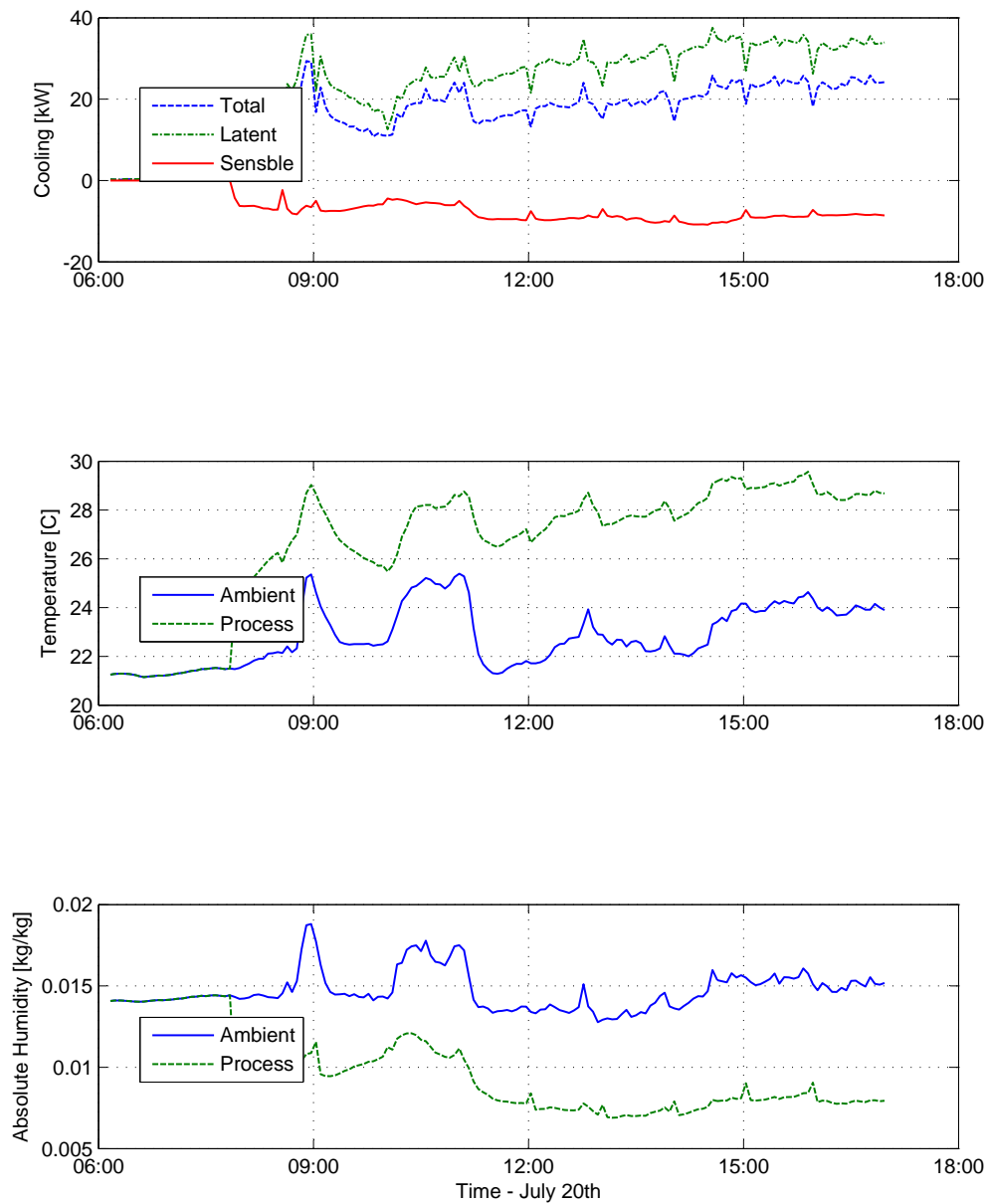


Figure A.9: Conditioner performance - July 20th

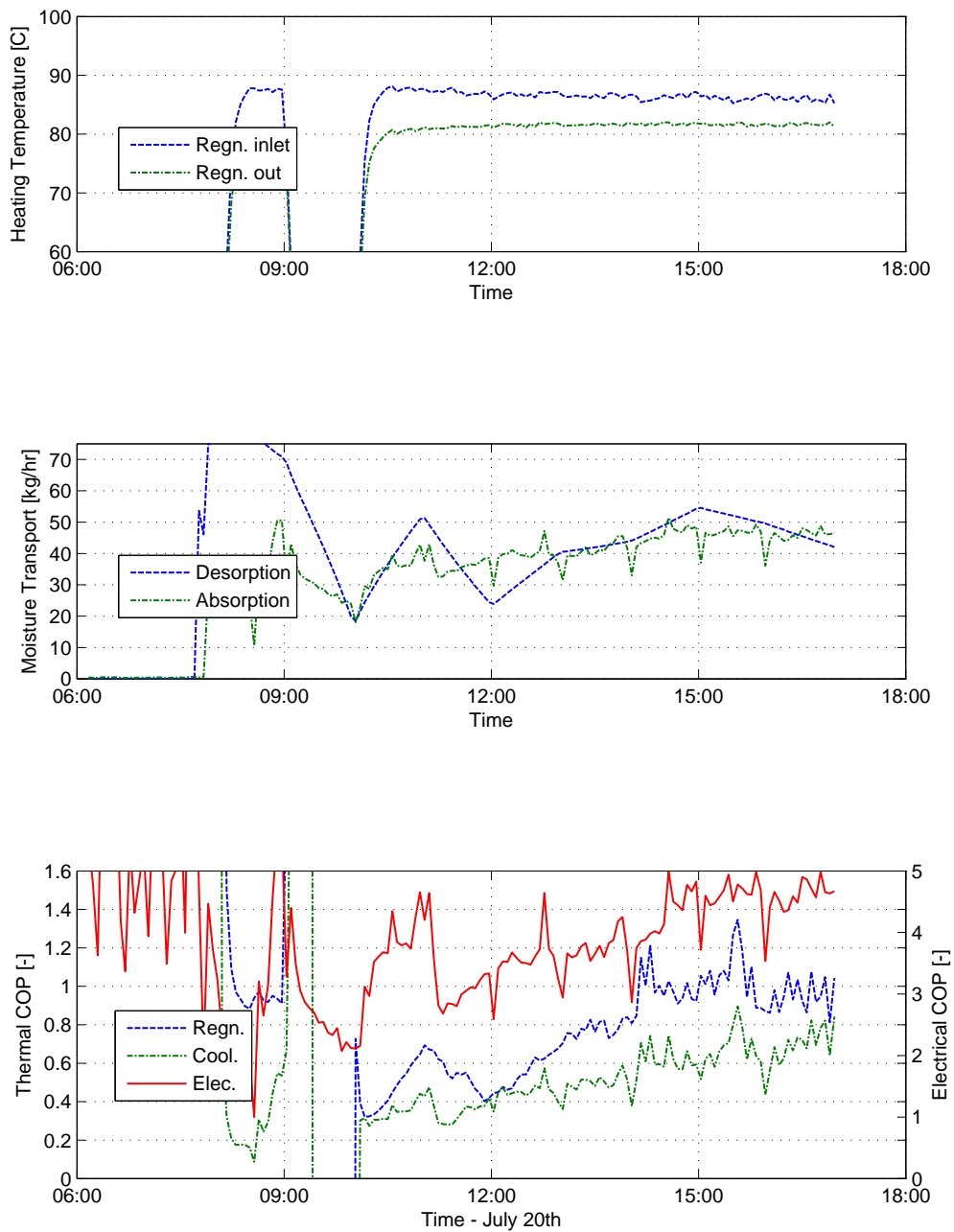


Figure A.10: Heating temperature & performance figures - July 20th

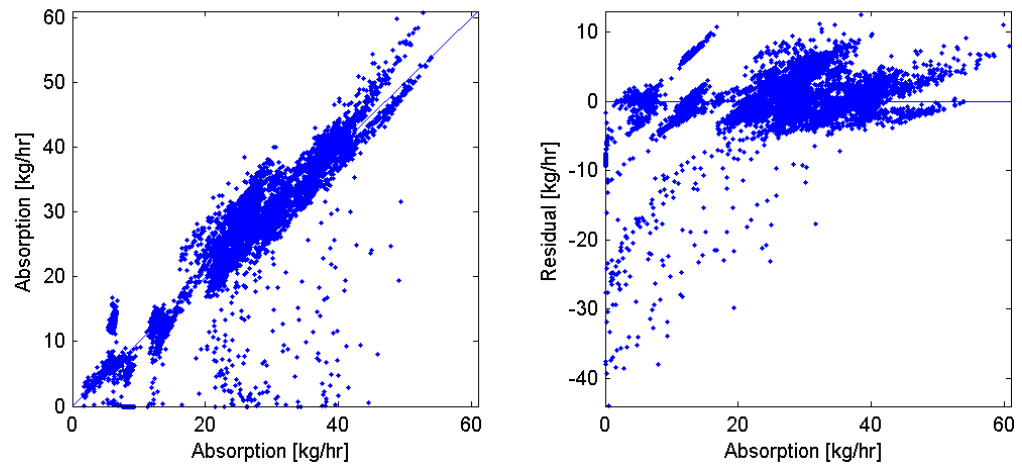


Figure A.11: Water absorption correlation for 2 variables

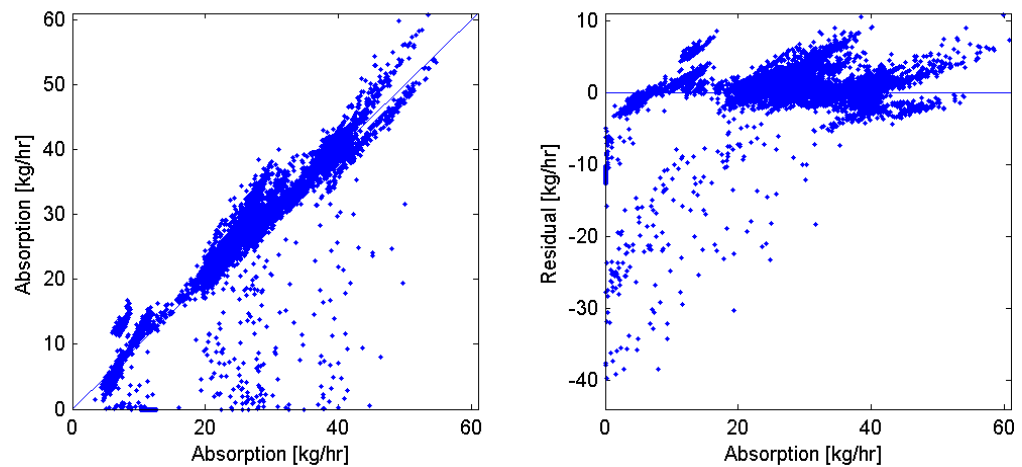


Figure A.12: Water absorption correlation for 3 variables

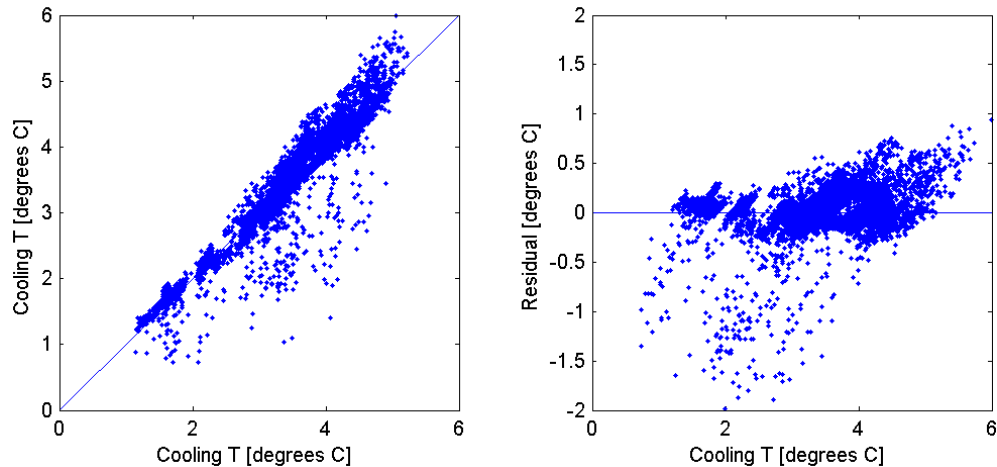


Figure A.13: Cooling water temperature change correlation for 2 variables

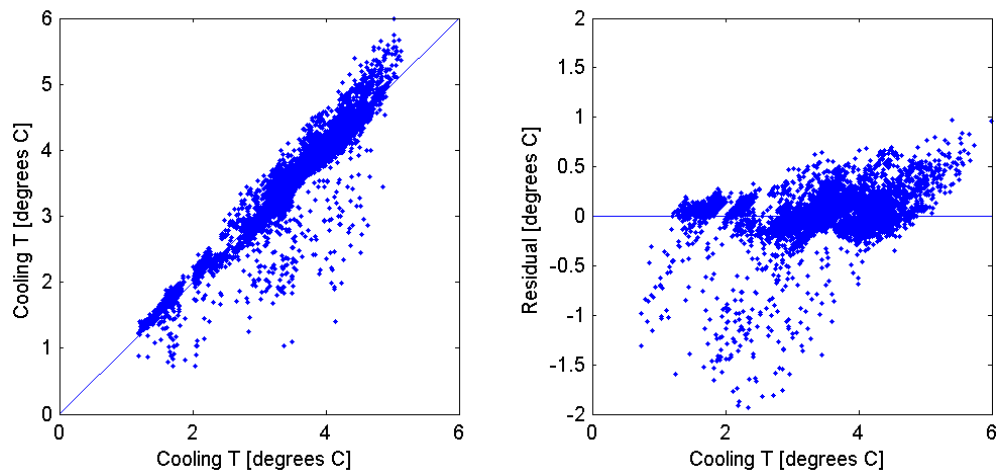


Figure A.14: Cooling water temperature change correlation for 3 variables

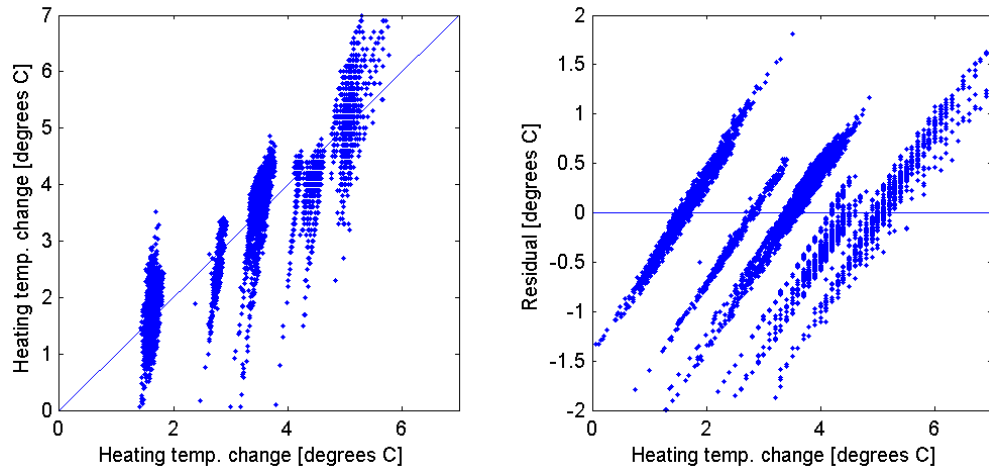


Figure A.15: Heating temperature change correlation for 2 variables

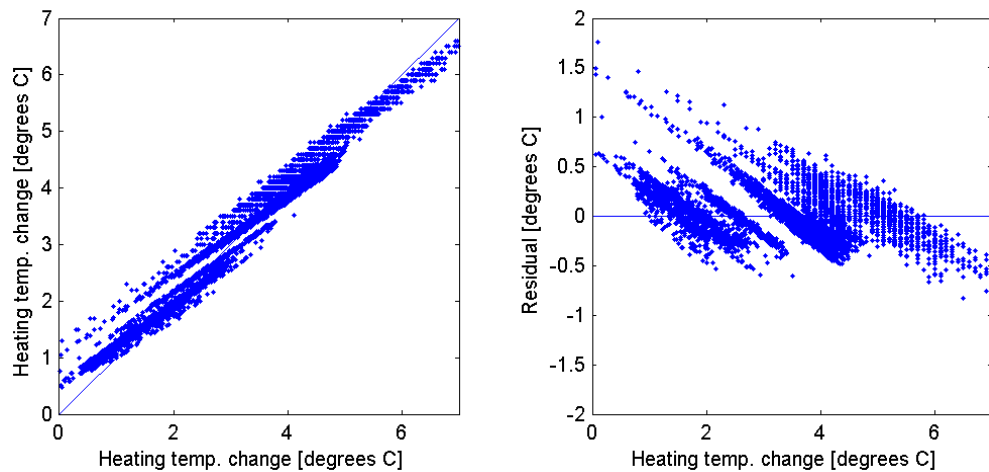


Figure A.16: Heating temperature change correlation for 3 variables

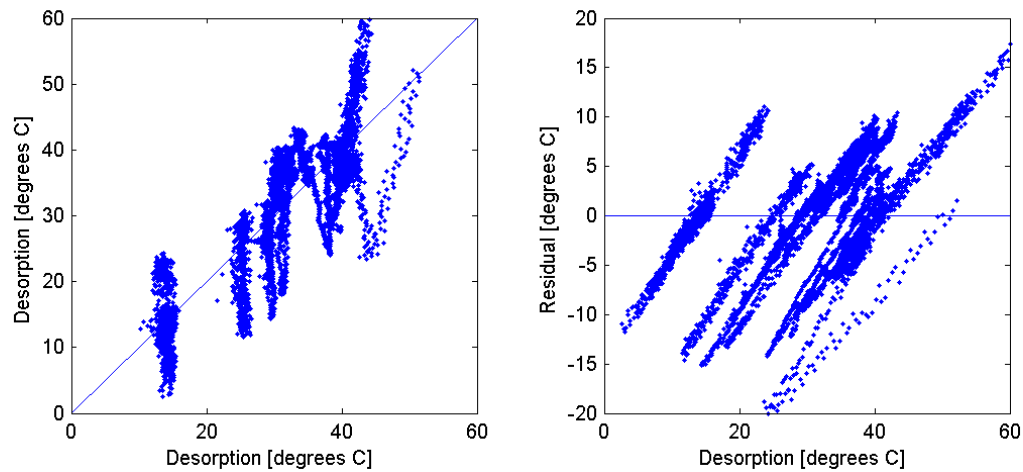


Figure A.17: Heating temperature change correlation for 2 variables

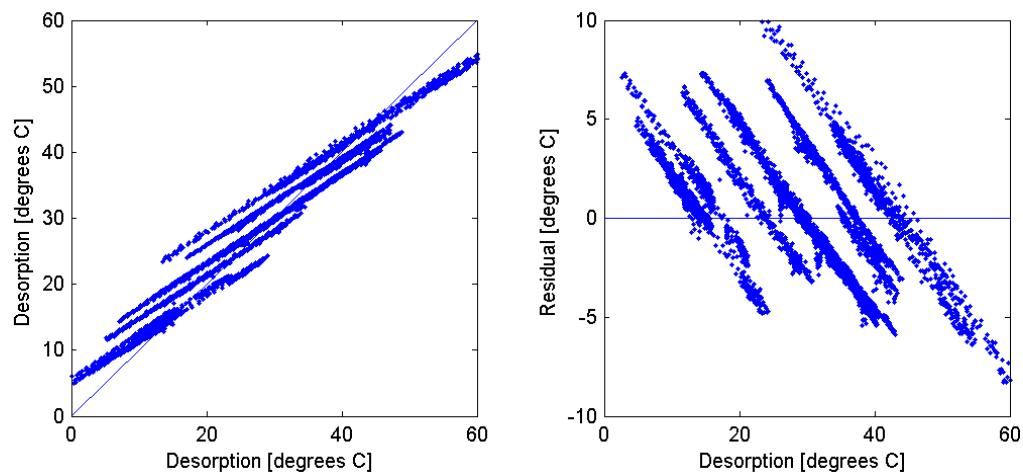


Figure A.18: Heating temperature change correlation for 3 variables

Appendix B

Data acquisition and control

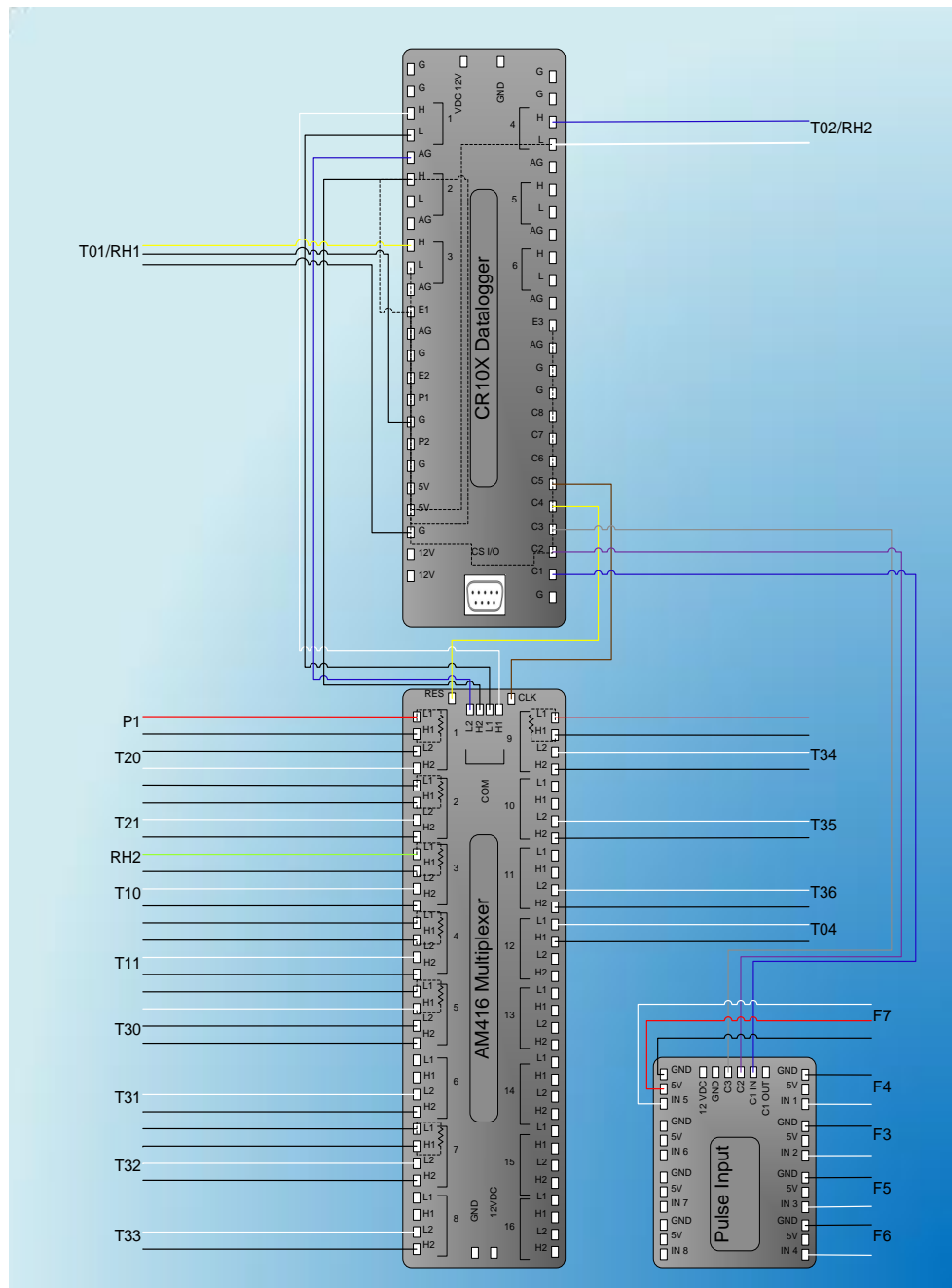


Figure B.1: Data Acquisition System Wiring

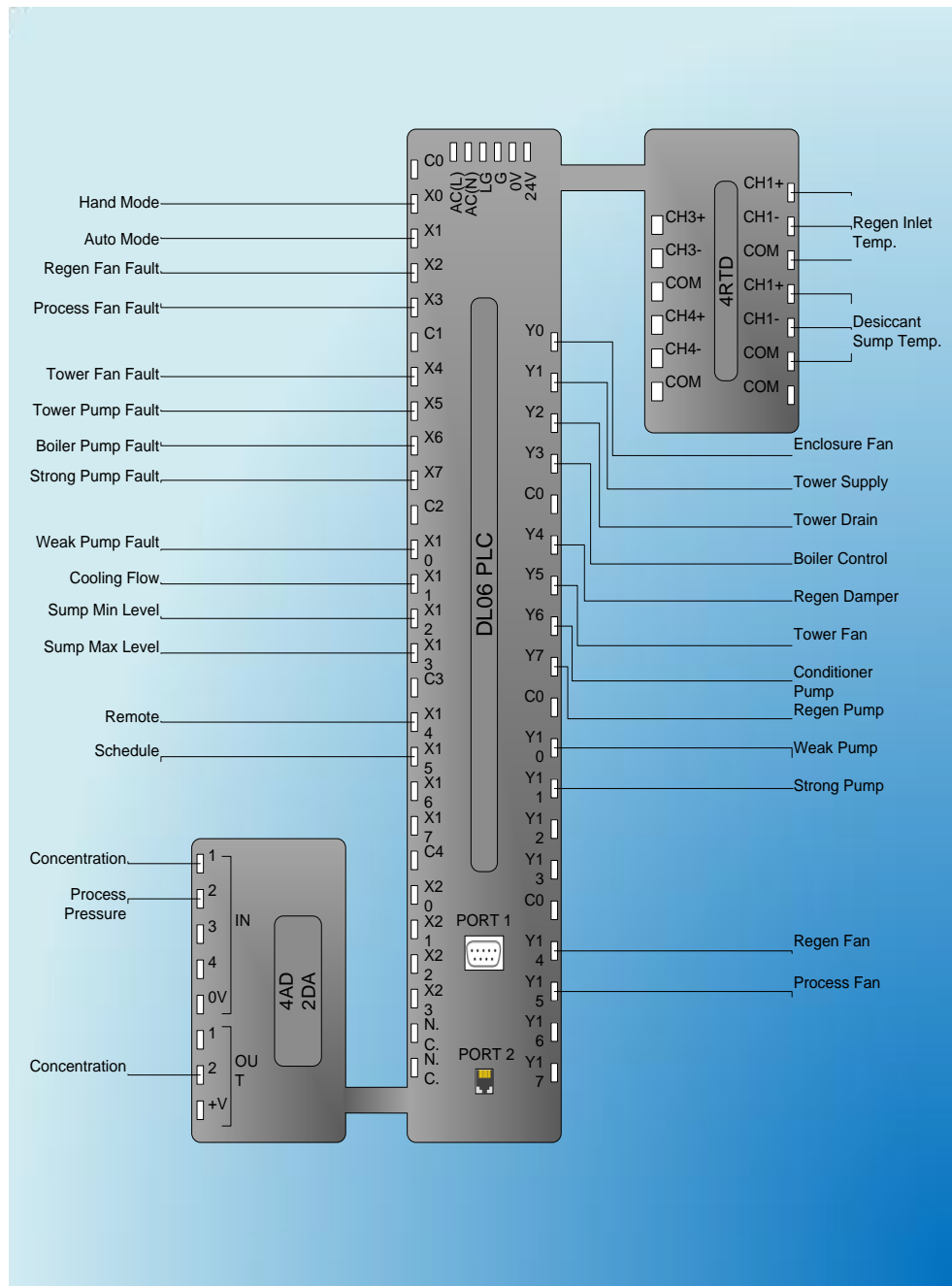


Figure B.2: Programmable Logic Controller Wiring

System	Tag	Label	Units	Location	Description	Sensor	Rated Accuracy
Desiccant	-	-	%	-	Concentration	Manual Data Collection	±2% LiCl
Process Air	F1	RUSKPAMS	in. water	Process outlet	Process Flow	Ruskin AMS 810	±3%
Heating	F3	LPMHot	Liter/min	Hot water supply	Regen Flow	AMCO M190 Hot Water Meter (1 1/2")	±1.5%
Cooling	F4	LPMCool	Liter/min	Cold water supply	Cooling flow	AMCO C700 Water Meter (1 1/2") Pulser Type SF	±1.5%
Desiccant	F5	LPMDesC	Liter/min	Absorber inlet	Strong flow (Abs)	Omega FTB6207-PS	±1.5%
Desiccant	F6	LPMDesR	Liter/min	Regenerator inlet	Weak flow (Regen)	Omega FTB6207-PS	±1.5%
Gas	F7	CFMNgas	Liter/min	Gas supply	Gas consumption	American Meter Company AC-250	±1.5%
Electrical	P1	Power	Watt	Main 3 phase line	Main Power	Watt Node WNB-3D-240-P	±0.5%
Process Air	RH1	RHamb	%	Outdoor	Outdoor RH	Campbell Scientific HMP45C-L25	±2% RH
Process Air	RH2	Rhprocess1	%	Process outlet	Process RH	Vaisala HMD60Y HUMICAP 180	±1.5% RH
Process Air	RH3	Rhprocess2	%	Process outlet	Process RH	Vaisala HMT330	±2% RH
Process Air	T01	Tamb	°C	Outdoor	Outdoor DB	Campbell Scientific HMP45C-L25	±0.3°C
Process Air	T02	Tprocess	°C	Process outlet	Process DB	Vaisala HMD60Y PT1000RTD	±0.15°C
Process Air	T03	Tprocess	°C	Process outlet	Process DB	Vaisala HMT330	±0.2°C
Heating	T10	THotIn	°C	Regen inlet	Regen inlet	10k thermistor (4159-3/16-6-25-TH44036)	±0.3°C
Heating	T11	THotOut	°C	Regen outlet	Regen outlet	10k thermistor (4159-3/16-6-25-TH44036)	±0.3°C
Cooling	T20	TCoolIn	°C	Absorber inlet	Absorber inlet	10k thermistor (4159-3/16-6-25-TH44036)	±0.3°C
Cooling	T21	TCoolOut	°C	Absorber outlet	Absorber outlet	10k thermistor (4159-3/16-6-25-TH44036)	±0.3°C
Desiccant	T30	TDesCIn	°C	Absorber inlet	Absorber inlet	10k thermistor (4159-1/8-6-25-TH44036-FEP)	±0.3°C
Desiccant	T31	TDesCOut	°C	Absorber outlet	Absorber outlet	10k thermistor (4159-1/8-6-25-TH44036-FEP)	±0.3°C
Desiccant	T32	TDesRIn	°C	Regenerator inlet	Regen inlet	10k thermistor (4159-1/8-6-25-TH44036-FEP)	±0.3°C
Desiccant	T33	TDesROut	°C	Regenerator outlet	Regen outlet	10k thermistor (4159-1/8-6-25-TH44036-FEP)	±0.3°C
Desiccant	T34	TDesHIn	°C	Regen HX inlet	Regen HX inlet	10k thermistor (4159-1/8-6-25-TH44036-FEP)	±0.3°C
Desiccant	T35	TDesHOut	°C	Regen HX outlet	Regen HX outlet	10k thermistor (4159-1/8-6-25-TH44036-FEP)	±0.3°C
Sump	T36	TDesSump	°C	Sump	Sump temperature	10k thermistor (4159-1/8-12-25-TH44036-FEP)	±0.3°C
Scavenging Air	T04	Treg	Celsius	Regen Outlet	Regen outlet	10k thermistor (H-MIX)	±0.3°C

Table B.1: Data acquisition specification and cross reference

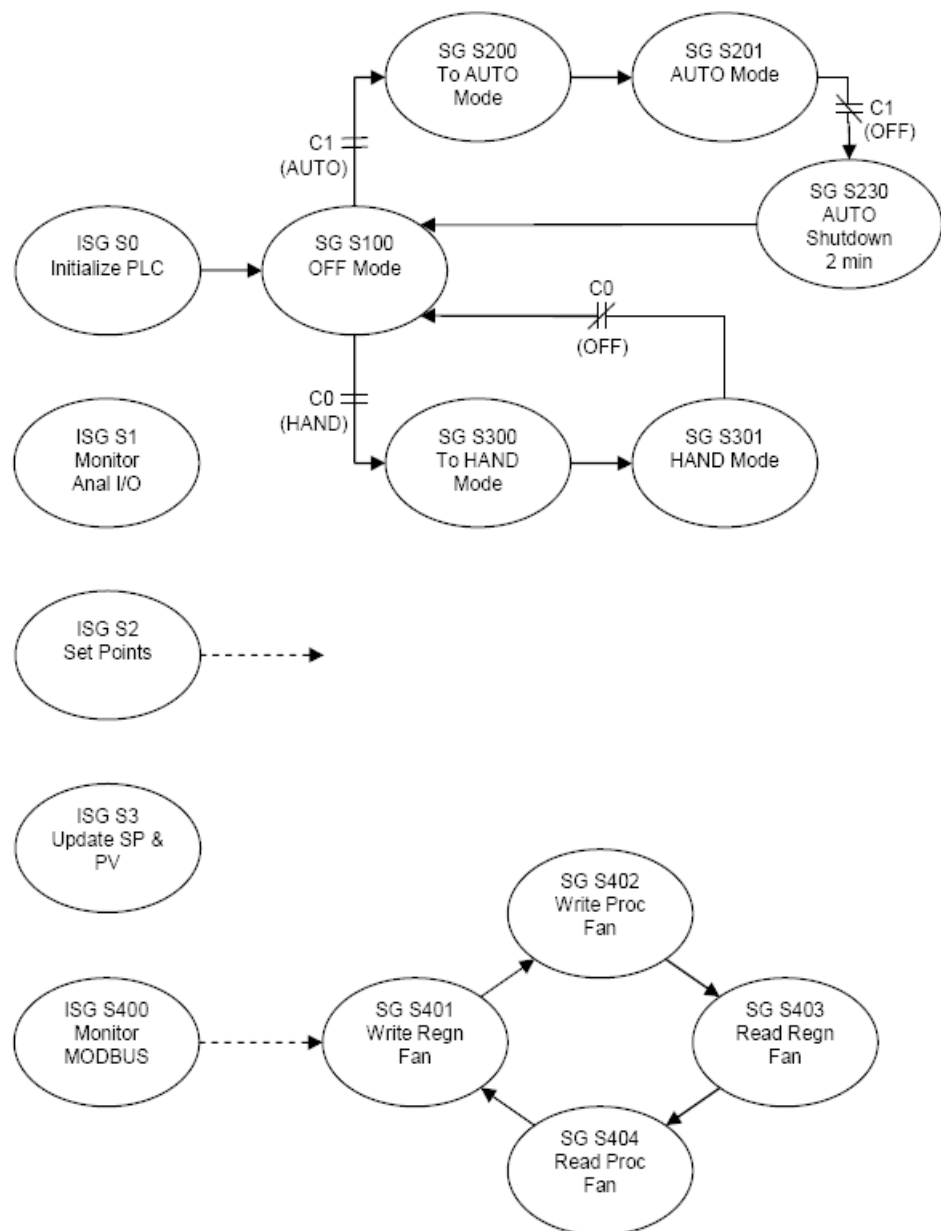


Figure B.3: Programmable Logic Controller Initialization Stage

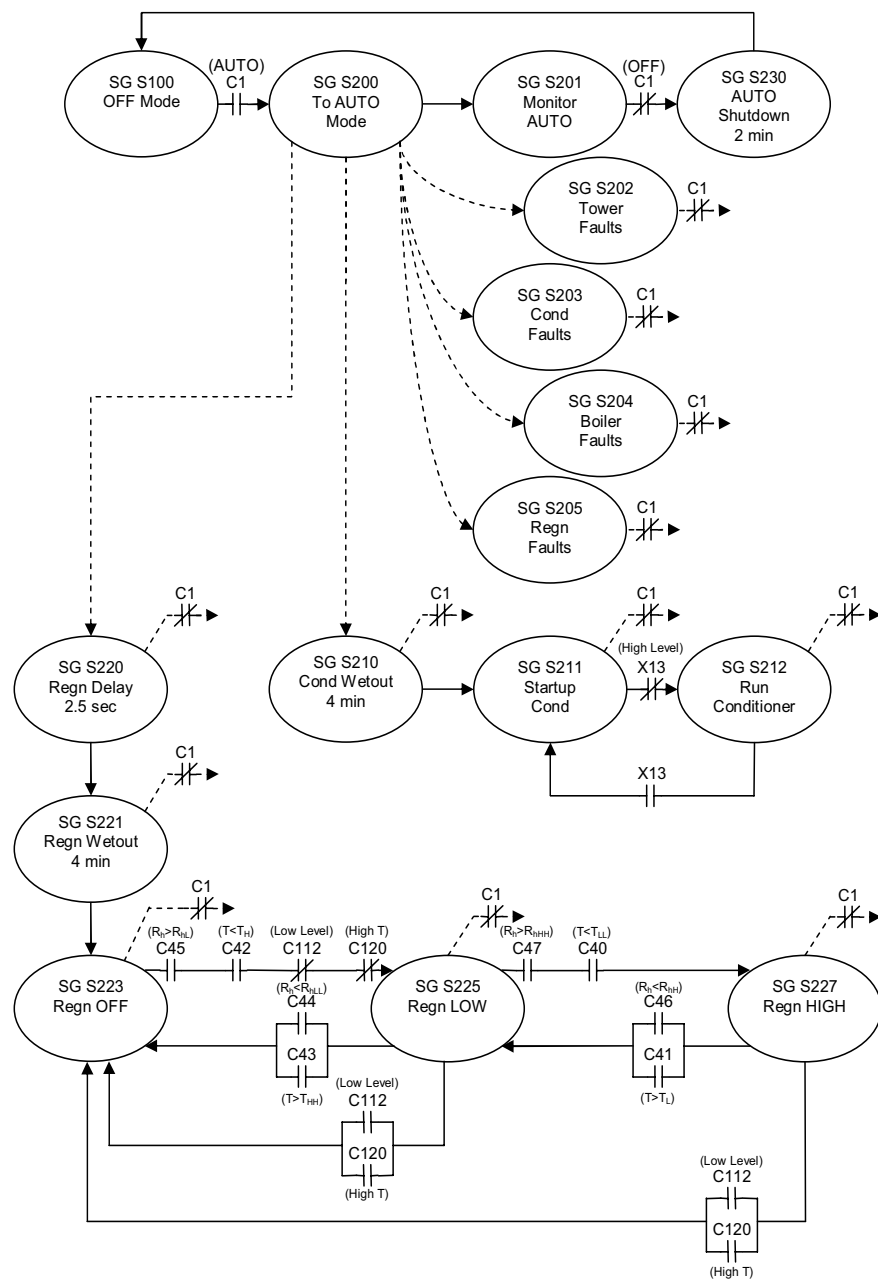


Figure B.4: Programmable Logic Controller Control Stage

Appendix C

Matlab data processing

C.0.1 Script: Air stream processing

```
% This script generates air state properties at three positions within the
% air flow path using the ambient, and two outlet T/RH sensors
% RH and T data is expanded to include W (humidity ratio) and H (enthalpy)
% using Ashrae correlations found in the following functions;
% function EnthalpyAir=EnthalpyAir(TC,W)
% function Wratio=Wratio(T,p,phi)
% Air.Amb - Ambient Sensor
% Air.Proc1 - AIL supplied sensor
% Air.Proc2 - SCL supplied sensor
% Air.Proc - Best sensor values, see '080611 Calibration report.pdf'

% Assumption;
AmbPres = 101300; % [Pa] Atmospheric pressure is constant at 1 atm

% Ambient air data
Air.Amb.Pres = AmbPres*ones(length(DatedData(:,1)),1);
Air.Amb.Temp = DatedData(:,L.Tamb_C);
Air.Amb.RH = DatedData(:,L.RHamb);
Air.Amb.W = Wratio(DatedData(:,L.Tamb_C),AmbPres,DatedData(:,L.RHamb));
Air.Amb.H = EnthalpyAir(DatedData(:,L.Tamb_C),Air.Amb.W);

% Original AIL supplied sensor
Air.Proc1.Pres = real(AmbPres*ones(length(DatedData(:,1)),1));
Air.Proc1.Temp = real(DatedData(:,L.T_fan));
Air.Proc1.RH = real(DatedData(:,L.RH_fan));
Air.Proc1.W = real(Wratio(DatedData(:,L.T_fan),AmbPres,DatedData(:,L.RH_fan)));
Air.Proc1.H = EnthalpyAir(DatedData(:,L.T_fan),Air.Proc1.W);

% Calibrated sensor air data (in duct)
Air.Proc2.Pres = AmbPres*ones(length(DatedData(:,1)),1);
Air.Proc2.Temp = DatedData(:,L.Tcal);
Air.Proc2.RH = DatedData(:,L.RHcal);
```

```

Air.Proc2.W = Wratio(DatedData(:,L.Tcal),AmbPres,DatedData(:,L.RHcal));
Air.Proc2.H = EnthalpyAir(DatedData(:,L.Tcal),Air.Proc2.W);

% This is the final outlet condition used, based on the sensor calibration
Air.Proc.Pres = Air.Proc1.Pres; % This is assumed pressure
Air.Proc.Temp = Air.Proc2.Temp; % Use SCL sensor
Air.Proc.RH = Air.Proc1.RH; % Use the AIL sensor
Air.Proc.W = Wratio(Air.Proc.Temp,AmbPres,Air.Proc.RH);
Air.Proc.H = EnthalpyAir(Air.Proc.Temp,Air.Proc.W);

% A 10k thermistor was added to the outlet of the regenerator
Air.Reg.Temp = DatedData(:,39);

% Flow rate as given by AMS
Air.FlowLPS = ...
    DatedData(:,L.RuskinAir)...    %
;

% Convert flow rate [L/s] to [kg/h]
Air.FlowKH = Air.FlowLPS * 60 * 60 / 1000 .* ... % Convert to m3/hr
interp1(AirProps.Temp,AirProps.Dens,... % Lookup table
    (Air.Proc.Temp + Air.Amb.Temp)/2, ... % Average air temperature
    'pchip');

% Recalibrate the air flow - AMS gives inaccurate data
Air.FlowKH = Air.FlowKH .* 1.54

% A regenerator flow rate of 430 cfm was measured
Air.FlowRegenKH = 430 * 0.4718 * 60 * 60 / 1000 .* ... % Convert to m3/hr
interp1(AirProps.Temp,AirProps.Dens,... % Lookup table
    (Air.Reg.Temp + Air.Amb.Temp)./2, ... % This is the average air temperature
    'pchip');

Air.FlowRegenKH = Air.FlowRegenKH.* (Air.Reg.Temp./Air.Reg.Temp);

clear AmbPres

```

C.0.2 Function: Humidity ratio calculation

```

% This function returns the humidity ratio given the rh, temperature,
% and pressure from Ashrae correlation
% T [C]
% p [Pa]
% rh [%]
% W [kg/kg]

function Wratio=Wratio(T,p,phi)

T = T + 273;
phi = phi/100;
% Finding W from eq. 22
% Where p_w is the partial pressure of water vapor and p is the
% total pressure.
% W = M_w/M_a;
%
% W = ----
%          M[w]
%          M[a]
%
% M_w is the mass of water, M_a is the mass of air

```

```
% W = .62198*x[w]/x[a];
%                               0.62198 x[w]
%                               -----
%                               x[a]
% x_w/x_a is the mole fraction ratio, multiplied by the ratio of
% molecular masses, 18.01528/28.9645 = 0.62198.
% The partial pressure of water, p_w is derived from;
% phi = (p_w)/(p_ws)

%Where p_ws [Pa] is the saturation pressure of water vapor in
%the absence of air at a given temperature
%The saturation pressure over liquid water for 0 to 200degC is;

C_8 = -5800.2206;
C_9 = 1.3914993;
C_10 = -0.48640239e-1;
C_11 = 0.41764768e-4;
C_12 = -0.14452093e-7;
C_13 = 6.5459673;

% Find p_ws from empirical fit against T
p_ws = exp(C_8./T+C_9+C_10.*T+C_11.*T.^2+C_12.*T.^3+C_13.*log(T));

% Use p_ws and rh to get p_w
p_w = p_ws.*phi;

% W is a function of p and p_w
Wratio = .62198.*p_w./(p-p_w);

end
```

C.0.3 Function: Air enthalpy calculation

```
% This function returns the enthalpy of the air from ASHRAE fundamentals
% T [C]
% W [kg/kg]

function EnthalpyAir=EnthalpyAir(TC,W)

EnthalpyAir = 1.006.*TC + W.*(2501+1.805.*TC);

end
```

C.0.4 Script: Enthalpy flow rates and performance factors

```
% This script compiles the enthalpy flow rates [kJ/hr]
% and performance parameters

%%%%%%%%%%%%%
% Water sorption rates
% For conditioner, both delta W and delta C give rate
% For regenerator, only delta C is available, until enthalpy balance is
% completed
%%%%%%%%%%%%%
Perf.C.WA_Air = Air.FlowKH.* (Air.Amb.W - Air.Proc.W); % [kg/hr]
```

```

Perf.C.WA_Des = Des.C.FlowInKH.* (Des.C.ConcIn./Des.C.ConcOut-1); % [kg/hr]
Perf.R.WR_Des = Des.R.FlowInKH.* (Des.R.ConcOut./Des.R.ConcIn-1); % [kg/hr]
% Can't calc R.WR_Air yet!

%%%%%%%%%%%%%
% Update desiccant data by adding the corrected outlet flow rate
%%%%%%%%%%%%%
Des.C.FlowOutKH_Air = Des.C.FlowInKH + Perf.C.WA_Air; % [kg/hr]
Des.C.FlowOutKH_Des = Des.C.FlowInKH + Perf.C.WA_Des; % [kg/hr]
Des.R.FlowOutKH_Des = Des.R.FlowInKH - Perf.R.WR_Des; % [kg/hr]

%%%%%%%%%%%%%
% Enthalpy of cooling water
%%%%%%%%%%%%%
Enthalpy.Cond.CW.In = ...
    Cold.FlowKH .* (... % Flow rate [kg/hr]
    Cold.Temp.In.* ... % Temp [deg C]
    interp1(WaterProps.Temp, ...
        WaterProps.SpecHeat,Cold.Temp.In,'pchip') ... Cp [kJ/kg/degC]
    ); % [kJ/hr]
Enthalpy.Cond.CW.Out = ...
    Cold.FlowKH .* (... % Flow rate [kg/hr]
    Cold.Temp.Out.* ... % Temp [deg C]
    interp1(WaterProps.Temp, ...
        WaterProps.SpecHeat,Cold.Temp.Out,'pchip') ... % Cp [kJ/kg/degC]
    ); % [kJ/hr]

%%%%%%%%%%%%%
% Enthalpy of heating water
%%%%%%%%%%%%%
Enthalpy.Regen.HW.In = ...
    Hot.FlowKH.* (... % Flow rate [kg/hr]
    Hot.Temp.In.* ... % Temp [deg C]
    interp1(WaterProps.Temp, ...
        WaterProps.SpecHeat,Hot.Temp.In,'pchip') ... % Cp [kJ/kg/degC]
    ); % [kJ/hr]
Enthalpy.Regen.HW.Out = ...
    Hot.FlowKH.* (... % Flow rate [kg/hr]
    Hot.Temp.Out.* ... % Temp [deg C]
    interp1(WaterProps.Temp, ...
        WaterProps.SpecHeat,Hot.Temp.Out,'pchip') ... % Cp [kJ/kg/degC]
    ); % [kJ/hr]

%%%%%%%%%%%%%
% Enthalpy of process air through conditioner
%%%%%%%%%%%%%
Enthalpy.Cond.Air.In = ... % [kJ/hr]
    Air.FlowKH.* ... % Flow rate [kg/hr]
    Air.Amb.H; % Enthalpy state in [kJ/kg]
Enthalpy.Cond.Air.Out = ... % [kJ/hr]
    Air.FlowKH.* ... % Flow rate [kg/hr]
    Air.Proc.H; % Enthalpy state in [kJ/kg]

%%%%%%%%%%%%%
% Enthalpy of scavenging air through regenerator
%%%%%%%%%%%%%
Enthalpy.Regen.Air.In = ...
    Air.FlowRegenKH.* ... % Flow rate [kg/hr]
    Air.Amb.H; % Enthalpy state in [kJ/hr]
% Can't calc Regen.Air.Out yet

```

```

%%%%% Enthalpy of desiccant stream through conditioner
% Uses concentration data
%%%%%
Enthalpy.Cond.Des.In = ...
    Des.C.FlowInKH.*( ... % Flow rate [kg/hr]
    Des.C.TempIn.*CpLiCl(Des.C.TempIn,Des.C.ConcIn) ... % Enthalpy in
    ); % kJ/hr
Enthalpy.Cond.Des.Out = ...
    Des.C.FlowOutKH_Air.*( ... % Flow rate [kg/hr]
    Des.C.TempOut.*CpLiCl(Des.C.TempOut,Des.C.ConcOut) ... % Enthalpy out
    ); % kJ/hr

%%%%% Enthalpy of desiccant stream through regenerator
% Uses concentration!!!!
%%%%%
Enthalpy.Regen.Des.In = ...
    Des.R.FlowInKH.*( ... % Flow rate [kg/hr]
    Des.R.TempIn.*CpLiCl(Des.R.TempIn,Des.R.ConcIn) ... % Enthalpy in
    ); % kJ/hr
Enthalpy.Regen.Des.Out = ...
    Des.R.FlowOutKH_Des.*( ... % Flow rate [kg/hr]
    Des.R.TempOut.*CpLiCl(Des.R.TempOut,Des.R.ConcOut) ... % Enthalpy out
    ); % kJ/hr

%%%%% Enthalpy flow rate of conditioner absorption water,
% calculated from desiccant
%%%%%
Enthalpy.Cond.WA_Des = Perf.C.WA_Des .* ...
    (interp1(WaterProps.Temp,WaterProps.Hfg, ... % Interpolate Hfg
    (Des.C.TempIn + Des.C.TempOut)./2,'pchip')... % Average desiccant temp
    + Dilution_Enthalpy(... % Calculate Hdil
    (Des.C.TempIn + Des.C.TempOut)./2,... % Average temperature
    (Des.C.ConcIn + Des.C.ConcOut)./2)... % Average concentration
    );

%%%%% Enthalpy flow rate of conditioner absorption water,
% calculated from air
%%%%%
Enthalpy.Cond.WA_Air = Perf.C.WA_Air .* ...
    (interp1(WaterProps.Temp,WaterProps.Hfg, ... % Interpolate Hfg
    (Des.C.TempIn + Des.C.TempOut)./2,'pchip')... % Average desiccant temp
    + Dilution_Enthalpy(... % Calculate Hdil
    (Des.C.TempIn + Des.C.TempOut)./2,... % Average temperature
    (Des.C.ConcIn + Des.C.ConcOut)./2)... % Average concentration
    ); % [kJ/h]

%%%%% Enthalpy flow rate of regenerator desorption water,
% calculated from desiccant
%%%%%
Enthalpy.Regen.WR_Des = Perf.R.WR_Des .* ...
    (interp1(WaterProps.Temp,WaterProps.Hfg, ... % Interpolate Hfg
    (Des.R.TempIn + Des.R.TempOut)./2,'pchip')... % Average desiccant temp
    + Dilution_Enthalpy(... % Calculate Hdil
    (Des.R.TempIn + Des.R.TempOut)./2,... % Average temperature

```

```

(Des.R.ConcIn + Des.R.ConcOut)./2)...
); % [kJ/h]

%%%%% Using a total regenerator enthalpy balance , the missing enthalpy,
% Air.Out, can be calculated
%%%%%
Enthalpy.Regen.Air.Out = Enthalpy.Regen.Air.In ...
+ Enthalpy.Regen.HW.In ...
+ Enthalpy.Regen.Des.In ...
- Enthalpy.Regen.HW.Out ...
- Enthalpy.Regen.Des.Out; % [kJ/hr]

%%%%% Calculate state value from the flow value
%%%%%
Air.Reg.H = Enthalpy.Regen.Air.Out./Air.FlowRegenKH; % [kJ/kg]

%%%%% Using the two air states, calculate humidity
%%%%%
Air.Reg.W = WRatioHT(Air.Temp,Air.Reg.H); % [kg/kg]

%%%%% With the change in air humidity, calculate the water desorption rate
%%%%%
Perf.R.WR_Air = Air.FlowRegenKH.* (Air.Reg.W - Air.Amb.W); % [kg/hr]

%%%%% Update desiccant data by adding the corrected outlet flow rate
%%%%%
Des.R.FlowOutKH_Air = Des.R.FlowInKH - Perf.R.WR_Air; % [kg/hr]

%%%%% With the desorption rate, calculate associated enthalpy flow rate
%%%%%
Enthalpy.Regen.WR_Air = Perf.R.WR_Air .* ...
(interp1(WaterProps.Temp,WaterProps.Hfg, ... % Interpolataate Hfg
(Des.R.TempIn + Des.R.TempOut)./2,'pchip')... % Average desiccant temp
+ Dilution_Enthalpy(... % Calculate Hdil
(Des.R.TempIn + Des.R.TempOut)./2,... % Average temperature
(Des.R.ConcIn + Des.R.ConcOut)./2)... % Average concentration
);

%%%%% Performance parameters
%%%%%
% Heat exchanger effectiveness
Perf.HX.eff = (Des.R.TempOut - Des.HX.TempOut) ./ (Des.R.TempOut - Des.HX.TempIn);

% Regenerator COP
Enthalpy.Regen.HW.Delta = ...
Enthalpy.Regen.HW.Out - Enthalpy.Regen.HW.In;

Perf.R.COPth_Des = -Enthalpy.Regen.WR_Des./Enthalpy.Regen.HW.Delta;
Perf.R.COPth_Air = -Enthalpy.Regen.WR_Air./Enthalpy.Regen.HW.Delta;

```

C.0.5 Script: Regression fitting routine

```

clear x1 x2 y X b stats x1fit x2fit X1FIT X2FIT YFIT b

%%%%%%%%%%%%%%%
% Choose and load independent and dependent variables
%%%%%%%%%%%%%%%
% Plot 1
x1 = Good.Air.Amb.W';
x2 = Good.Strong.C.In';
y = Good.C.Air.WA';

%%%%%%%%%%%%%%%
% Choose model of fit and perform regression
%%%%%%%%%%%%%%%
X = [ones(size(x1)) x1 x2 x1.*x2]; % Bi-linear, w/ interaction
b = regress(y,X);
stats = regstats(y,[x1 x2 x1.*x2], 'interaction'); % Perform fit
% beta - Regression coefficients
% covb - Covariance of regression coefficients
% yhat - Fitted values of the response data
% r - Residuals
% mse - Mean squared error
% rsquare - R2 statistic

%%%%%%%%%%%%%%%
% Correlation plot
%%%%%%%%%%%%%%%
figure
hold on
p1 = plot(yhat,y);
p2 = plot([-1000,1000],[-1000,1000])
axis([round(min(y)) round(max(y)) round(min(y)) round(max(y))])
set(p1,'Marker','.', 'LineStyle','none');
ylabel('Fitted')
xlabel('Input')
hold off

figure
hold on
p1 = plot(y,r);
p2 = plot([-1000,1000],[0,0]);
axis([round(min(y)) round(max(y)) round(min(r)) round(max(r))])
set(p1,'Marker','.', 'LineStyle','none');
ylabel('Residual')
xlabel('y')
hold off

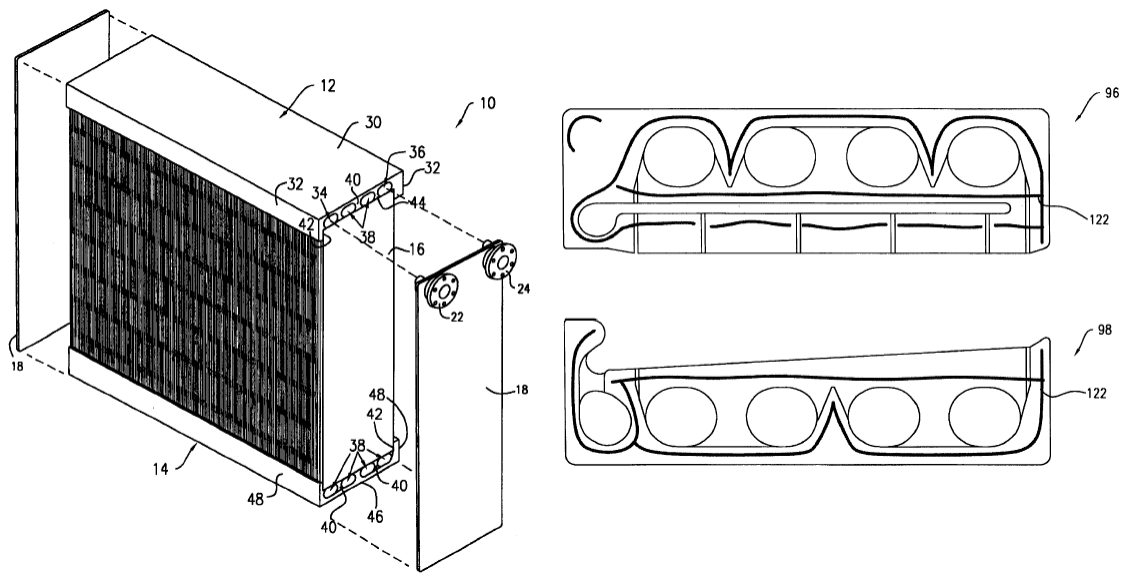
%%%%%%%%%%%%%%%
% 3D plot of data and model
%%%%%%%%%%%%%%%
hold on
%b = stats.beta;
scatter3(x1,x2,y) % Raw data
X = [x1,x2];
x1min = floor(min(x1)*1000)/1000;
x1max = floor(max(x1)*1000)/1000;
x1step = (x1max - x1min)/10;
x2min = floor(min(x2)*1000)/1000;
x2max = floor(max(x2)*1000)/1000;

```

```
x2step = (x2max - x2min)/10;
x1fit = (x1min:x1step:x1max); % x1 fit axis
x2fit = (x2min:x2step:x2max); % x2 fit axis
[X1FIT,X2FIT] = meshgrid(x1fit,x2fit);
YFIT = b(1) + b(2)*X1FIT + b(3)*X2FIT + b(4)*X1FIT.*X2FIT;
mesh(X1FIT,X2FIT,YFIT); % Fitted data
hold off
```

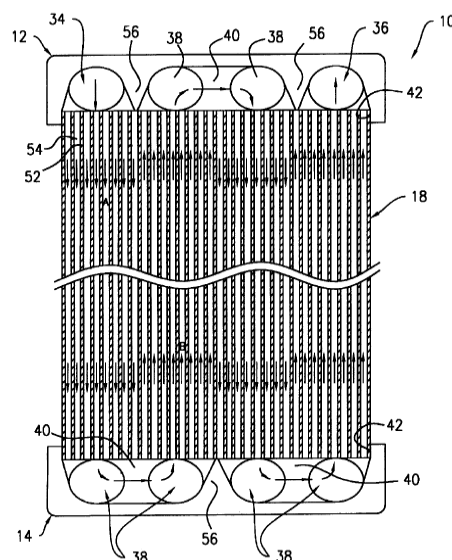
Appendix D

Conditioner Assembly Drawings

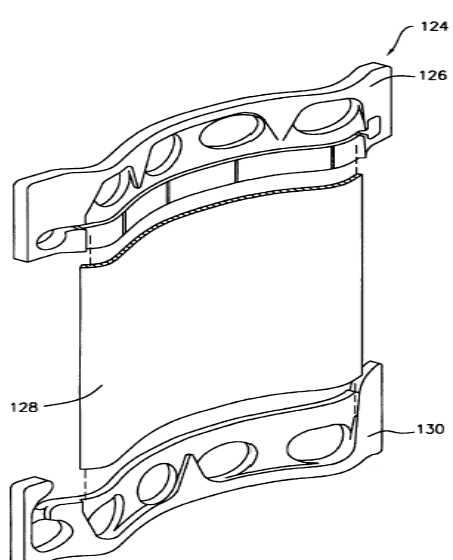


(a) Partial exploded view of conditioner exchanger assembly

(b) Bottom and top plate end-pieces with adhesive bead pattern



(c) Partial cross section of conditioner showing cooling water flow pattern



(d) Perspective view of plate and end piece conditioner assembly

Figure D.1: Conditioner assembly diagrams (U.S. patent 6745826)